

Anoxic Biodegradation of Naphthenic Acid Using Nitrite as an Electron Acceptor

A Thesis Submitted to the College of
Graduate Studies and Research
In Partial Fulfillment of the Requirements
For the Degree of Master of Science
In the Department of Chemical and Biological Engineering
University of Saskatchewan
Saskatoon

By
Fangzhou Dong

PERMISSION TO USE

In presenting this thesis in partial fulfillment of the requirements for a Postgraduate degree from the University of Saskatchewan, I agree that the Libraries of this University may make it freely available for inspection. I further agree that permission for copying of this thesis in any manner, in whole or in part, for scholarly purposes may be granted by the professor or professors who supervised my thesis work or, in their absence, by the Head of the Department or the Dean of the college in which my thesis work was done. It is understood that any copying or publication or use of this thesis or parts thereof for financial gain shall not be allowed without my written permission. It is also understood that due recognition shall be given to me and to the University of Saskatchewan in any scholarly use which may be made of any material in my thesis.

Requests for permission to copy or to make other use of material in this in whole or part should be addressed to:

Head of the Department of Chemical and Biological Engineering

University of Saskatchewan

Saskatoon, Saskatchewan

S7N 5A9

Canada

ABSTRACT

Extraction of bitumen from oil sands by surface mining and alkaline hot water process has generated large amount of oil sand process water (OSPW) which are contaminated by naphthenic acids (NAs). Due to the toxic and harmful nature of NAs, OSPW have been stored on-site in extremely large tailing ponds. With the understanding that the OSPW must be treated before their release into the natural water bodies and the need for reuse of the water, there is an urgent need to treat these OSPWs effectively and economically. Numerous works on different treatment methods including photocatalysis, ozonation, adsorption, phytoremediation, simulated wetlands and bioremediation have been conducted and bioremediation has been proved as one of the most feasible ways among these methods.

Research works on biodegradation of NAs, both aerobically and anoxically, have been conducted intensively in our research group in the past several years. Using surrogate NAs, specially trans-4-methyl-1-cyclohexane carboxylic acid (trans-4MCHCA), aerobic (Paslawski *et al.*, 2009a,b,c, Huang *et al.*, 2012; D'Souza *et al.*, 2013) and anoxic (Gunawan *et al.*, 2014) biodegradations of NA have been studied in batch, CSTR, biofilm system and circulating packed-bed bioreactor. Effects of naphthenic acid concentration, temperature, and naphthenic acid loading rate on the biodegradation process have been investigated (Paslawski *et al.*, 2009a,b,c, Huang *et al.*, 2012; D'Souza *et al.*, 2013; Gunawan *et al.*, 2014). The results of the anoxic biodegradation of trans-4MCHCA in the presence of nitrate as an electron acceptor revealed that its performance was similar or better than that of the aerobic biodegradation. The results of the anoxic biodegradation study also indicated the production of nitrite during the denitrification of nitrate and its subsequent consumption as part of biodegradation process. Given the importance of denitritation (nitrite reduction) as an essential step in anoxic biodegradation in the presence of nitrate, and the potential inhibitory effect of nitrite, the current research was conducted with the aim of investigating the performance of the anoxic biodegradation of

trans-4MCHCA in the presence of nitrite as an electron acceptor, using batch, CSTR and biofilm reactor.

In the current work, the results of batch studies showed that nitrite at concentration up to 690 mg L⁻¹ did not have a marked inhibitory effect but concentrations above 920 mg L⁻¹ imposed a strong inhibitory effect. The optimum temperature was found to be in the range 24 to 30 °C. Continuous anoxic biodegradation of trans-4MCHCA with nitrite in CSTR achieved the maximum trans-4MCHCA biodegradation rate of 14.4 mg L⁻¹ h⁻¹ at a trans-4MCHCA loading rate of 22.9 mg L⁻¹ h⁻¹, which was about seven folds lower than the maximum trans-4MCHCA biodegradation rate observed with nitrate as an electron acceptor (105.4 mg L⁻¹ h⁻¹; Gunawan, 2013). Both the trans-4MCHCA and nitrite degradation rates decreased with further increase of trans-4MCHCA loading rate. Using the experimental data the biokinetic coefficients Y (biomass yield), K_e (endogenous rate constant), μ_m (maximum specific growth rate) and K_s (saturation constant) were determined as 0.3 mg cell mg substrate⁻¹, ~0 h⁻¹, 0.4 h⁻¹ and 20.9 mg substrate L⁻¹, respectively.

Similar pattern was observed in the biofilm system wherein the maximum trans-4MCHCA biodegradation rate was 82.2 mg L⁻¹ h⁻¹ at a trans-4MCHCA loading rate of 171.8 mg L⁻¹ h⁻¹, was about five folds lower than the maximum trans-4MCHCA biodegradation rate observed when nitrate was used as an electron acceptor (435.8 mg L⁻¹ h⁻¹; Gunawan, 2013). The findings of current study suggested that the anoxic NA biodegradation in the presence of nitrite occurred at rates which were lower than those observed in the presence of nitrate, as well as those obtained under aerobic conditions with oxygen as the electron acceptor.

ACKNOWLEDGEMENTS

I would like to express my gratitude to my supervisor Dr. Mehdi Nemati for taking me as a Master of Science student and offering me constant guidance, encouragement, expertise, patience and detailed and constructive comments throughout the Master's program. I would also like to acknowledge the help and comments from my committee members, Dr. Yen-Han Lin and Dr. Venkatesh Meda. I also express my thanks to Richard Blondin and Rlee Prokopishyn for the great technical services and suggestions, and Kelly Bader, Jean Horosko and Jaime Provo for all the administrative and clerical work. My thanks also go to our lab members, Yetty Gunawan, Wen Wang, Yi Zhou, Lyman Moreno and Suraj Kumar for their advice and assistance during my research.

I would also like to thank my parents, the University of Saskatchewan, and Natural Sciences and Engineering Research Council of Canada (NSERC) for their financial support during my Master's program.

DEDICATION

To my parents Hao Dong and Fengxiang Zhao for their love and support.

TABLE OF CONTENTS

PERMISSION TO USE	i
ABSTRACT	ii
ACKNOWLEDGEMENTS	iv
DEDICATION	v
TABLE OF CONTENTS	vi
LIST OF TABLES	ix
LIST OF FIGURES	x
NOMENCLATURES AND ABBREVIATIONS.....	xvi
CHAPTER 1 INTRODUCTION	1
CHAPTER 2 LITERATURE REVIEW, KNOWLEDGE GAP AND RESEARCH OBJECTIVES	3
2.1 Overview of the Canadian Oil sand Industry	3
2.2 Oil Sand Process Water (OSPW)	3
2.3 Naphthenic Acids	4
2.3.1 Chemical and Physical Properties of Naphthenic Acids.....	5
2.3.2 Characterization of Naphthenic Acids	6
2.3.3 Toxicity of Naphthenic Acids	6
2.4 Treatment of Naphthenic Acids	7
2.4.1 Photocatalysis	8
2.4.2 Ozonation.....	9
2.4.3 Adsorption.....	10
2.4.4 Bioremediation.....	11
2.4.4.1 Phytoremediation	11
2.4.4.2 Simulated Wetlands Biodegradation	12
2.4.4.3 Aerobic Biodegradation	13
2.4.4.4 Anaerobic/Anoxic Biodegradation.....	16

2.5 Knowledge Gap and Research Objectives	17
CHAPTER 3 MATERIALS AND METHODS	19
3.1 Model Naphthenic Acid	19
3.2 Microbial Culture and Medium	19
3.3 Anoxic Biodegradation of trans-4MCHCA with Nitrite in Batch System.....	21
3.3.1 Effect of trans-4MCHCA Initial Concentration.....	21
3.3.2 Effect of Temperature	22
3.3.3 Inhibitory Effect of Nitrite	23
3.3.4 Control Experiments	23
3.4 Anoxic Biodegradation of trans-4MCHCA with Nitrite in the Continuous Stirred Tank Reactor (CSTR)	23
3.4.1 Experimental Set-up for Biodegradation in Continuous Stirred Tank Reactor (CSTR).....	23
3.4.2 Biokinetics and the Associated Coefficients.....	25
3.5 Anoxic Biodegradation of trans-4MCHCA with Nitrite in the Biofilm Reactor	27
3.6 Analytical Methods	29
3.6.1 Trans-4MCHCA Concentration	29
3.6.2 Nitrite Concentration	30
3.6.3 Biomass Measurement	31
3.6.4 Reproducibility and Data Uncertainty	31
CHAPTER 4 RESULTS AND DISCUSSION	32
4.1 Batch Biodegradation of trans-4MCHCA with Nitrite	32
4.1.1 Effect of trans-4MCHCA Initial Concentration.....	32
4.1.2 Effect of Temperature	35
4.1.3 Inhibitory Effect of Nitrite	39
4.2 Continuous Biodegradation of trans-4MCHCA with Nitrite in Stirred Tank Reactor.....	43
4.2.1 Effect of trans-4MCHCA Loading Rate	43

4.2.2 Determination of Associated Biokinetic Coefficients Using CSTR Data	46
4.3 Continuous Biodegradation of trans-4MCHCA with Nitrite in Biofilm Reactor	48
4.4 Comparison of trans-4MCHCA Biodegradation with Nitrite in CSTR and Biofilm System	57
4.5 Comparison of Anoxic Biodegradation of trans-4MCHCA with Nitrite and Nitrate as Electron Acceptor	58
4.5.1 Comparison of Biodegradation with Nitrite and Nitrate in a Batch System.....	58
4.5.2 Comparison of Biodegradation with Nitrite and Nitrate in a CSTR.....	59
4.5.3 Comparison of Biodegradation with Nitrite and Nitrate in a Biofilm System	60
CHAPTER 5 CONCLUSIONS AND RECOMMENDATIONS FOR FUTURE WORK	62
5.1 Conclusions.....	62
5.2 Recommendations for Future Work.....	64
REFERENCES	65
APPENDIX A	72
A1 Gas Chromatography (GC) Calibration Curve	72
A2 Ion Chromatography (IC) Calibration Curve.....	73
A3 Biomass Calibration Curve	74
APPENDIX B	75
B1 Samples of Gas Chromatogram.....	75
B2 Sample of Ion Chromatogram	76
APPENDIX C	77
Sample Calculations.....	77
APPENDIX D	79
Determination of Biokinetic Coefficients from CSTR Data.....	79
APPENDIX E	80
Data for Control Experiments	80

LIST OF TABLES

Table 4.1 Effect of trans-4MCHCA initial concentration on biodegradation rate of trans-4MCHCA and reduction rate of nitrite.....	35
Table 4.2 Effect of temperature on lag phase and complete biodegradation time.....	36
Table 4.3 Effect of temperature on biodegradation rate of trans-4MCHCA and nitrite reduction rate.....	39
Table 4.4 Effect of nitrite concentration on biodegradation rate of trans-4MCHCA and nitrite reduction rate.....	42
Table 4.5 Comparison of biokinetic coefficients for aerobic biodegradation (Paslawski <i>et al.</i> , 2009c) with anoxic biodegradation (present work) of trans-4MCHCA in CSTR.....	48
Table 4.6 Comparison of biodegradation rates of trans-4MCHCA obtained at various initial concentrations at room temperature (24 ± 2 °C) with nitrate (Gunawan <i>et al.</i> , 2014) and nitrite (present work).....	59
Table D.1 Data for CSTR modelling.....	79
Table E.1 Control experiment with 100 mg L^{-1} trans-4MCHCA and 460 mg L^{-1} nitrite in the absence of inoculum.....	81
Table E.2 Control experiment with 100 mg L^{-1} trans-4MCHCA in the absence of nitrite.....	81

LIST OF FIGURES

Figure 2.1 Generalized scheme for oil sands processing using water-based extraction processes (Masliyah <i>et al.</i> , 2004).....	4
Figure 3.1 Molecular structure of trans-4-methyl-1-cyclohexane carboxylic acid.....	19
Figure 3.2 Schematic diagram of experimental set-up for biodegradation studies in the continuous stirred tank reactor (CSTR).....	25
Figure 3.3 Schematic diagram of experimental set-up of the biofilm system.....	29
Figure 4.1 Biomass growth, trans-4MCHCA biodegradation and nitrite reduction observed with various initial concentrations of trans-4MCHCA at room temperature (24 ± 2 °C). Panel (A): 100 mg L ⁻¹ trans-4MCHCA and 460 mg L ⁻¹ nitrite, Panel (B): 250 mg L ⁻¹ trans-4MCHCA and 690 mg L ⁻¹ nitrite and Panel (C): 250 mg L ⁻¹ trans-4MCHCA and 828 mg L ⁻¹ nitrite. The error bars represent the standard deviations of multiple tests on each sample taken from the system and they may not be visible in some cases. ◆ Biomass concentration; □ trans-4MCHCA concentration; △ Nitrite ion concentration.....	33
Figure 4.2 Biomass growth, trans-4MCHCA biodegradation and nitrite reduction observed for 100 mg L ⁻¹ of trans-4MCHCA and 460 mg L ⁻¹ of nitrite at various temperatures. Panel (A) 10 °C, Panel (B) 15 °C, Panel (C) 20 °C, Panel (D) 24 ± 2 °C, Panel (E) 30 °C and Panel (F) 35 °C. The error bars represent the standard deviations of multiple tests on each sample taken from the system and they may not be visible in some cases. ◆ Biomass concentration; □ trans-4MCHCA concentration; △ Nitrite ion concentration.....	38

Figure 4.3 Biomass growth, trans-4MCHCA biodegradation and nitrite reduction patterns observed with 100 mg L⁻¹ of trans-4MCHCA with various nitrite concentrations at room temperature (24 ± 2 °C). Panel (A) 100 mg L⁻¹ trans-4MCHCA and 230 mg L⁻¹ nitrite, Panel (B) 100 mg L⁻¹ trans-4MCHCA and 460 mg L⁻¹ nitrite, Panel (C) 100 mg L⁻¹ trans-4MCHCA and 690 mg L⁻¹ nitrite, Panel (D) 100 mg L⁻¹ trans-4MCHCA and 920 mg L⁻¹ nitrite and Panel (E) 100 mg L⁻¹ trans-4MCHCA and 1150 mg L⁻¹ nitrite. The error bars represent the standard deviations of multiple tests on each sample taken from the system and they may not be visible in some cases. ♦ Biomass concentration; □ trans-4MCHCA concentration; ▲ Nitrite ion concentration.....41

Figure 4.4 Steady-state profiles of trans-4MCHCA and biomass concentrations observed in continuous stirred tank reactor (CSTR). Values reported are the average data for multiple samplings of the reactor over an extended period equal to three to five residence times after the establishment of steady state. Error bars represent the standard deviations and might not be visible in some cases. □ trans-4MCHCA residual concentration; ♦ biomass concentration.....44

Figure 4.5 Steady-state profiles of nitrite concentration observed in the continuous stirred tank reactor (CSTR). Values reported are the average data for multiple samplings of the reactor over an extended period equal to three to five residence times after the establishment of steady state. Error bars represent the standard deviations and might not be visible in some cases. ▲ nitrite concentration.....44

Figure 4.6 Removal rate and removal percentage of trans-4MCHCA as a function of its loading rate in continuous stirred tank reactor (CSTR). □ removal rate of trans-4MCHCA; ▲ removal percentage of trans- 4MCHCA.....45

Figure 4.7 Removal rate and removal percentage of nitrite as a function of trans-4MCHCA loading rate in continuous stirred tank reactor (CSTR). ○ removal rate of nitrite; ◇ removal percentage of nitrite.....46

Figure 4.8 Linear plot of $\frac{(S_0 - S)D}{X}$ against D.....47

Figure 4.9 Linear plot of $\frac{S}{D + K_e}$ against S.....47

Figure 4.10 Steady-state profiles of trans-4MCHCA and nitrite concentrations observed in the biofilm system at various loading rate of trans-4MCHCA. Values reported are the average data for multiple samplings of the reactor over an extended period equal to three to five residence times after the establishment of steady state. Error bars represent the standard deviations and might not be visible in some cases. □ trans-4MCHCA residual concentration; △ nitrite concentration.....49

Figure 4.11 Removal rate and removal percentage of trans-4MCHCA as a function of trans-4MCHCA loading rate in the biofilm system. □ removal rate of trans-4MCHCA; △ removal percentage of trans-4MCHCA.....50

Figure 4.12 Removal rate and removal percentage of nitrite as a function of trans-4MCHCA loading rate in the biofilm system. ○ removal rate of nitrite; ◇ removal percentage of nitrite.....51

Figure 4.13 Steady-state profile of trans-4MCHCA observed in the biofilm system with various feed trans-4MCHCA and nitrite concentrations. Values reported are the average data for multiple

samplings of the reactor over an extended period equal to three to five residence times after the establishment of steady state. Error bars represent the standard deviations and might not be visible in some cases. □ $53.9 \pm 5.9 \text{ mg L}^{-1}$ trans-4MCHCA and $498.9 \pm 16.6 \text{ mg L}^{-1}$ nitrite; □ $105.3 \pm 1.8 \text{ mg L}^{-1}$ trans-4MCHCA and $471.6 \pm 12.9 \text{ mg L}^{-1}$ nitrite; □ $252.7 \pm 6.4 \text{ mg L}^{-1}$ trans-4MCHCA and $815.9 \pm 10.3 \text{ mg L}^{-1}$ nitrite.....52

Figure 4.14 Steady-state profile of nitrite observed in the biofilm system with various feed trans-4MCHCA and nitrite concentrations. Values reported are the average data for multiple samplings of the reactor over an extended period equal to three to five residence times after the establishment of steady state. Error bars represent the standard deviations and might not be visible in some cases. △ $53.9 \pm 5.9 \text{ mg L}^{-1}$ trans-4MCHCA and $498.9 \pm 16.6 \text{ mg L}^{-1}$ nitrite; △ $105.3 \pm 1.8 \text{ mg L}^{-1}$ trans-4MCHCA and $471.6 \pm 12.9 \text{ mg L}^{-1}$ nitrite; △ $252.7 \pm 6.4 \text{ mg L}^{-1}$ trans-4MCHCA and $815.9 \pm 10.3 \text{ mg L}^{-1}$ nitrite.....53

Figure 4.15 Removal rate of trans-4MCHCA as a function of its loading rate in the biofilm system fed with various concentrations of trans-4MCHCA and nitrite. □ $53.9 \pm 5.9 \text{ mg L}^{-1}$ trans-4MCHCA and $498.9 \pm 16.6 \text{ mg L}^{-1}$ nitrite; □ $105.3 \pm 1.8 \text{ mg L}^{-1}$ trans-4MCHCA and $471.6 \pm 12.9 \text{ mg L}^{-1}$ nitrite; □ $252.7 \pm 6.4 \text{ mg L}^{-1}$ trans-4MCHCA and $815.9 \pm 10.3 \text{ mg L}^{-1}$ nitrite.....54

Figure 4.16 Removal percentage of trans-4MCHCA as a function of its loading rate in the biofilm system fed with various concentrations of trans-4MCHCA and nitrite. ○ $53.9 \pm 5.9 \text{ mg L}^{-1}$ trans-4MCHCA and $498.9 \pm 16.6 \text{ mg L}^{-1}$ nitrite; ○ $105.3 \pm 1.8 \text{ mg L}^{-1}$ trans-4MCHCA and $471.6 \pm 12.9 \text{ mg L}^{-1}$ nitrite; ○ $252.7 \pm 6.4 \text{ mg L}^{-1}$ trans-4MCHCA and $815.9 \pm 10.3 \text{ mg L}^{-1}$ nitrite.....55

Figure 4.17 Removal rate of nitrite as a function of trans-4MCHCA loading rate in the biofilm

system fed with various concentrations of trans-4MCHCA and nitrite. \diamond $53.9 \pm 5.9 \text{ mg L}^{-1}$ trans-4MCHCA and $498.9 \pm 16.6 \text{ mg L}^{-1}$ nitrite; \diamond $105.3 \pm 1.8 \text{ mg L}^{-1}$ trans-4MCHCA and $471.6 \pm 12.9 \text{ mg L}^{-1}$ nitrite; \diamond $252.7 \pm 6.4 \text{ mg L}^{-1}$ trans-4MCHCA and $815.9 \pm 10.3 \text{ mg L}^{-1}$ nitrite.....56

Figure 4.18 Removal percentage of nitrite as a function of trans-4MCHCA loading rate in the biofilm system fed with various concentrations of trans-4MCHCA and nitrite. \triangle $53.9 \pm 5.9 \text{ mg L}^{-1}$ trans-4MCHCA and $498.9 \pm 16.6 \text{ mg L}^{-1}$ nitrite; \triangle $105.3 \pm 1.8 \text{ mg L}^{-1}$ trans-4MCHCA and $471.6 \pm 12.9 \text{ mg L}^{-1}$ nitrite; \triangle $252.7 \pm 6.4 \text{ mg L}^{-1}$ trans-4MCHCA and $815.9 \pm 10.3 \text{ mg L}^{-1}$ nitrite.....57

Figure 4.19 Comparison of trans-4MCHCA and nitrite removal rates in the CSTR and biofilm system. Panel (A) \square trans-4MCHCA removal rate profiles of CSTR operating with $101.6 \pm 5.4 \text{ mg L}^{-1}$ trans-4MCHCA and $492.5 \pm 14.8 \text{ mg L}^{-1}$ nitrite; \circ trans-4MCHCA removal rate profiles in biofilm system operating with $53.9 \pm 5.9 \text{ mg L}^{-1}$ trans-4MCHCA and $498.9 \pm 16.6 \text{ mg L}^{-1}$ nitrite; Panel (B) \square nitrite removal rate profiles of CSTR operating with $101.6 \pm 5.4 \text{ mg L}^{-1}$ trans-4MCHCA and $492.5 \pm 14.8 \text{ mg L}^{-1}$ nitrite; \circ nitrite removal rate profiles of biofilm system operating with $53.9 \pm 5.9 \text{ mg L}^{-1}$ trans-4MCHCA and $498.9 \pm 16.6 \text{ mg L}^{-1}$ nitrite.....58

Figure 4.20 Removal rate of trans-4MCHCA as a function of its loading rate in the presence of nitrate and nitrite ions as electron acceptors in the CSTR. \diamond Biodegradation of $232.5 \pm 22.9 \text{ mg L}^{-1}$ trans-4MCHCA with $613.7 \pm 10.5 \text{ mg L}^{-1}$ nitrate (data was taken from Gunawan *et al.*, 2014); \square Biodegradation of $101.6 \pm 5.4 \text{ mg L}^{-1}$ trans-4MCHCA with $492.5 \pm 14.8 \text{ mg L}^{-1}$ nitrite.....60

Figure 4.21 Removal rate of trans-4MCHCA as a function of its loading rate in the presence of

nitrate and nitrite ions as electron acceptors in the biofilm system. \diamond Biodegradation of 50.3 ± 3.1 mg L⁻¹ trans-4MCHCA with 316.1 ± 22.8 mg L⁻¹ nitrate (data was taken from Gunawan *et al.*, 2014); \square Biodegradation of 53.9 ± 5.9 mg L⁻¹ trans-4MCHCA with 498.9 ± 16.6 mg L⁻¹ nitrite.....61

Figure A.1 Calibration curve developed for various trans-4MCHCA concentrations. Error bars represent standard deviations in 3 trans-4MCHCA concentration readings.....72

Figure A.2 Calibration curve developed for various nitrite concentrations. Error bars represent standard deviations in 4 nitrite concentration readings.....73

Figure A.3 Biomass calibration curve.....74

Figure B.1 The representative Varian-430 GC chromatogram of trans-4MCHCA.....75

Figure B.2 The representative Dionex ICS-2500 IC chromatogram of nitrite.....76

Figure E.1 Control experiments with 100 mg L⁻¹ trans-4MCHCA and 460 mg L⁻¹ nitrite in the absence of inoculum. The error bars represent the standard deviations of multiple tests on each sample taken from the system and they may not be visible in some cases. \diamond Biomass concetnration; \square trans-4MCHCA concetnration; \triangle Nitrite ion concetnration.....80

NOMENCLATURES AND ABBREVIATIONS

Nomenclature

D: dilution rate (h^{-1})

HRT: hydraulic residence time (h)

K_e : endogenous rate constant (h^{-1})

K_s : saturation constant ($\text{mg substrate L}^{-1}$)

Q: volumetric flow rate of the influent and the effluent (mL h^{-1})

r_x : biomass growth rate ($\text{mg cell}^{-1} \text{mg substrate}^{-1} \text{h}^{-1}$)

r_s : substrate utilization rate ($\text{mg substrate L}^{-1} \text{h}^{-1}$)

S_0 : feed trans-4MCHCA concentration (mg L^{-1})

S: residual trans-4MCHCA concentration (mg L^{-1})

V: working volume of the bioreactor (mL)

X_0 : feed biomass concentration ($\text{mg cell dry weight L}^{-1}$)

X: biomass concentration in the bioreactor ($\text{mg cell dry weight L}^{-1}$)

Y: biomass yield ($\text{mg cell mg substrate}^{-1}$)

μ : specific growth rate (h^{-1})

μ_m : maximum specific growth rate (h^{-1})

Abbreviations

CAPP: Canadian Association of Petroleum Producers

CPBB: Circulating Packed-bed Bioreactor

CSS: Cyclic Steam Stimulation

CSTR: Continuous Stirred Tank Reactor

ESI: Electron Spray Ionization

FID: Flame Ionization Detection

FTIR: Fourier Transform Infrared

GC: Gas Chromatography

GCOS: Great Canadian Oil Sands

HPLC: High Performance Liquid Chromatography

IC: Ion Chromatography

ISB: Immobilized Soil Bioreactor

ICR: Immobilized Cell Bioreactor

MS: Mass Spectrometry

NAs: Naphthenic Acids

OD: Optical Density

OSPW: Oil Sand Process Water

SAGD: Steam-assisted Gravity Drainage

Trans-4MCHCA: Trans-4-methyl-1-cyclohexane carboxylic acid

TOC: Total Organic Carbon

TAO: Total Acid-extractable Organics

UV: Ultraviolet

CHAPTER 1 INTRODUCTION

As of 2014, Canada has the world's third largest oil reserves of 173 billion barrels, third to Venezuela and Saudi Arabia. Of the total reserves, 169 billion barrels are from the oil sands. Athabasca, Peace River and Cold Lake in Northern Alberta are the three main regions where these oil sand deposits are located (CAPP, 2014). As the majority of the oil reserve is in the form of oil sands, recovery methods that are different from the traditionally-used oil well extraction method are widely used in Alberta in order to separate bitumen from oil sands. Currently, both surface mining and *in-situ* extraction, are used and contribute to around 850,000 b day⁻¹ and 1.1 million b day⁻¹, respectively to the total crude oil production (CAPP, 2014).

The rapid increase in crude oil production requires a sustainable supply of fresh water to meet the water consumption, especially for the surface mining of oil sands. Recovering bitumen from oil sands requires large volume of fresh water, which results in generation of toxic slurry called oil sand process water (OSPW) that consist of sand, clay, unrecovered hydrocarbons and water. Currently, 2-2.5m³ of fresh water is used for production of each cubic meter of synthetic crude oil from surface mining, and 0.5 m³ of fresh water in case of *in situ* extraction (CAPP, 2011; Toor *et al.*, 2013a). The main cause of toxicity in OSPW is believed to be naphthenic acids (NAs) (MacKinnon and Boerger, 1986). Subsequent studies have revealed the impact of NAs on the environment, aquatic lives (Videla *et al.*, 2009) and animals (Rogers *et al.*, 2002). Due to the low treatment efficiency of natural degradation in tailing ponds and the zero discharge policy put in place by the Government of Alberta, the OSPWs are currently stored in extremely large tailings ponds on site (Dominski, 2007). The area of the tailing ponds in 2011 was greater than 170 km² (Gunawan *et al.*, 2014). With the rising concern in the increasing volume of the OSPW and the potential risk of leakage and damage to the underground water system and environment, more efficient and economical methods for the treatment of OSPW are required.

Research works have been conducted on different treatment methods including photocatalysis, ozonation, adsorption, phytoremediation, simulated wetlands and bioremediation in the past and bioremediation has been proven as one of the most feasible techniques among these methods. Both aerobic and anoxic biodegradation of NAs have been investigated intensively in our research group in the past few years (Paslawski *et al.*, 2009a, b, c; Huang *et al.*, 2012; D'Souza *et al.*, 2013; Gunawan *et al.*, 2014) and a recent research done by Gunawan *et al.* (2014) on a surrogate NA (trans-4-methyl-1-cyclohexane carboxylic acid, trans-4MCHCA) has shown that anoxic biodegradation of NA coupled with denitrification could be used as an effective alternative to aerobic conditions. This work also indicated that nitrite was generated during the biodegradation of NA under denitrifying conditions and that the produced nitrite was eventually used by microbial culture for biodegradation of NA. Considering the known inhibitory effect of nitrite and the fact that reduction of nitrate during biodegradation of NA results in the formation of nitrite, an understanding of the process of anoxic NA biodegradation with nitrite as an electron acceptor (denitrification) is essential. This is very important due to the fact that there is not any information in the literature with regard to biodegradation of NAs coupled with denitrification process. Thus, in the current work anoxic biodegradation of naphthenic acids in the presence of nitrite is being investigated.

This thesis consists of five chapters including Chapter 1 Introduction, Chapter 2 Literature Review, Knowledge Gap and Research Objectives, Chapter 3 Material and Methods, Chapter 4 Results and Discussion and Chapter 5 Conclusions and Recommendations for Future work.

CHAPTER 2 LITERATURE REVIEW, KNOWLEDGE GAP AND RESEARCH OBJECTIVES

2.1 Overview of the Canadian Oil sand Industry

With the total global oil reserves being 173 billion barrels, Canada has the world's third largest oil reserves after Venezuela and Saudi Arabia (CAPP, 2014). A large part of Canada's oil reserve is in the form of oil sands and are mainly located in Northern Alberta and Saskatchewan (Athabasca, Cold Lake, and Peace River). These oil sand reserves are recoverable in the form of bitumen and currently two methods for oil recovery are employed: surface mining and *in situ* extraction (e.g. cyclic steam stimulation, CSS and steam-assisted gravity drainage, SAGD) (CAPP, 2014). Both surface mining and *in-situ* extraction need large amounts of water to recover the bitumen from oil sands. Canadian Association of Petroleum Producers (CAPP) reported that in the year of 2013, out of 1.9 million b day⁻¹ of produced crude oil about 0.8 million b day⁻¹ were recovered by surface mining techniques. Due to the heavy and viscous nature of bitumen, most of the current surface mining production is based on the modified Clark hot water extraction process (Gunawan *et al.*, 2014), which uses hot alkaline water (50 - 80 °C) to separate bitumen from oil sand ore (Holowenko *et al.*, 2002). In current integrated surface mining operations, approximately 2-2.5m³ of fresh water is used to produce 1m³ of synthetic crude oil (Toor *et al.*, 2013a). Meanwhile, *in situ* extraction method required about half a barrel of water for each recovered barrel of crude oil (CAPP, 2011). With the increase in global demand of oil, surface mining production is forecasted to grow to 1.6 million b day⁻¹ and *in situ* production is forecasted to grow to 3.2 million b day⁻¹ by 2030 (CAPP, 2014), which means about 3.2 to 4 million b day⁻¹ and 1.6 million b day⁻¹ of fresh water will be required for each process, respectively.

2.2 Oil Sand Process Water (OSPW)

Although the majority (80 to 95 percent) of the water used in the oil sands projects is recycled (CAPP, 2011; Government of Alberta, 2014), the water that cannot be recycled, known as oil

sand process water (OSPW), is retained in the tailing ponds on site because of its toxic nature and the zero discharge policy put in place by the Government of Alberta. Tailings in these ponds usually consist of water, sand, clay, some residual bitumen, and most importantly, naphthenic acids (Gunawan *et al.*, 2014), which are proven to be toxic to a number of species, including mammals and fish (MacKinnon and Boerger, 1986; Rogers *et al.*, 2002; Smith *et al.*, 2008). The accumulated tailings are projected to have a volume of 1 billion m³ by 2025 (Del Rio *et al.*, 2006). Generation of tailings has resulted in the expansion of the tailing ponds with the total area of which exceeded 170 km² in 2011 (Gunawan *et al.*, 2014). Figure 2.1 summarizes the extraction and upgrading of bitumen, and the generation of tailings (Masliyah *et al.*, 2004).

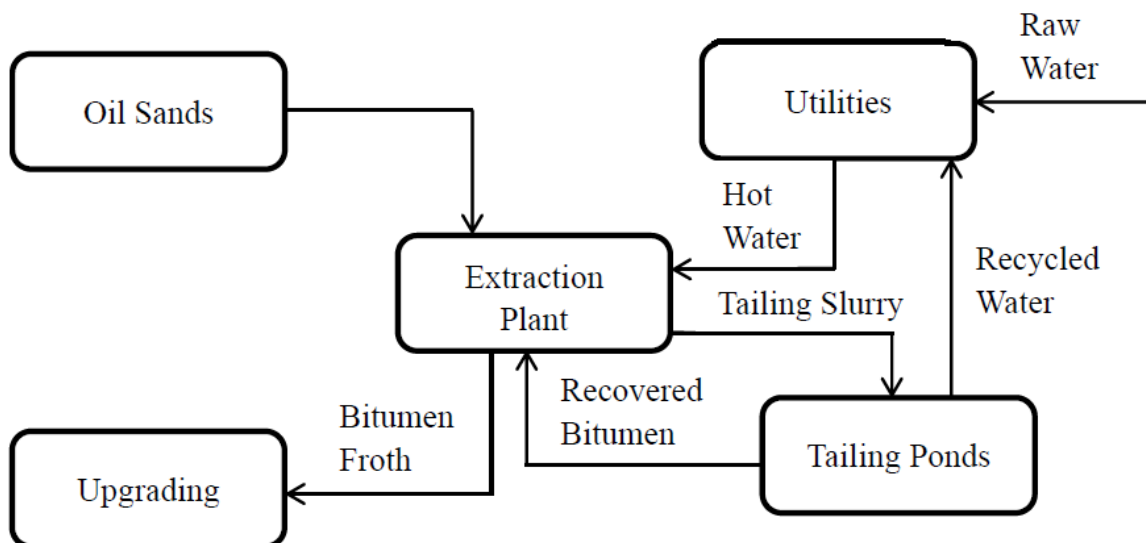


Figure 2.1 Generalized scheme for oil sands processing using water-based extraction processes (Masliyah *et al.*, 2004)

2.3 Naphthenic Acids

The use of modified Clark hot water extraction method results in transfer of some toxic contaminants, particularly naphthenic acids that have both acute and chronic toxicity (Toor *et al.*, 2013b), into the aqueous phase when the water and oil sands are contacted. Naphthenic acids are a mixture of cycloaliphatic carboxylic acids, alkyl-substituted acyclic carboxylic acids (classical NAs) and some minor compounds (non-classical NAs) like aromatic acids, olefinic acids,

hydroxyl acids, dibasic acids. Some NAs contain multiple hydroxyl/carboxyl groups or heteroatoms such as N and S (D'Souza *et al.*, 2013; Johnson *et al.*, 2013). The general formula for the majority of the NAs is $C_nH_{2n+z}O_2$, where n stands for the carbon number and z characterizes the hydrogen atom deficiency resulting from ring formation (Paslawski, 2008). Z can only be either zero or a negative even integer. For example, when z is equal to zero, it means saturated linear NAs; when z equals to -2 or -4, it represents monocyclic NAs and bicyclic NAs respectively (Huang, 2011). It also should be pointed out that the majority of NAs in OSPW are those having z values between -8 and -12, with almost no or little portion of them having z values between 0 and -6 (Azad *et al.*, 2013).

The current concentration of NAs in OSPW is estimated between 40 to 130 mg L⁻¹ (D'Souza *et al.*, 2013) and it will be more and more concentrated because of the recycling of the water. With the total volume of OSPW is projected to be 1 billion m³ by 2025, the amount of NAs in SPW will exceed at least 40,000 tons by that time. Although they appear naturally in the oil sands extraction and upgrading processes and bring many problems such as corrosion for refineries and reducing the crude oil quality, NAs also have a variety range of industrial uses including fuel additives, wood preservatives, paint driers, aluminum ceramics, anti-wear lubricants, and in the process of manufacturing tires (Brient *et al.*, 1995; Gunawan, 2013).

2.3.1 Chemical and Physical Properties of Naphthenic Acids

Naphthenic acids (NAs) are clear or brown viscous liquids or powders that are soluble in some organic solvents. The solubility of NAs in water is determined by the pH of the water. Increase of pH increases the solubility of NAs in water (Azad *et al.*, 2013). Their color, odour and stability vary according to their structures (e.g. the presence of phenolic groups and/or the heteroatoms). The boiling points of NAs are within the range of 250 to 350 °C (Brient *et al.*, 1995). The volatility of NAs are extremely low with the Henry's constant being $8.56 \times 10^{-6} \text{ m}^3\text{-atm mol}^{-1}$ (Rogers *et al.*, 2002).

Chemically, NAs behave similar to carboxylic acids with a pH between 4.8 and 9.9, weaker than acetic acid but stronger than phenol. The acid dissociation (pK_a) value of NAs is of almost 5 (Brient *et al.*, 1995; Azad *et al.*, 2013).

2.3.2 Characterization of Naphthenic Acids

Many analytical methods, including Fourier transform infrared spectrometry (FTIR) (MacKinnon and Boerger, 1986; Scott *et al.*, 2008), Gas chromatography (GC) (Jones *et al.*, 2001; Paslawski *et al.*, 2009b,c; Huang *et al.*, 2012; D'Souza *et al.*, 2013; Gunawan *et al.*, 2014), Mass Spectrometry (MS) (Hsu *et al.*, 2000), Gas chromatography-mass spectrometry (GC-MS) (Clemente *et al.*, 2003; Scott *et al.*, 2008; Damasceno *et al.*, 2014), Electron spray ionization-mass spectrometry (ESI-MS) (Headley *et al.*, 2002b; Martin *et al.*, 2008; Damasceno *et al.*, 2014; Goff *et al.*, 2014), High performance liquid chromatography (HPLC) (Yen *et al.*, 2004; Scott *et al.*, 2005), High performance liquid chromatography-mass spectrometry (HPLC-MS) (Pereira *et al.*, 2013) have been employed to study of NAs individually in mixture and separately both qualitatively and quantitatively.

Fourier transform infrared spectrometry (FTIR) is the most widely used in industries to determine bulk concentration of NAs in OSPW. However, FTIR readings can be easily interfered by other non-toxic organic compounds, thus they may give higher values of NAs concentration in OSPW (Scott *et al.*, 2008). GC or GC/MS usually have advantage in separating the individual NAs from the mixture over HPLC, but because of the extremely complexity of the NAs mixture present in OSPW, completely isolation and characterization of individual NAs still cannot be achieved (Quagraine *et al.*, 2005).

2.3.3 Toxicity of Naphthenic Acids

The toxicity of OSPW was first noticed in 1975. Hrudey (1975) reported acute toxicity to

rainbow trout that were exposed to drainage water from the Great Canadian Oil Sands (GCOS, the precursor to Suncor) lease (Allen 2008). The primary toxic component to aquatic organisms was believed to be naphthenic acids, although thousands of organic/inorganic contaminants present of OSPW (Rogers *et al.*, 2002). Due to their nature of having both the hydrophobic alkyl groups and a hydrophilic carboxylic group at the same time, NAs are considered to be surfactants that can easily penetrate the cell walls and cause membrane disruption (Rogers *et al.*, 2002). Numerous works have been conducted to identify the toxicity of NAs to different species including rainbow trout and water fleas (MacKinnon and Boerger, 1986), mammals (Wistar rats) (Rogers *et al.*, 2002) and fish (Dokholyan and Magomedov, 1983; Scarlett *et al.*, 2013). Due to the technical difficulties in separating and analyzing the individual NAs from the complex mixture, most of the toxicity research treated the NAs mixture as a whole, so that the most toxic compound in the NAs mixture is still unknown (Quagraine *et al.*, 2005). Holowenko *et al.* (2002) reported that the toxicity decreased with the increase of carbon number (n). In this work “C₂₂+cluster” was used as a parameter to determine the relationship between toxicity and the NAs distribution. The acute toxicity of both Suncor samples and Syncrude samples were found to decrease when the proportion of the “C₂₂⁺cluster” increased (Holowenko *et al.*, 2002).

2.4 Treatment of Naphthenic Acids

With the understanding that the tailing ponds must be reclaimed in the near future and the water retained inside must be reused or returned to the natural water bodies, treatment of waters contaminated with naphthenic acids have been studied intensively. Several treatment methods including photocatalysis (Doll and Frimmel, 2005; Mishra *et al.*, 2010b), ozonation (Scott *et al.*, 2008; Martin *et al.*, 2010; Hwang *et al.*, 2013; Pereira *et al.*, 2013), adsorption (Zubot *et al.*, 2012; Azad *et al.*, 2013), phytoremediation (Knight *et al.*, 1999; McMartin, 2003; Quagraine *et al.*, 2005; Biryukova *et al.*, 2007; Quesnel *et al.*, 2011), simulated wetlands (Toor *et al.*, 2013a,b) and aerobic/anoxic biodegradation (Herman *et al.*, 1994; Paslawski *et al.*, 2009a,b,c; Huang *et al.*, 2012; D’Souza *et al.*, 2013; Gunawan *et al.*, 2014) have been proposed and studied. Some of

these methods will be discussed briefly in the follow sections.

2.4.1 Photocatalysis

The process of photocatalysis is based on the reduction and oxidation (redox) reactions which form electron-hole pairs and generate free radicals for secondary reactions through the photo-excitation (Linsebigler *et al.*, 1995). Microwave treatment of NAs in the presence of TiO₂ catalyst, an example of photocatalysis, was studied as an alternative treatment of degradation of NAs (Mishra *et al.*, 2010a). Microwave system was reported to successfully degrade both OSPW NAs and commercial Fluka NAs, with the presence of TiO₂ as catalyst, in short period of time. TiO₂ was chosen because it is active, cheap, non-toxic, chemically stable, and did not subject to photo corrosion (Doll and Frimmel, 2005). However, it should be pointed out that Mishra *et al.* also observed a slight increase in toxicity after the treatment in OSPW NAs samples (Mishra *et al.*, 2010a).

Photo-excitation can also be achieved by using UV or visible lights, with UV₂₅₄ has been reported to be the optimum wavelength to treat the NAs (McMartin *et al.*, 2004; Mishra *et al.*, 2010b; Afzal *et al.*, 2012). Mishra *et al.* (2010b) used UV₂₅₄ together with TiO₂ as catalyst to treat both commercial NAs and OSPW NA extracts. The photocatalytic system effectively degraded the NAs and removed acute toxicity in a relatively short time (half-life values ranging between 1.6 and 17.4 h). Although TiO₂ has been used widely as catalyst in many works and proven to be successful, its disadvantages cannot be ignored. For instance performance of TiO₂ as catalyst can be easily suppressed by some other ions commonly present in OSPW including chloride (Cl⁻) and bicarbonate (HCO₃⁻) (Bessa *et al.*, 1999). Furthermore, the separation of TiO₂ and any other catalyst after treatment is also a problem that limits the industrial application of photocatalysis.

2.4.2 Ozonation

Ozonation is a treatment technique that applies ozone as a powerful oxidizing agent to break down NAs, even the most recalcitrant ones, to CO₂ or less harmful compounds and reduces the toxicity of OSPW. It is a highly efficient method and can remove naphthenic acids and their associated acute toxicity in short time (Scott *et al.*, 2008). Scott *et al.* (2008) reported that >95 % of the NAs in OSPW can be degraded after 130 min ozonation, with the residual NAs concentration <2 mg L⁻¹. The Microtox bioassay result indicated the acute toxicity as zero. Pereira *et al.* (2013) examined effect of ozonation on not only classical NAs, but also some with heteroatom-containing compounds such as O_x, NO_x, SO_x, NO₂S, N and S. The result showed that ozonation with 50 mg O₃ L⁻¹ had degraded all the organic compounds with only some small residual amount of SO_x and O_x that led to the residual toxicity (Pereira *et al.*, 2013).

However, because ozone cannot be stored or transported, the relatively high cost of generating ozone on-site to handle the large volume of OSPW makes its use as the sole treatment approach impractical (Scott *et al.*, 2008). Thus many researchers have focused on the combination of ozonation and biodegradation (Martin *et al.*, 2010; Hwang *et al.*, 2013). Furthermore, as clear evidence has shown that ozone has the preference of reacting with NAs that have higher carbon numbers and higher hydrogen deficiency numbers (Islam *et al.*, 2014) which is exactly complementary to biodegradation, ozonation was widely used as a pre-treatment method to degrade the biopersistent proportion of NAs in the OSPW or to break down the highly branched and highly cyclic proportion of NAs to smaller and more linear forms, which are more amenable to biodegradation. Ozonation has not only accelerated the total NA biodegradation half-life from 83 days (without ozonation) to 48 days with ozone-degraded OSPW, but also accelerated the removal of toxicity of OSPW (Martin *et al.*, 2010). Hwang *et al.* (2013) reported that combined ozonation and biodegradation process removed 99 % of the NAs and 87.2 % of the TAO (total acid-extractable organics) from the OSPW, compared to 13.8 % and 18.5 %, respectively, for unozonated OSPW. Brown *et al.* (2013) found that ozonation at 50 mg L⁻¹ concentration

significantly improved the *in situ* biodegradability of the dissolved organic carbon and most importantly, ozonation did not negatively affect the performance of the indigenous microbial communities for degrading the dissolved organic carbon in OSPW.

The drawbacks of ozonation, besides the high operation cost, includes the increase of toxicity (Pereira *et al.*, 2013) and the limitation of mass transfer from gas phase (ozone) to liquid phase (OSPW) (D'Souza 2012). Pereira *et al.* (2013) suggested that ozone may react with other chemicals in OSPW and generate more toxic compounds (e.g. halogenated compounds) that may have higher toxicity based on certain endpoints.

2.4.3 Adsorption

Adsorption of NAs using different types of adsorbents is another method that is under investigation. Some adsorbents are proved to effectively remove NAs from OSPW, including activated carbon, nickel (Ni) based alumina (Ni-Al₂O₃) and petroleum coke (Zubot *et al.*, 2012; Azad *et al.*, 2013). Azad *et al.* (2013) reported that 50.4 % and 39.9 % total organic carbon (TOC) were removed when using activated carbon and Ni-Al₂O₃ as adsorbents, respectively. They also found out that the Ni loading was influential in the removal of TOC and the effectiveness of adsorbents may be improved by decreasing the total dissolved salts in OSPW (Azad *et al.*, 2013). Zubot *et al.* (2012) used petroleum coke, a by-product of bitumen upgrading, as adsorbent to treat the OSPW and found that total acid-extractable organics (TAO) and toxicity decreased after treatment. The adsorption capacity was found to be 0.26 mg NA g⁻¹ of adsorbent for typical OSPW with initial TAO of 60 mg L⁻¹.

The disadvantage that limited the widespread use of adsorption is the generation of used adsorbents as a secondary pollutant. Further research work is needed on how to recover the adsorbents economically or how to environmentally dispose the used adsorbents.

2.4.4 Bioremediation

Bioremediation is one of the most cost-effective and environmental friendly way to for the treatment of wastewaters (Scott *et al.*, 2008). NAs with lower carbon number and those with least cyclic proportion are more susceptible to the natural biodegradation, which may take up to 12 to 14 years (Toor *et al.*, 2013b). Moreover, commercial NAs are more amenable for biodegradation than NAs from OSPW (Del Rio *et al.*, 2006; Misiti *et al.*, 2013c). The organisms commonly used for bioremediation includes algae, plants, and bacteria. As living organism is more susceptible to the ambient environment; many researches have been conducted to evaluate the factors that may affect the performance of bioremediation, including but not limited to the species of the organism, type of the substrate, temperature and pH, the configuration of bioreactors, etc..

This section summarizes the latest progresses in bioremediation of oil sand process waters using four different approaches of: phytoremediation, simulated wetlands biodegradation, aerobic microbial biodegradation and anaerobic/anoxic microbial biodegradation.

2.4.4.1 Phytoremediation

Phytodegradation employs rhizobacterial attached to the extensive root systems of the plants. There are basically two processes involved in removal of contaminants (i) the stimulation of rhizobacterial transformation; (ii) the slowing of contaminant transport from the rooting zone as a result of adsorption or increased evapotranspiration and plant uptake followed by metabolism, volatilization, or accumulation (McMartin, 2003; Quagraine *et al.*, 2005).

A recent Study on aerobic degradation using rhizobacterial showed that they can degrade lower molecular mass NAs from the initial concentration of 135 mg L⁻¹ to 10 mg L⁻¹ in 10 days. (Biryukova *et al.*, 2007). Five different types of rhizobacterial from the soil of five different plant species were examined in this study and they all showed the preference to degrade NAs with

lower molecular mass. Quesnel *et al.* (2011) reported that the marine alga *Dunaliella tertiolecta* was able to tolerate five model NAs (cyclohexane carboxylic acid, cyclohexane acetic acid, cyclohexane propionic acid, cyclohexane butyric acid and 1, 2, 3, 4-tetrahydro-2-naphthoic acid) at concentrations as high as 300 mg L⁻¹, and it could completely degrade four of them at 200 mg L⁻¹, which is a level higher than current NAs concentration in any OSPW, within 42 days. The metabolic pathways for these four model NAs were explained as β -oxidation and step-wise β -oxidation (Quesnel *et al.*, 2011). However, as shown in these research works, phytodegradation was incapable of degrading all NAs presented in OSPW. The biodegradation was selective and the residual recalcitrant fraction of NAs in the OSPW after treatment was the major problem that limited its application (Biryukova *et al.*, 2007; Quesnel *et al.*, 2011). Furthermore, due to the concern of leaching of NAs to the groundwater, heavy metal build up, and long-term plant productivity, the application of phytodegradation on a large-scale have been limited (Knight *et al.*, 1999).

2.4.4.2 Simulated Wetlands Biodegradation

Simulated wetlands with sediments have been used in laboratory studies as a representation of constructed wetlands which could be used for the reclamation of tailing ponds and the treatment of OSPW. Indigenous microbial communities and laboratory microorganisms were employed to treat NAs from different sources at different concentrations. Toor *et al.* (2013a) reported that significant NAs biodegradation and reduction in toxicity were achieved for both Suncor and Syncrude OSPW samples over an extended hydraulic residence time (HRT) of 52 weeks. In both samples the NAs fraction with low molecular weight and those with less rings tended to be biodegraded faster and more completely. The treatment efficiency for Syncrude NAs ranged from 61 % to 75 % based on different n and z numbers, and 56 % to 96 % for Suncor NAs. The residual toxicity after treatment was resulted from the persistent fraction of NAs in OSPW (Toor *et al.*, 2013a). In another research conducted by Toor *et al.* (2013b), although increase of HRT from 40d to 400d resulted in a greater reduction in total NAs in both OSPWs, complete removal

of the persistent fraction of NAs still could not be achieved. Around 18 % of the NAs in OSPW remained after the simulated wetlands treatment (Toor *et al.*, 2013b).

2.4.4.3 Aerobic Biodegradation

Aerobic biodegradation with the aim of enhancing the natural biodegrading process, which may take up to 12 to 14 years (Toor *et al.*, 2013b) has been studied extensively in the past few decades using different types of bacteria, different NAs and different bioreactors. The source and chemical structure of NAs plays an important role in determining the efficiency of aerobic biodegradation (Holowenko *et al.*, 2002; Han *et al.*, 2008; Smith *et al.*, 2008; Scott *et al.*, 2008; Johnson *et al.*, 2011; Misiti *et al.*, 2013a). The lower molecular weight and linear fraction NAs with less branching are more susceptible to biodegradation while those heavier and more cyclic NAs are resistant to biodegradation (Holowenko *et al.*, 2002; Smith *et al.*, 2008; Paslawski *et al.*, 2009b; Johnson *et al.*, 2011; Misiti *et al.*, 2013c). The commercially available NAs, which contained less complex NAs, were proved to be biodegraded easier and faster than those NAs from OSPW (Scott *et al.*, 2008). Different geometric NA isomers also have shown to have different degradation rates (Headley *et al.*, 2002a). Headley *et al.* (2002a) reported that both trans-4-methyl-cyclohexane-acetic acid (trans-4MACH) and trans-4-methyl-cyclohexane carboxylic acid (trans-4MCCH) were degraded faster than their cis- counterparts (cis-4MACH and cis-4MCCH); the rate constant (K) for the former two was about 4 times greater than the other two. The configuration of the bioreactors was also found to affect the treatment efficiency significantly. So far, batch reactor (Paslawski *et al.*, 2009b; Misiti *et al.*, 2013a), continuous stirred tank reactor (CSTR) (Paslawski *et al.*, 2009c), immobilized soil bioreactor (ISB) (McKenzie *et al.*, 2014), immobilized cell bioreactor (ICR) (Paslawski *et al.*, 2009a,c) and circulating packed-bed bioreactor (CPBB) (Huang *et al.*, 2012; D'Souza *et al.*, 2013) have been studied and immobilized cell bioreactor (ICB) was found to have advantage over the others since it increased the biomass hold-up in the bioreactor, regardless of the increase or decrease of the hydraulic residence time (HRT). Some other factors such as temperature, pH, and dissolved

oxygen concentration have also been examined and proved to have significant impact on biodegradation process (Paslawski, 2008). The results that achieved by these studies and the latest progresses are summarized briefly in the following sections.

Misiti *et al.* (2013a) reported that *Pseudomonas* and *Microbulbifer* were able to degrade up to 85 % of the commercial NAs mixture but only a small proportion of the NAs was completely mineralized to CO₂ (28.5 %). Batch reactors were used in this research and different initial NAs concentrations ranging from 60 mg L⁻¹ to 270 mg L⁻¹ were examined. The residual NAs concentration increased from 15.1 mg L⁻¹ to 44.5 mg L⁻¹ with the increase of initial NAs concentration from 60 to 270 mg L⁻¹ after a 3-day treatment (Misiti *et al.*, 2013a). This confirmed the previous research carried by Herman *et al.* (1994) in which the microbial activity mineralized approximately 20 % of the organic carbon in an extracted NAs sample from the OSPW and around 50 % of the organic carbon in a commercial mixture of NAs. Herman *et al.* (1994) determined the dominated species in the mixture as *Pseudomonas stutzeri*, *Alcaligenes denitrificans*, *Acinetobacter calcoaceticus* and *Pseudomonas fluorescens* and that all species contributed in biodegradation of NAs. Apart from the research on mixed NAs from commercial source and OSPW, aerobic batch biodegradation process of several commercially available pure model NAs have been conducted as well. Huang *et al.* (2012) reported that the biodegradability of three model NAs, trans-4-methyl-cyclohexane carboxylic acid (trans-4MCHCA), trans-4-methyl-cyclohexane acetic acid (trans-MCHAA) and cis-4-methyl-cyclohexane acetic acid (cis-MCHAA) were different because of their different carbon numbers and their spatial arrangements. Regardless of the initial concentration, trans-4MCHCA was always gone through biodegradation with the fastest rate and that the degradation rate of trans-MCHAA was around 2 times higher than that of cis-MCHAA (Huang *et al.*, 2012). This confirmed the previous conclusion made by Headley *et al.* (2002a) that geometric arrangement of the atoms would affect the biodegradation process. The aerobic biodegradation of non-classical NAs, for example aromatic alkanolic naphthenic acids, were also carried out recently in batch reactors, although

they only make up a very small fraction in the NAs (Johnson *et al.*, 2013). Being the most recalcitrant compounds, Johnson *et al.* (2013) reported that *Pseudomonas putida* KT2440 could only degrade (4'-n-butylphenyl)-4-butanoic acid (n-BPBA) with no effect on (4'-t-butylphenyl)-4-butanoic acid (t-BPBA). These authors also noticed that the increase of NAs concentration resulted in the decrease of biodegradation ability of *Pseudomonas putida* KT2440 and a decrease in cell numbers, which suggested that NAs may inhibit the bacterial activity due to their toxicity (Johnson *et al.*, 2013). Similar observation was also reported by Misiti *et al.* (2013c) whereby growth inhibition ranging from 10 % to 59 % was observed in activated sludge heterotrophic microcosms which were exposed to NA concentrations higher than 100 mg L⁻¹.

While the majority of the aerobic biodegradation research works used batch reactors, some researchers evaluated continuous aerobic biodegradation and proved that the configuration of the bioreactor was a key factor for achieving higher biodegradation rates. Paslawski *et al.* (2009c) reported that the maximum aerobic biodegradation rates for a surrogate NA, trans-4-methy-1-cyclohexane carboxylic acid (trans-4MCHCA), in continuously stirred tank reactor (CSTR) and immobilized cell reactor (ICR) were 9.6 mg L⁻¹ h⁻¹ and 916.7 mg L⁻¹ h⁻¹, respectively, at the residence times of 40 h and 1.6 h, respectively. Circulating packed-bed bioreactor (CPBB) has also been used to study aerobic biodegradation of single or mixed commercially available NAs. Huang *et al.* (2012) reported a maximum aerobic biodegradation rate of trans-4-methy-1-cyclohexane carboxylic acid (trans-4MCHCA) in a CPBB as 209 mg L⁻¹ h⁻¹ at the residence time of 0.2 h, while the maximum aerobic biodegradation rates for cis- and trans-4-methy-cyclohexane carboxylic acid (cis-/trans-4MCHAA) were 4.2 mg L⁻¹ and 8.7 mg L⁻¹, respectively, at residence time of 3.3 h. D'Souza *et al.* (2013) reported that the aerobic biodegradation rate of octanoic acid stayed the same in the presence of other NAs compounds (trans-4MCHCA and cis- and trans-4MCHAA) in the bioreactor. The maximum aerobic biodegradation rate of octanoic acid was found to be 372 mg L⁻¹ h⁻¹ at the loading rate of 666.7 mg L⁻¹ h⁻¹. The interaction of different NAs compounds in the bioreactor was intricate since the

presence of octanoic acid inhibited degradation of trans-4MCHCA but accelerated the biodegradation of cis- and trans-4MCHAA (D'Souza *et al.*, 2013). McKenzie *et al.* (2014) used immobilized soil bioreactor (ISB) to degrade mixed NAs from OSPW aerobically and obtained a maximum NAs biodegradation rate of $0.1 \text{ mg L}^{-1} \text{ h}^{-1}$ at a residence time of 160 h.

2.4.4.4 Anaerobic/Anoxic Biodegradation

Anaerobic or anoxic biodegradation of hydrocarbons has been studied intensively in the recent decades due to its intrinsic advantage of eliminating the aeration cost. Although many works have been done on the biodegradation of hydrocarbons, information on anoxic biodegradation of NAs is limited. This was due to general belief that anaerobic or anoxic biodegradation is not as effective as aerobic biodegradation. The latest developments in anaerobic or anoxic biodegradation of NAs are summarized in this section.

Evans (1977) pointed out to three routes for anaerobic biodegradation of aromatic hydrocarbons and their respective pathways, which were 1) photometabolism, 2) nitrate respiration and 3) methanogenic fermentation. In anaerobic respiration, instead of using molecular oxygen as an oxidizer and electron acceptor, some other electron acceptors, such as nitrate, nitrite, sulphate, carbon dioxide, etc. must be presented (Evans 1977; Foght 2008). Foght's (2008) provided a detailed look on the pathways, enzymes and terminal electron acceptors in a anaerobic biodegradation of several common aromatic hydrocarbons including benzene, toluene, xylenes, ethylbenzene, naphthalene, and phenanthrene, and the effect of all of the common terminal electron acceptors as mentioned above. The author also suggested that most of the aromatic hydrocarbons were degraded through the β -oxidation process (Foght, 2008).

While the anaerobic biodegradation of hydrocarbons, especially aromatic hydrocarbons is relatively well understood, the information on anaerobic biodegradation of NAs is limited. In an earlier work in our group, the anoxic biodegradation of a surrogate NA,

trans-4-methyl-1-cyclohexane carboxylic acid (trans-4MCHCA), in the presence of nitrate as an electron acceptor was evaluated (Gunawan *et al.*, 2014). The maximum removal rate observed in the anoxic CSTR was $105.4 \text{ mg L}^{-1} \text{ h}^{-1}$ compared to $9.6 \text{ mg L}^{-1} \text{ h}^{-1}$ for aerobic CSTR, and $2,028.1 \text{ mg L}^{-1} \text{ h}^{-1}$ in anoxic biofilm reactor compared to $924.4 \text{ mg L}^{-1} \text{ h}^{-1}$ in the aerobic reactor. These findings indicated that anoxic degradation could be as or even more effective than the aerobic degradation (Gunawan *et al.*, 2014). NAs have been reported to have significant inhibitory effect on some biodegradation processes including nitrification (NAs concentration $> 400 \text{ mg L}^{-1}$) and fermentation/methanogenesis (NAs concentration $> 200 \text{ mg L}^{-1}$); but no inhibitory effect was observed in the denitrification process, in which nitrate was used as electron acceptor (Misiti *et al.*, 2013b).

2.5 Knowledge Gap and Research Objectives

Various physicochemical and biological options for treatment of NAs have been investigated due to the detrimental environmental effects of naphthenic acid containing OSPW. Due to its practicality and feasibility, bioremediation has been identified as one of the most suitable approach with the focus of majority of earlier works being on biodegradation of NAs under aerobic conditions. Earlier work in our group has shown that NAs biodegradation can be carried out successfully under aerobic conditions, as well anoxically with nitrate as the electron acceptor and that nitrite is produced as a result of nitrate reduction and subsequently used as an electron acceptor during NAs biodegradation. However, the impact of nitrite and its potential inhibitory effect on the biodegradation of NAs is not well understood. Thus, there is a need to investigate the biodegradation of NAs coupled with denitrification and to establish the biokinetic of this process, and a need to compare the performance of the biodegradation processes in the presence of nitrate and nitrite as electron acceptors. The specific objectives of this research are as follows:

1. To evaluate the effect of trans-4MCHCA concentration and temperature on its anoxic biodegradation coupled with denitrification in a batch system;
2. To evaluate the inhibitory effect of nitrite on biodegradation of trans-4MCHCA in a

batch system;

3. To study the biokinetics of the anoxic biodegradation of trans-4MCHCA coupled with denitritation in continuous reactors with freely suspended cells (i.e. CSTR);
4. To investigate the potential for improving the anoxic biodegradation rate through application of biofilm system;
5. To compare the biodegrading process in the presence of nitrate and nitrite as electron acceptors.

CHAPTER 3 MATERIALS AND METHODS

3.1 Model Naphthenic Acid

Previous studies suggested that three different groups of naphthenic acids can be used for biodegradation studies in the laboratory scale: pure commercially available NAs, mixed commercially available NAs (i.e. Fluka or Kodak), and NAs extracted from the OSPW. (Holowenko *et al.*, 2001).

Based on the previous research carried out on aerobic and anoxic biodegradation of NAs (Paslawski *et al.*, 2009; Huang *et al.*, 2012; D'souza *et al.*, 2013; Gunawan *et al.*, 2014), trans-isomer of 4-methyl-1-cyclohexane carboxylic acid (referred to as trans-4MCHCA, Alfa Aesar, 98 % purity, CAS No. 13064-83-0) was selected in the current research to evaluate its biodegradation with nitrite. This allowed the comparison of trans-4MCHCA biodegradation in the presence of nitrate (Gunawan *et al.*, 2014) and nitrite. The formula of trans-4MCHCA is $C_8H_{14}O_2$ with the molecular weight being 142.2 g mol^{-1} . At room temperature, trans-4MCHCA appears as a white crystalline solid and its molecular structure is shown in Figure 3.1.

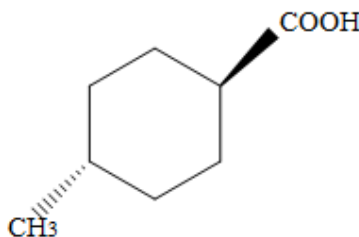


Figure 3.1 Molecular structure of trans-4-methyl-1-cyclohexane carboxylic acid

3.2 Microbial Culture and Medium

The mixed culture used in current research was originally enriched from the soil of an industrial site contaminated with heavy hydrocarbons and had been used in earlier works under both aerobic and anoxic conditions (Paslawski *et al.*, 2009; Huang *et al.*, 2012; D'souza *et al.*, 2013;

Gunawan *et al.*, 2014). The culture had been examined by EPCOR-Quality Assurance Lab, Edmonton, Canada and the two dominant species in this mixed culture had been identified as *Pseudomonas aeruginosa* and *Variovorax paradoxus* (Huang *et al.*, 2012). Since then the culture has been acclimated to the biodegradation of NAs under anoxic condition using nitrate as electron acceptor (Gunawan *et al.*, 2014). Nitrate was substituted by nitrite at the beginning of this research and after some repeated runs, the mixed culture showed the ability for anoxic degradation of trans-4MCHCA with nitrite as an electron acceptor. Subculturing was carried out using 150 mL serum bottles containing 90 mL of sterilized McKinney's modified medium with 100 mg L⁻¹ trans-4MCHCA and 460 mg L⁻¹ nitrite (corresponding sodium nitrite concentration: 690 mg L⁻¹) and 10 % (v/v) inoculum. Prior to inoculation, trans-4MCHCA and nitrite were added to medium and stirred vigorously for three hours to ensure complete dissolution of trans-4MCHCA and nitrite. Following this the medium was purged with nitrogen gas for around 5 minutes before inoculation. This ensured the anoxic condition prevailed inside the serum bottle. The nitrogen gas was introduced to the medium through a nylon membrane with the pore diameter of 0.2 µm (VWR) to maintain the sterile conditions of the medium. The subculturing was carried out every 14 days. All batch, CSTR and biofilm reactor experiments were carried out using a 7 day old stock culture as inoculum.

McKinney's modified medium (Hill & Robinson, 1975; Paslawski *et al.*, 2009) was used throughout this research for the growth of the mixed culture and for conducting the biodegradation experiments. McKinney's modified medium has the following composition: KH₂PO₄ (840 mg L⁻¹), K₂HPO₄ (750 mg L⁻¹), (NH₄)₂SO₄ (474 mg L⁻¹), NaCl (60 mg L⁻¹), CaCl₂ (60 mg L⁻¹), MgSO₄.7H₂O (60 mg L⁻¹) and Fe(NH₄)₂(SO₄)₂.6H₂O (20 mg L⁻¹). Trace solution was added to the McKinney's modified medium at 0.1 % v/v ratio. Trace solution consists of: H₃BO₃ (600 mg L⁻¹), CoCl₃ (400 mg L⁻¹), ZnSO₄.7H₂O (200 mg L⁻¹), MnCl₂ (60 mg L⁻¹), NaMoO₄.2H₂O (60 mg L⁻¹), NiCl₂ (40 mg L⁻¹) and CuCl₂ (20 mg L⁻¹).

3.3 Anoxic Biodegradation of trans-4MCHCA with Nitrite in Batch System

Batch experiments were conducted to examine the microbial growth, biodegradation of trans-4MCHCA, and nitrite reduction kinetics. All batch experiments were carried out in 150 mL serum bottles as described previously. Three sets of experiments were carried out to examine the effects of three factors on the biodegradation process: 1)- effect of trans-4MCHCA initial concentration, 2)- effect of temperature, and 3)- inhibitory effect of nitrite.

Assuming that the final product of trans-4MCHCA oxidation is carbon dioxide and the final product of nitrite reduction is nitrogen gas, the anoxic biodegradation coupled with the reduction of nitrite can be described by Equation 3.1:



Using the stoichiometry of the reaction given above, theoretically 452.98 mg nitrite is required to biodegrade every 100 mg trans-4MCHCA. However, one should note that some trans-4MCHCA might be oxidized by residual oxygen in the system in which case less nitrite will be required for complete degradation of trans-4MCHCA.

3.3.1 Effect of trans-4MCHCA Initial Concentration

Effect of trans-4MCHCA initial concentration was studied using 100 and 250 mg L⁻¹ of trans-4MCHCA. These two concentrations were selected consistently with the previous research on trans-4MCHCA biodegradation with nitrate (Gunawan *et al.*, 2014). Sodium nitrite was added to the McKinney's modified medium containing trans-4MCHCA to provide the nitrite ions. The concentration of nitrite was adjusted based on the initial concentration of trans-4MCHCA. For the 100 mg L⁻¹ trans-4MCHCA, 90 mL McKinney's modified medium containing 100 mg L⁻¹ trans-4MCHCA and 460 mg L⁻¹ (10 mM) nitrite was added to a serum bottle. Three hours of vigorously stirring and 5 minutes of nitrogen gas purging were conducted before the inoculation.

10 mL of a 7-day old culture was used as the inoculum. For the 250 mg L⁻¹ trans-4MCHCA experiment, 80 mL McKinney's modified medium containing mg L⁻¹ trans-4MCHCA and 650 mg L⁻¹ (15 mM) nitrite was tested initially. However, results indicated that nitrite was not sufficient so another set of experiment with 250 mg L⁻¹ trans-4MCHCA was conducted with 828 mg L⁻¹ (18 mM) nitrite. All the serum bottles were maintained at room temperature (24 ± 2 °C). First sample (initial reading of optical density, residual trans-4MCHCA concentration and residual nitrite concentration) was taken immediately after the inoculation and the following samples were taken on daily basis. The optical density and the residual concentration of trans-4MCHCA were determined in these samples. Measurement of trans-4MCHCA was done in triplicates and the average value of the data and associated standard deviations were used to present the results. Higher concentrations of trans-4MCHCA (>250 mg L⁻¹) were not tested as concentrations higher than 250 mg L⁻¹ required nitrite at concentrations higher than 650 mg L⁻¹ which based on our preliminary tests imposed severe inhibition on microbial activity.

3.3.2 Effect of Temperature

Effect of temperature was studied using two temperature controlled environmental chambers to achieve different temperatures below and above the room temperature (24 ± 2 °C) including 10, 15, 20, 30 and 35 °C. All experiments were carried out in 150 mL serum bottles using McKinney's medium containing 90 mg L⁻¹ trans-4MCHCA and 460 mg L⁻¹ nitrite. The inoculum for experiments conducted at 20 and 30 °C was a seven-day old stock culture grown at room temperature (24 ± 2 °C). The resulting culture at 20 °C was used as inoculum in the experiment at 15 °C, and the culture developed at 15 °C was used as inoculum for experiments at 10 °C. In a similar manner the culture developed at 30 °C was used as inoculum for experiments at 35 °C. All the procedures including sampling, and analyses were similar to those described in the preceding section.

3.3.3 Inhibitory Effect of Nitrite

Inhibitory effect of nitrite was studied by varying the nitrite concentrations while maintaining the trans-4MCHCA concentration at 100 mg L^{-1} . The nitrite concentrations of 230, 690, 920 and 1150 mg L^{-1} were tested. All experiments were conducted at room temperature ($24 \pm 2 \text{ }^{\circ}\text{C}$) in 150 mL serum bottles. In the experiments with 230 and 690 mg L^{-1} nitrite 10 mL of a 7-day old culture grown on 100 mg L^{-1} trans-4MCHCA and 460 mg L^{-1} nitrite were used. The culture developed with 690 mg L^{-1} nitrite was used as inoculum in the experiments with 920 mg L^{-1} nitrite and the culture developed with 920 mg L^{-1} nitrite was used as inoculum in the experiment with 1150 mg L^{-1} nitrite. All the other procedures were similar to those described earlier.

3.3.4 Control Experiments

To assess the extent of abiotic oxidation of naphthenic acid, control experiments were conducted using McKinney's medium containing 100 mg L^{-1} trans-4MCHCA and 460 mg L^{-1} nitrite in the absence of inoculum. Experiments were carried out in a 150 mL serum and at room temperature. All the other procedures were similar to those described earlier (See Appendix E).

3.4 Anoxic Biodegradation of trans-4MCHCA with Nitrite in the Continuous Stirred Tank Reactor (CSTR)

3.4.1 Experimental Set-up for Biodegradation in Continuous Stirred Tank Reactor (CSTR)

Continuous stirred tank reactor (CSTR) used in this research was a glass vessel with diameter of 5.3 cm and height of 14.6 cm. There were two ports with the same diameter of 0.6 cm for the influent and the effluent on the upper part of the vessel. The bioreactor had a third port with the diameter of 1.6 cm in the middle for sampling. The working volume of the reactor was 200 mL. A magnetic stirrer was used to provide mixing inside the reactor and to keep the cells suspended. Feed was introduced into the reactor using a variable flow peristaltic pump. A schematic of the experimental system is shown in Figure 3.2. The reactor was run initially in the batch mode using McKinney's modified medium with 100 mg L^{-1} trans-4MCHCA and 460 mg L^{-1} nitrite.

Upon completion of the batch, indicated by a high and stable optical density and a zero concentration of trans-4MCHCA, the system was switched to continuous mode by pumping in McKinney's modified medium containing trans-4MCHCA (average concentration: 101.6 ± 5.4 mg L⁻¹) and nitrite (average concentration: 492.5 ± 14.8 mg L⁻¹) into the reactor. The feed had been purged by nitrogen gas before being used to maintain the anoxic condition in the system. The flow rate was initially set at 5 mL h⁻¹ and then increased at 5 to 10 mL h⁻¹ increments until the cell washout occurred (i.e. significant decrease in optical density and increase in residual trans-4MCHCA and nitrite concentrations). Overall 9 flow rates in the range of 5 to 71.3 mL h⁻¹ (5, 10.5, 15.8, 25.6, 35, 41.7, 50.8, 61, and 71.3 mL h⁻¹) were tested. Each flow rate was maintained until the system reached steady state condition. Steady state condition was assumed by stable readings in optical density, residual concentrations of trans-4MCHCA and nitrite for several consecutive samples. Once steady-state condition was established the reactor was maintained at the same flow rate for 2-3 days (or at least three sampling events) before increasing the flow rate to the next levels. Samples were taken following the same procedure described for the batch experiments and were analyzed for the biomass, residual trans-4MCHCA and residual nitrite concentrations. The average values of biomass, residual trans-4MCHCA and nitrite concentrations and associated standard deviations for these three samples were then calculated and used to present the results. Dilution rate (influent flow rate divided by the volume of the reactor), trans-4MCHCA loading rate (concentration of trans-4MCHCA in the feed times its corresponding dilution rate), trans-4MCHCA removal rate (the difference of influent and effluent trans-4MCHCA concentrations times the corresponding dilution rate), nitrite removal rate (the difference of influent and effluent nitrite concentrations times the corresponding dilution rate), trans-4MCHCA removal percentage (the difference of influent and effluent trans-4MCHCA concentrations divided by influent trans-4MCHCA concentration) and nitrite removal percentage (the difference of influent and effluent nitrite concentrations divided by influent nitrite concentration) were calculated and used in presenting the results.

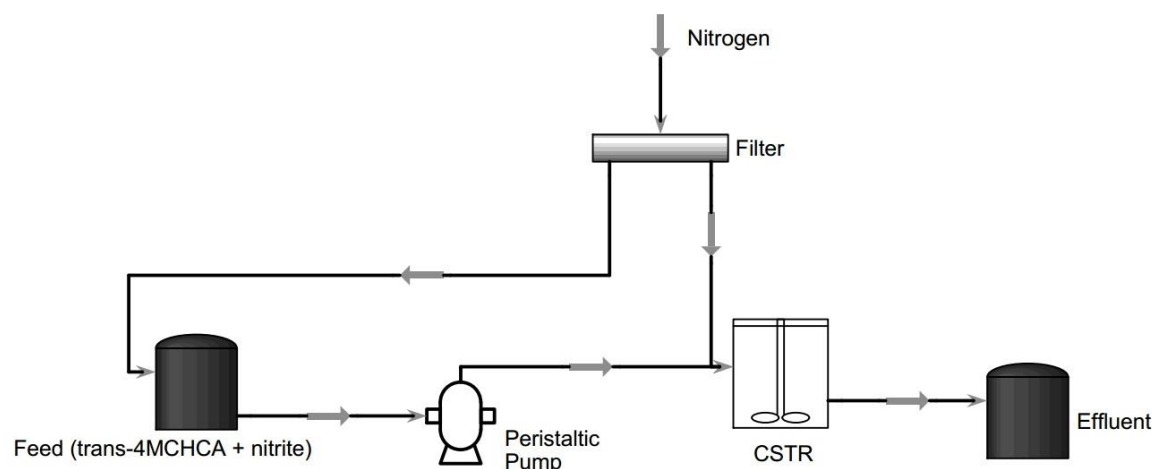


Figure 3.2 Schematic diagram of experimental set-up for biodegradation studies in the continuous stirred tank reactor (CSTR)

Two sets of control experiments were carried out in the CSTR: 1)- McKinney's modified medium containing 100 mg L^{-1} trans-4MCHCA and 460 mg L^{-1} nitrite with no inoculum was fed to the CSTR. Two different flow rates of 9.4 and 18.3 mL h^{-1} were tested in this negative control experiment and each flow rate was maintained for three days; 2)- McKinney's modified medium containing 100 mg L^{-1} trans-4MCHCA with no nitrite was fed to a CSTR which contained McKinney modified medium with 100 mg L^{-1} trans-4MCHCA and 460 mg L^{-1} nitrite inoculated with a seven-day old stock culture and already undergone batch biodegradation (i.e. CSTR contained bacterial population but trans-4MCHCA and nitrite were already consumed) to confirm that nitrite was required as the terminal electron acceptor and also to assess the extent of potential aerobic biodegradation, if any. One flow rate of 10.7 mL h^{-1} was tested in this negative control experiment and it was maintained for six days. All the procedures for sampling and analyses for these two control experiments were same as those described for the CSTR experiment (See Appendix E).

3.4.2 Biokinetics and the Associated Coefficients

Mass balances for substrate and biomass, as described below, together with the experimental data were used to determine the biokinetics coefficients for microbial growth and biodegradation. The

Monod expression was used to describe the microbial growth kinetics (Shuler and Kargi, 2002).

Data used in this section is presented in Appendix D.

Mass balance for the substrate:

$$QS_0 - QS - Vr_s = 0 \quad (3.2)$$

$$D = \frac{Q}{V} \quad (3.3)$$

$$r_s = \frac{Q(S_0 - S)}{V} = D(S_0 - S) \quad (3.4)$$

Also

$$r_s = -\frac{ds}{dt} = \frac{\frac{dx}{dt}}{Y} = \frac{\mu X}{Y} \quad (3.5)$$

$$D(S_0 - S) = \frac{\mu X}{Y} \quad (3.6)$$

$$X = \frac{DY(S_0 - S)}{\mu} \quad (3.7)$$

Mass balance for the biomass:

$$QX_0 - QX + Vr_x = 0 \quad (3.8)$$

Assuming negligible biomass in the feed stream:

$$X_0 = 0$$

$$r_x = \frac{QX}{V} = DX \quad (3.9)$$

$$r_x = \mu X - K_e X \quad (3.10)$$

$$DX = \mu X - K_e X \quad (3.11)$$

$$\mu = D + K_e \quad (3.12)$$

Substituting μ in Equation 3.7 with Equation 3.12:

$$X = \frac{DY(S_0 - S)}{D + K_e} \quad (3.13)$$

$$DY(S_0 - S) = DX + K_e X \quad (3.14)$$

$$\frac{(S_0 - S)D}{X} = \frac{D}{Y} + \frac{K_e}{Y} \quad (3.15)$$

Using the experimental data one can plot $\frac{(S_0 - S)D}{X}$ against D which results in a line where

slope of the line represents $\frac{1}{Y}$ and the intercept is $\frac{K_e}{Y}$.

$$\text{From Equation 3.12: } D = \mu - K_e \quad (3.16)$$

$$\text{Monod equation: } \mu = \frac{\mu_m S}{K_s + S} \quad (3.17)$$

$$D = \frac{\mu_m S}{K_s + S} - K_e \quad (3.18)$$

$$D + K_e = \frac{\mu_m S}{K_s + S} \quad (3.19)$$

$$\frac{\mu_m S}{D + K_e} = K_s + S \quad (3.20)$$

$$\frac{S}{D + K_e} = \frac{S}{\mu_m} + \frac{K_s}{\mu_m} \quad (3.21)$$

Using the experimental data one can plot $\frac{S}{D + K_e}$ against S which results in a line where slope

of the line represents $\frac{1}{\mu_m}$ and the intercept is $\frac{K_s}{\mu_m}$.

3.5 Anoxic Biodegradation of trans-4MCHCA with Nitrite in the Biofilm Reactor

The biofilm reactor was a glass vessel with the diameter of 4.4 cm and the height of 28.0 cm.

The influent port was at the bottom of the glass vessel with a diameter of 1.0 cm and the effluent port with the diameter of 1.2 cm was on the upper part of the glass vessel. Effluent port was also used for sampling. The sand particles which had the average diameter of 225 μm (mesh size: -50 to +70) were used as matrix for establishment of biofilm. Glass beads which had the average diameter of 1.0 cm, with a little sponge, were placed under the sands to support the sand particles. The working volume of the reactor was ~ 27 mL. The biofilm reactor had been set up during the previous work on anoxic biodegradation of trans-4MCHCA with nitrate experiment. A linear naphthenic acid, octanoic acid, and nitrate had been used as feed to develop the biofilm. McKinney's modified medium containing trans-4MCHCA (concentration: 53.9 ± 5.9 mg L⁻¹) and nitrite (498.9 ± 16.6 mg L⁻¹) was fed into the reactor by a peristaltic pump at the beginning of the current experiments. The trans-4MCHCA concentration was consistent with previous nitrate experiment (Gunawan *et al.*, 2014) to make it easier to compare the performance of the system with nitrate and nitrite. Figure 3.3 shows the biofilm reactor set-up. The feed was purged by nitrogen gas before being used to ensure the anoxic condition in the system. The flow rate was initially set at 2.5 mL h⁻¹ and then increased at 5 to 10 mL h⁻¹ increments until the maximum treatment capacity was achieved (i.e. significant increase in residual trans-4MCHCA and nitrite concentrations). Overall 11 flow rates in the range of 2.5 to 132 mL h⁻¹ (2.5, 5, 11.5, 23, 41, 56.7, 71.3, 87, 107, 120 and 132 mL h⁻¹) were tested. Each flow rate was maintained until the system reached steady state conditions. Steady state conditions were assumed by relatively constant values of residual trans-4MCHCA and nitrite concentrations over several consecutive sampling events. Once steady-state conditions established the reactor was maintained at the same flow rate for 2-3 days (or at least three sampling events) before increasing the flow rate to the next levels. Samples were taken following the same procedure described for the batch experiments and were analyzed for the residual trans-4MCHCA and residual nitrite concentrations. The average values of residual trans-4MCHCA and nitrite concentrations and associated standard deviations for these three samples were then calculated and used to present the results. The trans-4MCHCA loading rate, trans-4MCHCA removal rate, nitrite removal rate, trans-4MCHCA removal

percentage and nitrite removal percentage were also calculated and used in the same way as previously described for the CSTR experiments.

As part of the experimental runs and to examine the effect of trans-4MCHCA concentration, experiments with higher trans-4MCHCA concentrations ($105.3 \pm 1.8 \text{ mg L}^{-1}$ and $253.6 \pm 5.9 \text{ mg L}^{-1}$ respectively) experiments were also conducted after finishing the run with $53.9 \pm 5.9 \text{ mg L}^{-1}$ trans-4MCHCA and $498.9 \pm 16.6 \text{ mg L}^{-1}$ nitrite. For the $105.3 \pm 1.8 \text{ mg L}^{-1}$ trans-4MCHCA and $471.6 \pm 12.9 \text{ mg L}^{-1}$ nitrite experiment, overall 7 flow rates in the range of 13.4 to 106.7 mL h^{-1} (13.4, 40.3, 49.0, 64.2, 83.0, 100.7 and 106.7 mL h^{-1}) were tested, while for experiments with $253.6 \pm 5.9 \text{ mg L}^{-1}$ trans-4MCHCA and $814.6 \pm 18.2 \text{ mg L}^{-1}$ nitrite, overall 6 flow rates in the range of 10.8 to 49 mL h^{-1} (10.8, 17.5, 21.3, 24.6, 28.0 and 49.0 mL h^{-1}) were tested.

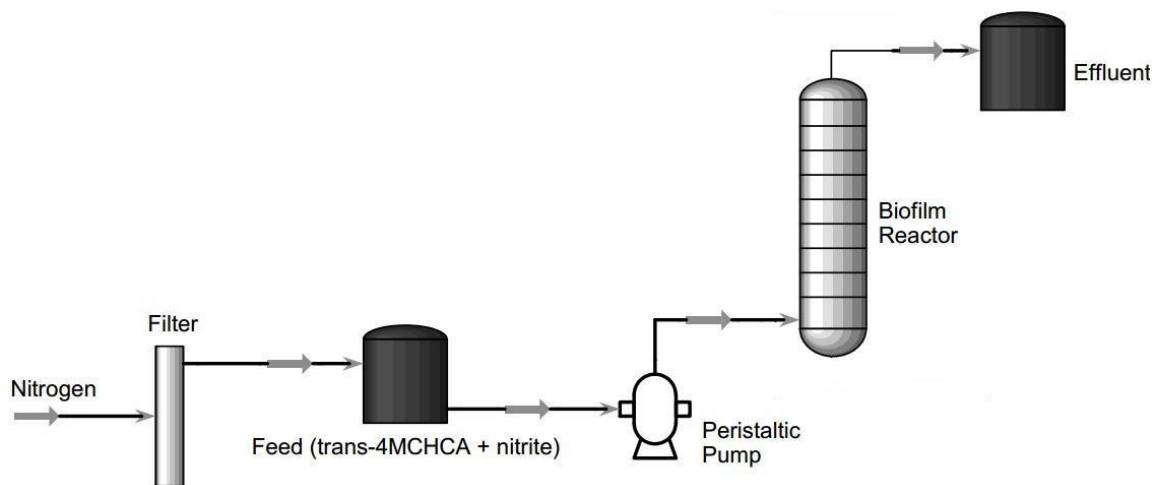


Figure 3.3 Schematic diagram of experimental set-up of the biofilm system

3.6 Analytical Methods

3.6.1 Trans-4MCHCA Concentration

Based on the earlier research (Gunawan *et al.*, 2014), gas chromatograph (GC) with flame ionization detector (GC-FID) was selected to analyze the trans-4MCHCA concentration. The gas chromatograph was a Varian-430 GC with a J&W DB-FFAP column. The GC column had the

following specifications: length: 15 m, inside diameter: 0.53 mm and film thickness: 1 μm . Helium (He) was used as the carrier gas. The system was operated under the following conditions: H_2 flow rate of 30 mL min^{-1} ; He flow rate of 16 mL min^{-1} ; air flow rate of 300 mL min^{-1} , injector splitless, injector and detector temperatures of 250°C . The column oven had initial temperature of 40°C which then was increased to 200°C at a rate of $10^\circ\text{C min}^{-1}$. The run time of the system, for each injection, was 16 minutes. Samples were taken from the batch, CSTR and biofilm reactors using a glass hypodermic syringe with a stainless steel needle. The solution inside the syringe was then filtered using a stainless steel cartridge with a $0.22 \mu\text{m}$ pore diameter nylon membrane filter (GE magna) placed inside the stainless steel cartridge. Filtered solution was collected using 2 mL transparent vials and analyzed immediately to determine the trans-4MCHCA concentration. Samples were analyzed in triplicate, where each sample had injection volume of $1.0 \mu\text{L}$. Three injections of Millipore water at the beginning of the GC analysis sequence and between every three to four samples were made to prevent the possible accumulation of the trans-4MCHCA in the column. All the samples were stored immediately in the -80°C freezer after being analyzed for possible future re-analysis. The retention time of trans-4MCHCA was 14.01 ± 0.5 minutes. The trans-4MCHCA calibration curve was made using six standard solutions (10, 20, 40, 60, 80 and 100 mg L^{-1} trans-4MCHCA in sterile modified McKinney's medium). The correlation coefficient of the calibration curve was 99.8 % (See Appendix A1).

3.6.2 Nitrite Concentration

Nitrite concentration was determined using a Dionex ICS-2500 ion chromatograph (IC) with a conductivity detector (CD25A). The analytical column used was IonPac AS11-HC with its guard column selected as IonPac AG11-HC. The KOH eluent gradient was initially at 12.0 mM and then ramped to 37.0 mM . The eluent flow rate was at 1.0 mL h^{-1} . The injection volume of each sample was $25.0 \mu\text{L}$. Filtered samples were firstly diluted 10 times by mixing $100 \mu\text{L}$ of the sample solution with $900 \mu\text{L}$ Millipore water. They were then further diluted 4 times by mixing

250 μL of the diluted solution with 750 μL Millipore water. This was necessary to ensure the final nitrite concentration fitted in the desired ion chromatograph calibration range. Calibration of the ion chromatograph was made using standard nitrite solutions with concentrations ranging from 0 to 25 mg L^{-1} (0, 5, 10, 15, 20, and 25 mg L^{-1}). The average retention time for nitrite was 4.5 ± 0.1 minutes. The correlation coefficient for the nitrite calibration curve was 99.3 % (See Appendix A2).

3.6.3 Biomass Measurement

Optical density (OD) was measured as a representative of biomass in the samples using a Mini Shimadzu (model 1240) ultraviolet (UV) spectrophotometer at a wavelength of 620 nm. The clear modified McKinney's media was used as blank. Samples were tested in triplicate. A calibration curve between optical density and cell dry weight (biomass concentration) was developed at the end of the experiment. The correlation coefficient for the calibration curve was 99.9 % (See Appendix A3).

3.6.4 Reproducibility and Data Uncertainty

Some of the batch experiments were carried out more than once to determine the reproducibility of the results. In the continuous experiments (CSTR and biofilm system), at least three samples were taken over an extended period equal to three to five residence times following the establishment of steady state conditions at each flow rate. The average value of the biomass, nitrite and trans-4MCHCA concentrations in the repeated samples and/or multiple analyses, and the associated standard deviations were used to present the results.

CHAPTER 4 RESULTS AND DISCUSSION

Biodegradation of trans-4MCHCA and denitrification (nitrite reduction) were carried out in both batch and continuous systems. The effects of initial concentration of trans-4MCHCA, temperature and the inhibitory effect of nitrite on biodegradation and denitrification were examined in the batch system. The effects of concentration and volumetric loading rate of trans-4MCHCA on its biodegradation and removal rate of nitrite were studied in continuous stirred tank reactor (CSTR) and biofilm system. This chapter presents the results of these studies and compares the results obtained with nitrite as an electron acceptor with those achieved with nitrate as part of an earlier reported work (Gunawan *et al.*, 2014).

4.1 Batch Biodegradation of trans-4MCHCA with Nitrite

Batch experiments of anoxic biodegradation of trans-4MCHCA were carried out to examine the effects of three variables: A) initial concentration of trans-4MCHCA, B) temperature, and C) inhibitory effect of nitrite.

4.1.1 Effect of trans-4MCHCA Initial Concentration

Biodegradation of trans-4MCHCA and denitrification were studied using 100 and 250 mg L⁻¹ of trans-4MCHCA with 460 and 640/828 mg L⁻¹ of nitrite, respectively. Profiles of trans-4MCHCA and nitrite concentrations observed in these experiments are shown in Figure 4.1.

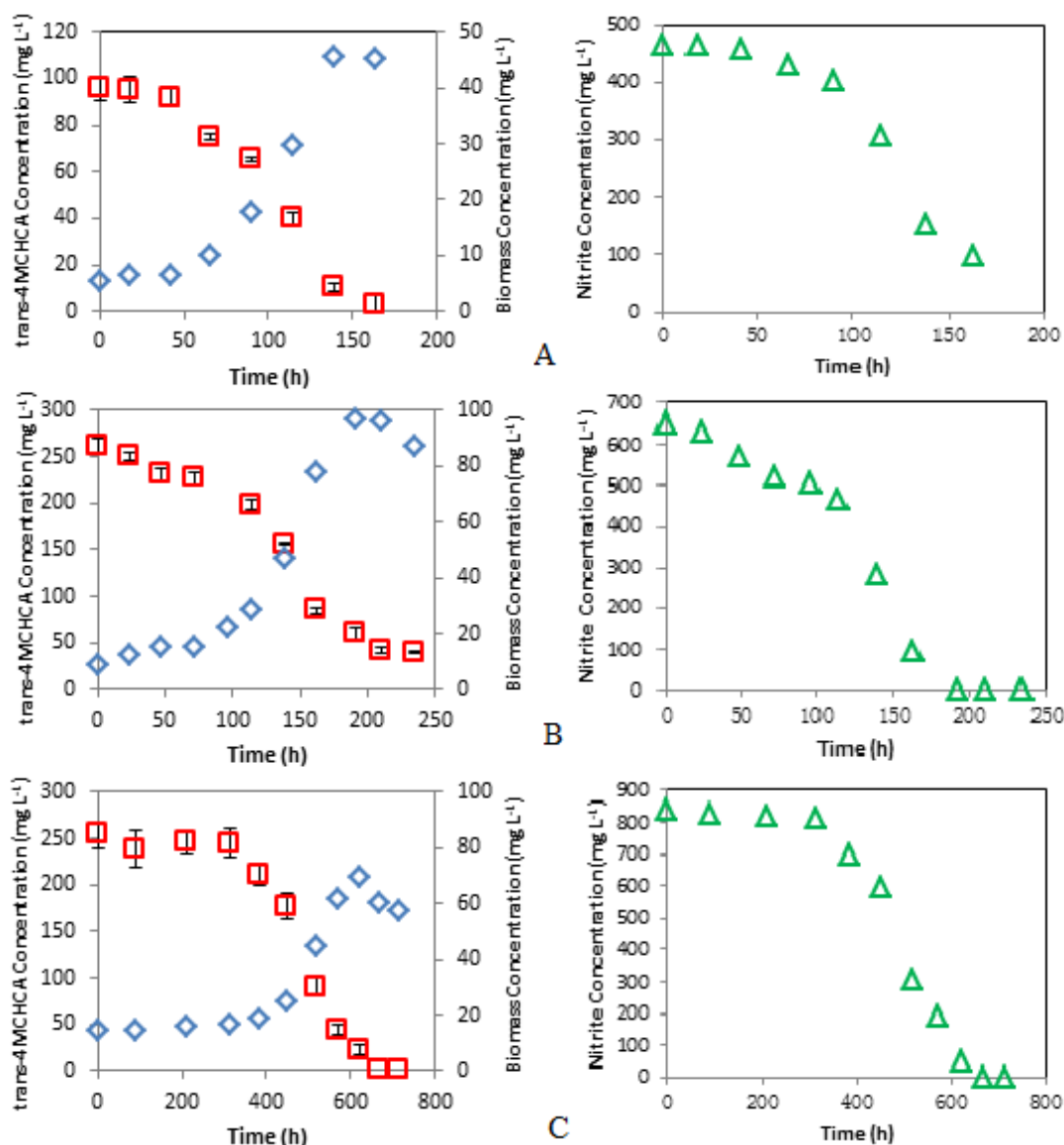


Figure 4.1 Biomass growth, trans-4MCHCA biodegradation and nitrite reduction observed with various initial concentrations of trans-4MCHCA at room temperature (24 ± 2 °C). Panel (A): 100 mg L⁻¹ trans-4MCHCA and 460 mg L⁻¹ nitrite, Panel (B): 250 mg L⁻¹ trans-4MCHCA and 690 mg L⁻¹ nitrite and Panel (C): 250 mg L⁻¹ trans-4MCHCA and 828 mg L⁻¹ nitrite. The error bars represent the standard deviations of multiple tests on each sample taken from the system and they may not be visible in some cases. \diamond Biomass concentration; \square trans-4MCHCA concentration; \triangle Nitrite ion concentration.

As seen an increase in trans-4MCHCA concentration from 100 mg L⁻¹ to 250 mg L⁻¹ resulted in longer lag phase in microbial activity, as well as an increase in final biomass concentration. The initial concentration of nitrite, added to the system as an electron acceptor, was adjusted based on

the initial concentration of trans-4MCHCA. The above biodegradation profiles show that once cells started to grow (increase in biomass concentration), trans-4MCHCA concentration declined, coupled with decrease in nitrite concentration. Figure 4.1 (A) shows that 460 mg L⁻¹ nitrite was in excess for biodegradation of 100 mg L⁻¹ trans-4MCHCA. The maximum biomass concentration observed was around 45 mg L⁻¹ and observed when trans-4MCHCA concentration decreased to zero at around 163 h. The corresponding residual nitrite concentration was around 99 mg L⁻¹. With 250 mg L⁻¹ trans-4MCHCA, an initial nitrite concentration of 640 mg L⁻¹ was not sufficient and a residual trans-4MCHCA concentration of 40 mg L⁻¹ was observed (Figure 4.1 (B)). This confirmed the coupling of biodegradation and nitrite reduction and that when nitrite was not sufficient, biodegradation of trans-4MCHCA did not proceed (i.e. concentration remained constant), and biomass concentration started to decline. The maximum biomass concentration observed in this experiment was around 97 mg L⁻¹ and observed at around 192 h. The repeat of this experiment with a higher level of nitrite (828 mg L⁻¹) resulted in complete biodegradation of 250 mg L⁻¹ trans-4MCHCA (Figure 4.1 (C)). However, due to the inhibitory effect of nitrite on biodegradation process, an extended lag phase and a marked increase in biodegradation time were observed. Complete biodegradation in this case took around 713 h and the maximum biomass concentration at around 624 h was 69 mg L⁻¹. The results obtained in these two experiments further confirmed that the reduction of nitrite ions was coupled with biodegradation (oxidation) of trans-4MCHCA, whereby the presence of sufficient nitrite led to complete biodegradation of trans-4MCHCA. Experiments with higher concentration of trans-4MCHCA were not carried out as higher concentration of trans-4MCHCA needed higher level of nitrite which based on our experimental observation would have imposed a severe inhibition on microbial activity and biodegradation. As indicated earlier and as shown in Figure 4.1 (C), increase in initial nitrite concentration resulted in longer lag phase in the system (an indication of adaptation period of microorganisms). A lag phase of around 312 h was observed with 828 mg L⁻¹ (Figure 4.1 (C)) nitrite compared with almost no or much shorter lag phases with 460 mg L⁻¹ nitrite (Figure 4.1 (A)) and 690 mg L⁻¹ nitrite (Figure 4.1 (B)), respectively.

Biodegradation rates of trans-4MCHCA and reduction rates of nitrite were calculated using the slopes of the linear parts of trans-4-MCHCA and nitrite concentration profiles (lag phases and stationary phases were excluded) for different initial trans-4-MCHCA and nitrite concentrations and shown in Table 4.1.

Table 4.1 Effect of trans-4MCHCA initial concentration on biodegradation rate of trans-4MCHCA and reduction rate of nitrite

Trans-4MCHCA Concentration (mg L ⁻¹)	Nitrite Concentration (mg L ⁻¹)	Biodegradation Rate of trans-4MCHCA (mg L ⁻¹ h ⁻¹)	Reduction Rate of Nitrite (mg L ⁻¹ h ⁻¹)
100	460	0.81 (0.96)*	3.03 (0.87)*
250	640	1.10 (0.94)*	3.45 (0.89)*
250	828	0.75 (0.98)*	2.49 (0.98)*

*The number in the parentheses represents R² values.

As seen in Table 4.1, the biodegradation rate of trans-4MCHCA and reduction rate of nitrite at 100 mg L⁻¹ trans-4-MCHCA with 460 mg L⁻¹ nitrite were close to that obtained with 250 mg L⁻¹ trans-4-MCHCA with 828 mg L⁻¹ nitrite, while the biodegradation rate of trans-4MCHCA and reduction rate of nitrite for 250 mg L⁻¹ trans-4MCHCA with 640 mg L⁻¹ nitrite were higher (1.1 mg L⁻¹ h⁻¹ and 3.5 mg L⁻¹ h⁻¹ respectively). Although increase in trans-4MCHCA concentration from 100 mg L⁻¹ to 250 mg L⁻¹ with 640 mg L⁻¹ nitrite increased both the biodegradation rate and the reduction rate, the biodegradation was incomplete due to absence of sufficient nitrite. When nitrite concentration was increased to 828 mg L⁻¹, the biodegradation was complete but both the biodegradation and the nitrite reduction rates became slower due to the inhibitory effect of nitrite at high concentration.

4.1.2 Effect of Temperature

The effect of temperature on biodegradation of trans-4MCHCA and reduction of nitrite was also

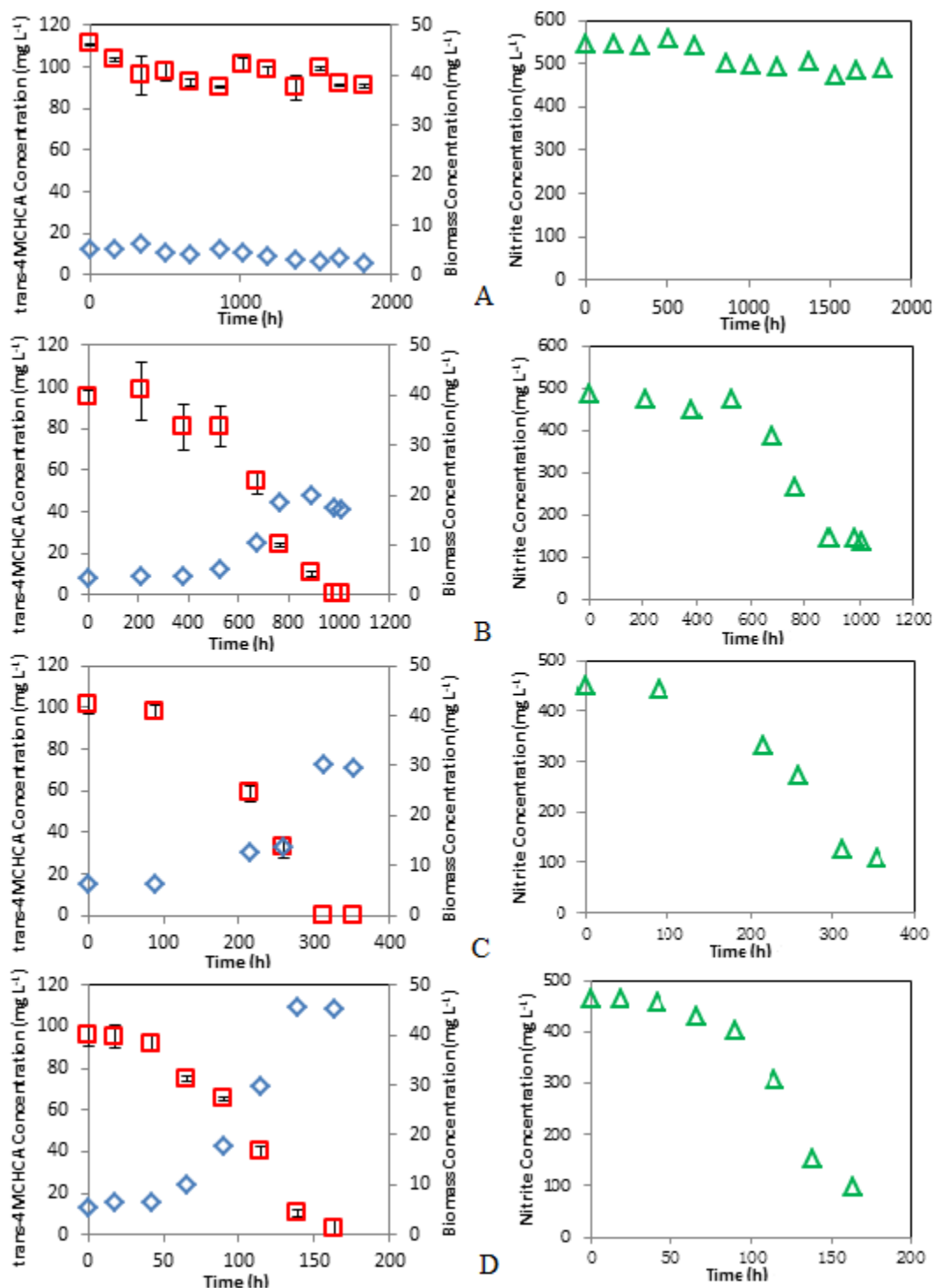
examined. These experiments were carried out at six different temperatures ranging from 10 to 35 °C, with the same initial trans-4-MCHCA and nitrite concentrations of 100 and 460 mg L⁻¹, respectively. Profiles of trans-4-MCHCA and nitrite concentrations observed in these experiments are shown in Figure 4.2. Temperature is considered to be one of the important factors affecting the biodegradation. As seen in Figure 4.2, except for a temperature of 10 °C (Figure 4.2 (A)), decrease in both trans-4-MCHCA and nitrite concentrations and increase in biomass concentration were observed due to microbial activity for all other tested temperature. The results showed an optimum temperature range of 24 ± 2 to 30 °C (Figure 4.2 (D) and (E)). Application of a high temperature of 35 °C (Figure 4.2 (F)) and low temperatures of 15 and 20 °C, (Figures 4.2 (B) and 4.2 (C)) negatively impacted the biodegradation process. This was clear from increase of lag phase and total biodegradation time, as well as the decrease in maximum biomass concentration. The maximum biomass concentrations at 24 and 30 °C were around 45 mg L⁻¹ (Figure 4.2 (D)) and 41 mg L⁻¹ (Figure 4.2 (E)) respectively, while values of 20, 30 and 32 mg L⁻¹ were observed at 15, 20 and 35 °C, respectively. Moreover, the increases in lag phases and the time required for complete biodegradation further confirmed that the optimum temperature for microbial activity and biodegradation was in the range 24 to 30 °C (see Table 4.2 for comparison of the data).

Table 4.2 Effect of temperature on lag phase and complete biodegradation time

Temperature (°C)	Lag Phase (h)	Complete Biodegradation Time (h)	Maximum Biomass Concentration (mg L ⁻¹)
10	N/A	N/A	N/A
15	215	980	20
20	20	312	30
24 ± 2	~ 0	163	45
30	39	164	41
35	96	310	32

It also should be pointed out that negative impact of temperatures outside the optimum range was

more severe when temperatures below the optimum range were used. As shown in Figure 4.2 (A), at 10 °C no microbial activity was observed as it is evident from the relatively constant trans-4MCHCA, nitrite and biomass concentrations over an extended period of 1823 h.



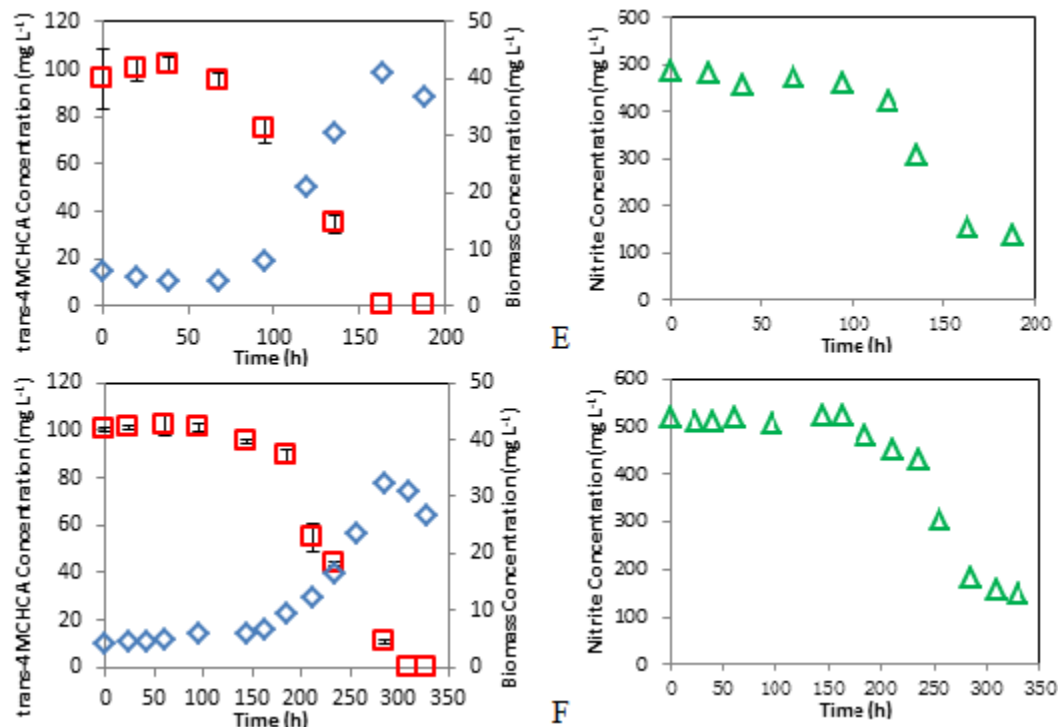


Figure 4.2 Biomass growth, trans-4MCHCA biodegradation and nitrite reduction observed for 100 mg L⁻¹ of trans-4MCHCA and 460 mg L⁻¹ of nitrite at various temperatures. Panel (A) 10 °C, Panel (B) 15 °C, Panel (C) 20 °C, Panel (D) 24 ± 2 °C, Panel (E) 30 °C and Panel (F) 35 °C. The error bars represent the standard deviations of multiple tests on each sample taken from the system and they may not be visible in some cases. ♦ Biomass concentration; □ trans-4MCHCA concentration; △ Nitrite ion concentration.

Using the slopes of the linear parts of trans-4-MCHCA and nitrite concentration profiles (lag phase and stationary phase were excluded), the biodegradation and nitrite reduction rates were calculated at different temperatures and presented in Table 4.3.

Table 4.3 Effect of temperature on biodegradation rate of trans-4MCHCA and nitrite reduction rate

Temperature (°C)	Biodegradation Rate of trans-4MCHCA (mg L ⁻¹ h ⁻¹)	Reduction Rate of Nitrite (mg L ⁻¹ h ⁻¹)
10	N/A	N/A
15	0.1 (0.94)*	0.5 (0.84)*
20	0.4 (0.96)*	1.3 (0.91)*
24 ± 2	0.8 (0.96)*	3.0 (0.87)*
30	0.8 (0.96)*	3.4 (0.85)*
35	0.5 (0.93)*	1.9 (0.81)*

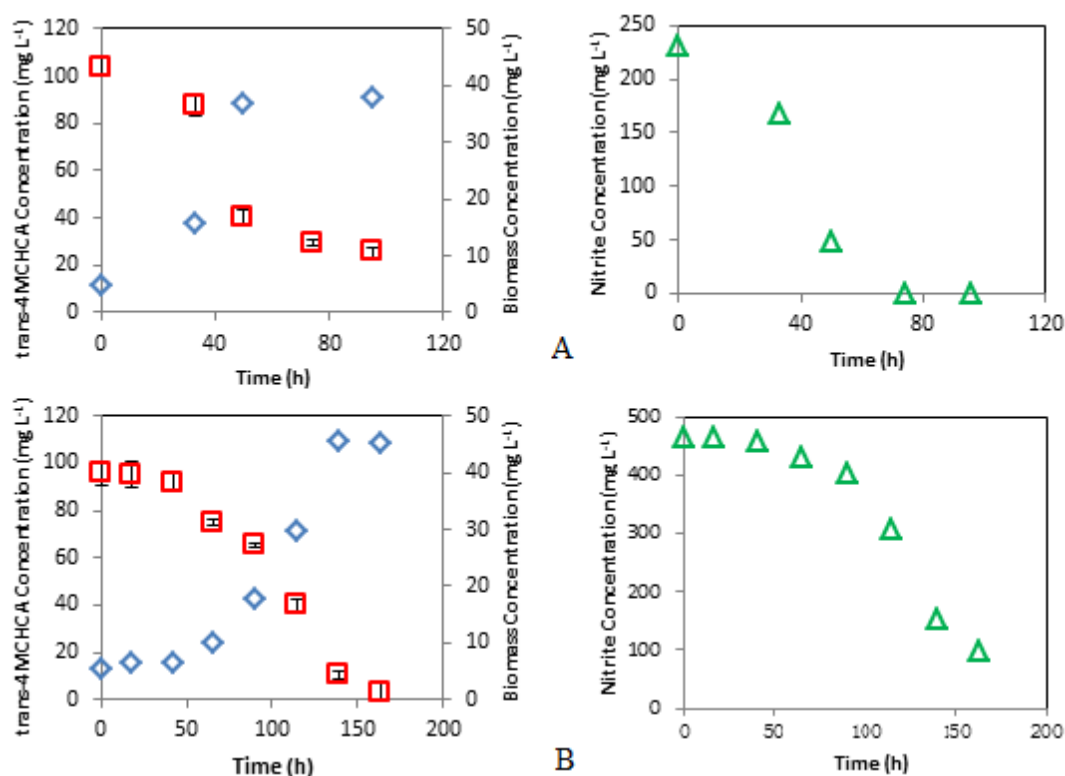
*The number in the parentheses represents R² values.

The highest biodegradation rate of trans-4MCHCA was 0.8 mg L⁻¹ h⁻¹ and observed at 30 °C, with the corresponding nitrite reduction rate (also the highest value) being 3.4 mg L⁻¹ h⁻¹. The trans-4MCHCA biodegradation rate and the nitrite deduction rate at 24 ± 2 °C were 0.8 mg L⁻¹ h⁻¹ and 3.0 mg L⁻¹ h⁻¹, respectively. Higher and lower temperatures decreased both biodegradation and nitrite reduction rates, confirming that the optimum tempertraure range was 24 to 30 °C. Similar trends in dependency of biodegradation and nitrite reduction rates on temperature were clear indication of biodegradation and nitrite reduction coupling.

4.1.3 Inhibitory Effect of Nitrite

To assess the potential inhibitory effect of nitrite on the biodegradation process which was evident from longer time required for biodegradation of 250 mg L⁻¹ trans-4MCHCA with 828 mg L⁻¹ nitrite when compared with that in the presence of 640 mg L⁻¹ nitrite, biodegradation experiments with 100 mg L⁻¹ trans-4MCHCA and five different initial nitrite concentrations were carried out at room temperature. An initial concentration of 100 mg L⁻¹ was selected because of the comparatively shorter time required for complete biodegradation. Initial nitrite concentrations tested were 230, 460, 690, 920 and 1150 mg L⁻¹. Profiles of biodegradation and nitrite reduction for these experiments are shown in Figure 4.3. Increase of lag phase and

biodegradation time was observed as a result of increase in nitrite concentration. As shown in Figures 4.3 (A) and (B), at lower nitrite concentrations of 230 and 460 mg L⁻¹ no lag phases were detected, while the lag phases of 67 h, 48 h and 137 h were observed with 690 mg L⁻¹ (Figure 4.3 (C)), 920 mg L⁻¹ (Figure 4.3 (D)) and 1150 mg L⁻¹ (Figure 4.3 (E)) nitrite, respectively. Decrease of biomass yield was also observed with the increase of nitrite concentration. The highest biomass concentrations with 230 mg L⁻¹ (Figure 4.3 (A)), 460 mg L⁻¹ (Figure 4.3 (B)), 690 mg L⁻¹ (Figure 4.3 (C)), 920 mg L⁻¹ (Figure 4.3 (D)) and 1150 mg L⁻¹ (Figure 4.3 (E)) nitrite were 53, 46, 31, 33 and 29 mg L⁻¹, respectively.



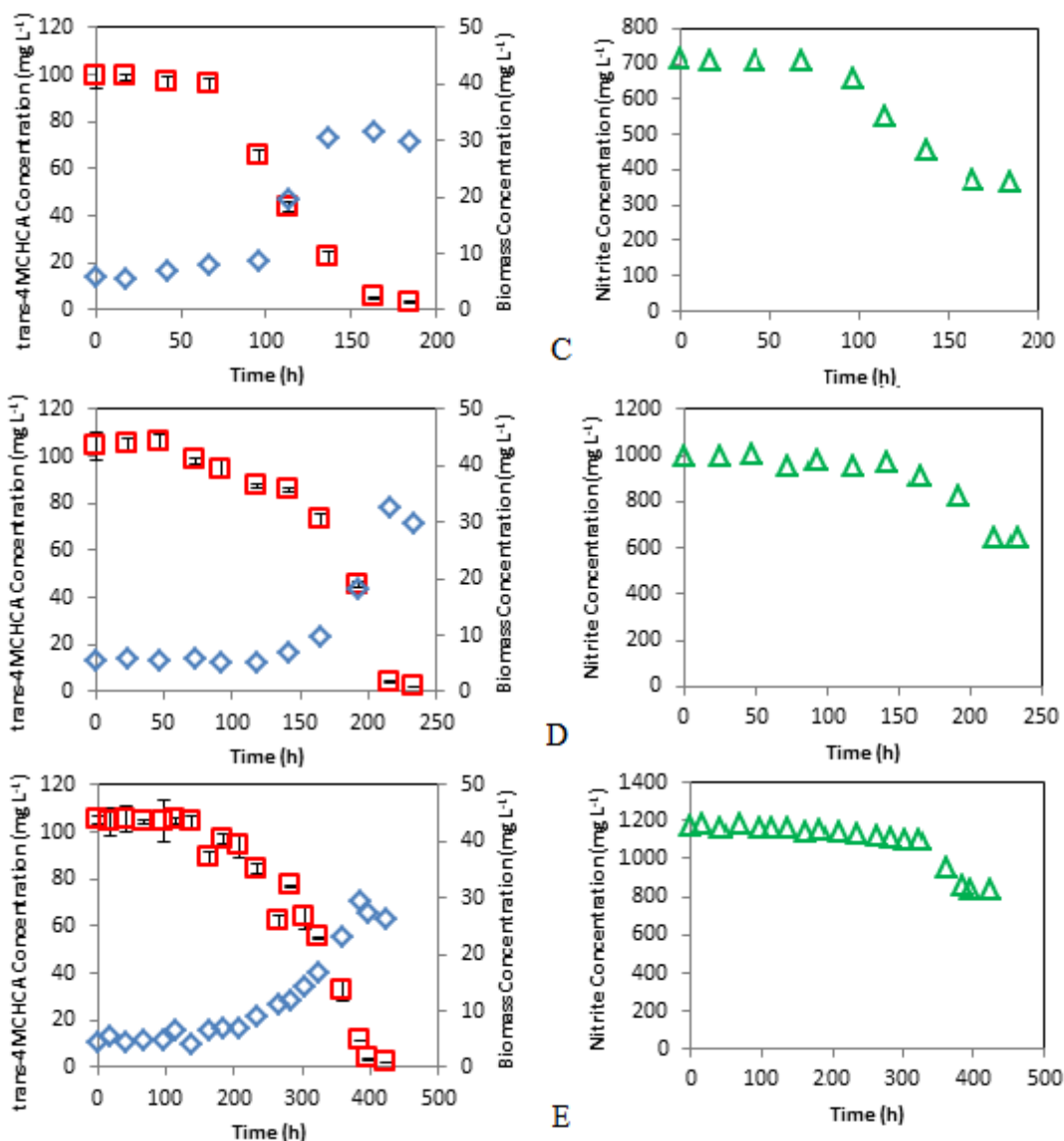


Figure 4.3 Biomass growth, trans-4MCHCA biodegradation and nitrite reduction patterns observed with 100 mg L⁻¹ of trans-4MCHCA with various nitrite concentrations at room temperature (24 ± 2 °C). Panel (A) 100 mg L⁻¹ trans-4MCHCA and 230 mg L⁻¹ nitrite, Panel (B) 100 mg L⁻¹ trans-4MCHCA and 460 mg L⁻¹ nitrite, Panel (C) 100 mg L⁻¹ trans-4MCHCA and 690 mg L⁻¹ nitrite, Panel (D) 100 mg L⁻¹ trans-4MCHCA and 920 mg L⁻¹ nitrite and Panel (E) 100 mg L⁻¹ trans-4MCHCA and 1150 mg L⁻¹ nitrite. The error bars represent the standard deviations of multiple tests on each sample taken from the system and they may not be visible in some cases. ◇ Biomass concentration; □ trans-4MCHCA concentration; △ Nitrite ion concentration.

As shown in Figure 4.3, increase of initial trans-4MCHCA concentration in the range 230 mg L⁻¹ to 460 mg L⁻¹ did not affect the biodegradation rate of trans-4MCHCA or reduction rate of nitrite.

Nitrite at concentration up to 690 mg L⁻¹ did not have a marked inhibitory effect but concentrations above 920 mg L⁻¹ imposed a strong inhibitory effect. Figure 4.3 (A) shows that with 230 mg L⁻¹ nitrite and 100 mg L⁻¹ trans-4MCHCA biomass concentration went up to around 53 mg L⁻¹ but the lack of nitrite ions as electron acceptors led to incomplete biodegradation and a residual trans-4MCHCA concentration of around 25 mg L⁻¹ was observed at the end of the experiment when nitrite concentration decreased to zero. Data presented in Figure 4.3 (B) revealed that application of 460 mg L⁻¹ nitrite resulted in complete biodegradation. Further increase in nitrite concentration caused a much stronger inhibitory effect on biodegradation process (Figures 4.3 (C, D and E)). Using the slopes of the linear parts of trans-4-MCHCA and nitrite concentration profiles, the biodegradation and nitrite reduction rates at different nitrite concentrations were calculated and presented in Table 4.4.

Table 4.4 Effect of nitrite concentration on biodegradation rate of trans-4MCHCA and nitrite reduction rate

Nitrite Concentration (mg L ⁻¹)	Biodegradation Rate of trans-4MCHCA (mg L ⁻¹ h ⁻¹)	Reduction Rate of Nitrite (mg L ⁻¹ h ⁻¹)
230	1.08 (0.89)*	3.30 (0.94)*
460	0.81 (0.96)*	3.03 (0.87)*
690	0.70 (0.93)*	2.45 (0.86)*
920	0.52 (0.82)*	1.69 (0.70)*
1150	0.36 (0.90)*	1.15 (0.73)*

*The number in the parentheses represents R² values.

As seen in this table the maximum biodegradation rate of trans-4MCHCA and reduction rate of nitrite (1.1 mg L⁻¹ h⁻¹ and 3.3 mg L⁻¹ h⁻¹) were observed with the lowest nitrite concentration of 230 mg L⁻¹, although this amount of nitrite was not sufficient to fully biodegrade 100 mg L⁻¹ trans-4MCHCA. Both trans-4MCHCA biodegradation rate and nitrite reduction rate decreased with further increase in nitrite concentration.

4.2 Continuous Biodegradation of trans-4MCHCA with Nitrite in Stirred Tank Reactor

4.2.1 Effect of trans-4MCHCA Loading Rate

The effect of volumetric loading rate of trans-4MCHCA on its biodegradation and reduction of nitrite was examined in the CSTR at room temperature (24 ± 2 °C). According to the results obtained from batch experiments, initial concentrations of trans-4MCHCA and nitrite were set at 100 mg L^{-1} and 460 mg L^{-1} respectively. Residual trans-4MCHCA and nitrite concentrations were monitored on a regular basis to assess the performance of the CSTR under different trans-4MCHCA volumetric loading rates. The bioreactor was initially operated in batch mode to increase the bacteria population (biomass concentration). Following the completion of the batch (complete biodegradation of trans-4MCHCA) the CSTR was switched to continuous mode by feeding it with modified McKinney's medium containing $101.6 \pm 5.4 \text{ mg L}^{-1}$ trans-4MCHCA and $492.5 \pm 14.8 \text{ mg L}^{-1}$ nitrite at a flow rate of 5 mL h^{-1} (corresponding trans-4MCHCA loading rate: $2.7 \text{ mg L}^{-1} \text{ h}^{-1}$; residence time: 40 h). When steady state was reached, flow rate was then increased incrementally (5 to 10 mL h^{-1} increase) until cell wash out occurred. Figures 4.4 and 4.5 show the dependency of the residual trans-4MCHCA, nitrite and biomass concentrations on the dilution rate. The increase in dilution rate led to increases in residual trans-4MCHCA and nitrite concentrations. As seen in Figure 4.4, up to the dilution rate of around 0.1 h^{-1} , residual trans-4MCHCA concentration was low ($<4 \text{ mg L}^{-1}$); the biomass concentration passed through a maximum value of around 66 mg L^{-1} at the dilution rate of 0.1 h^{-1} and then started to decrease. Increase of the residual trans-4MCHCA and nitrite concentrations and decrease in the biomass concentration were observed with further increase of the dilution rate. As shown in Figures 4.4 and 4.5, cell wash-out occurred at a dilution rate of 0.4 h^{-1} where the residual trans-4MCHCA and nitrite concentrations were 95 mg L^{-1} and 475 mg L^{-1} , respectively, which were quite close to the respective concentrations in the feed (trans-4MCHCA and nitrite concentrations at $101.6 \pm 5.4 \text{ mg L}^{-1}$ and $492.5 \pm 14.8 \text{ mg L}^{-1}$, respectively). The corresponding biomass concentration at this dilution rate was around 3.7 mg L^{-1} . It should be pointed out that the wash-out occurred gradually and not as a sudden phenomenon.

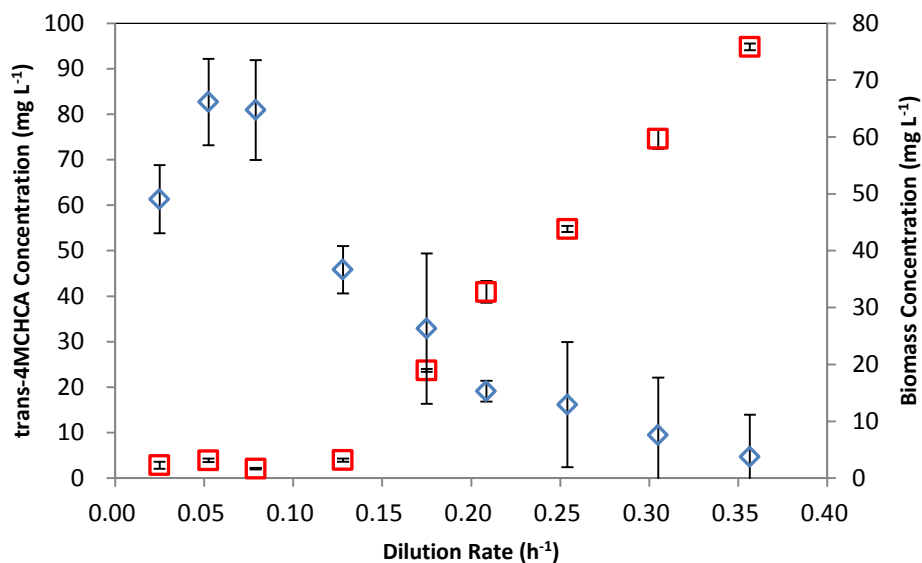


Figure 4.4 Steady-state profiles of trans-4MCHCA and biomass concentrations observed in continuous stirred tank reactor (CSTR). Values reported are the average data for multiple samplings of the reactor over an extended period equal to three to five residence times after the establishment of steady state. Error bars represent the standard deviations and might not be visible in some cases. \square trans-4MCHCA residual concentration; \diamond biomass concentration.

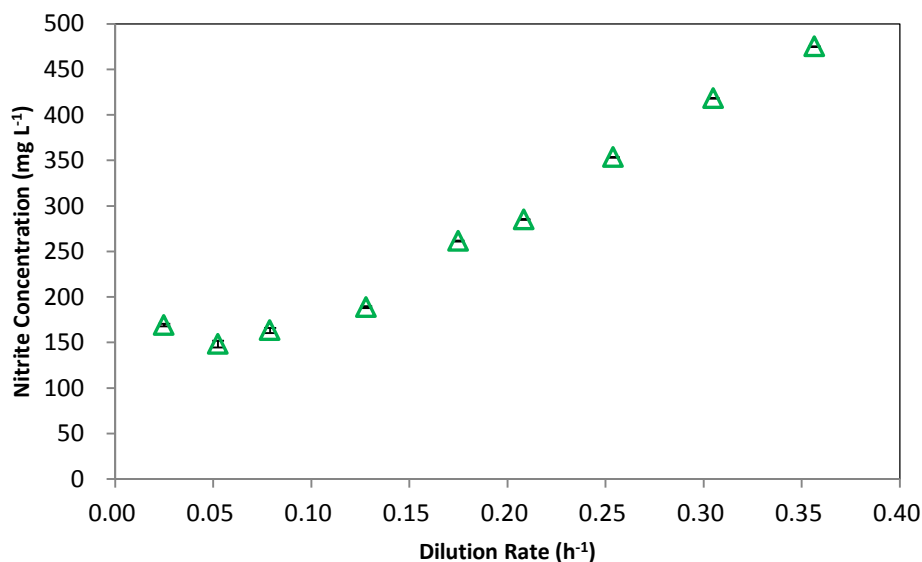


Figure 4.5 Steady-state profiles of nitrite concentration observed in the continuous stirred tank reactor (CSTR). Values reported are the average data for multiple samplings of the reactor over an extended period equal to three to five residence times after the establishment of steady state. Error bars represent the standard deviations and might not be visible in some cases. \triangle nitrite concentration.

Figure 4.6 shows the dependency of trans-4MCHCA removal rate and its removal percentage on trans-4MCHCA loading rate in the CSTR. The dependency of nitrite removal rate and its removal percentage on trans-4MCHCA loading rate is shown in Figure 4.7. Generally the removal percentages for both trans-4MCHCA and nitrite decreased with the increase of trans-4MCHCA loading rate. Up to the trans-4MCHCA loading rate of $12.6 \text{ mg L}^{-1} \text{ h}^{-1}$ (corresponding residence time: 7.8 h), the removal percentage for trans-4MCHCA was high ($>95 \%$). The removal percentages of both trans-4MCHCA and nitrite started to decrease with the further increase of the trans-4MCHCA loading rate. The lowest removal percentages for trans-4MCHCA and nitrite (6.6 % and 5.3 % respectively) were observed at the wash-out. The trans-4MCHCA and nitrite removal rates, however, passed through maximum values of 14.4 and $44.2 \text{ mg L}^{-1} \text{ h}^{-1}$, respectively, at a trans-4MCHCA loading rate of $22.9 \text{ mg L}^{-1} \text{ h}^{-1}$ (corresponding residence time: 4.8 h). The corresponding removal percentage for trans-4MCHCA and nitrite were 62.8 % and 42.7 %, respectively.

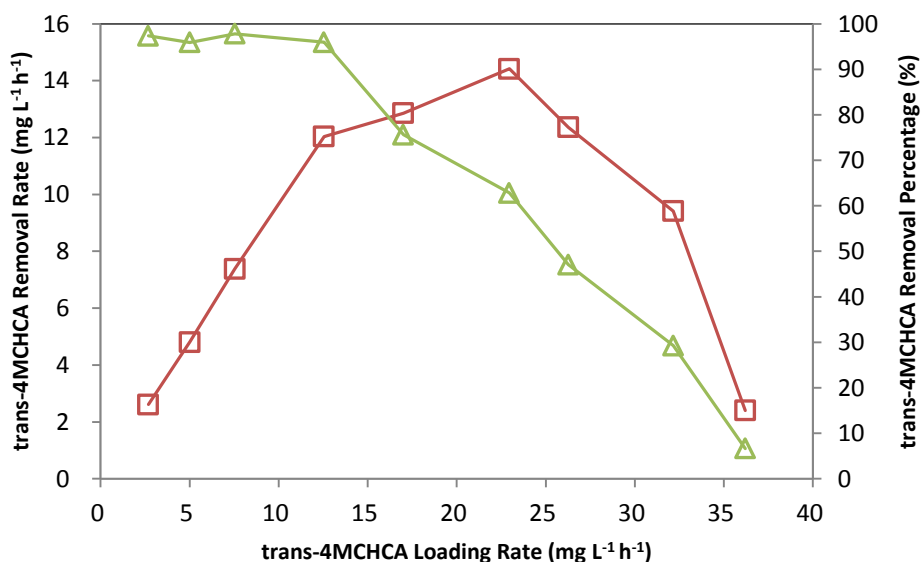


Figure 4.6 Removal rate and removal percentage of trans-4MCHCA as a function of its loading rate in continuous stirred tank reactor (CSTR). \square removal rate of trans-4MCHCA; \triangle removal percentage of trans- 4MCHCA.

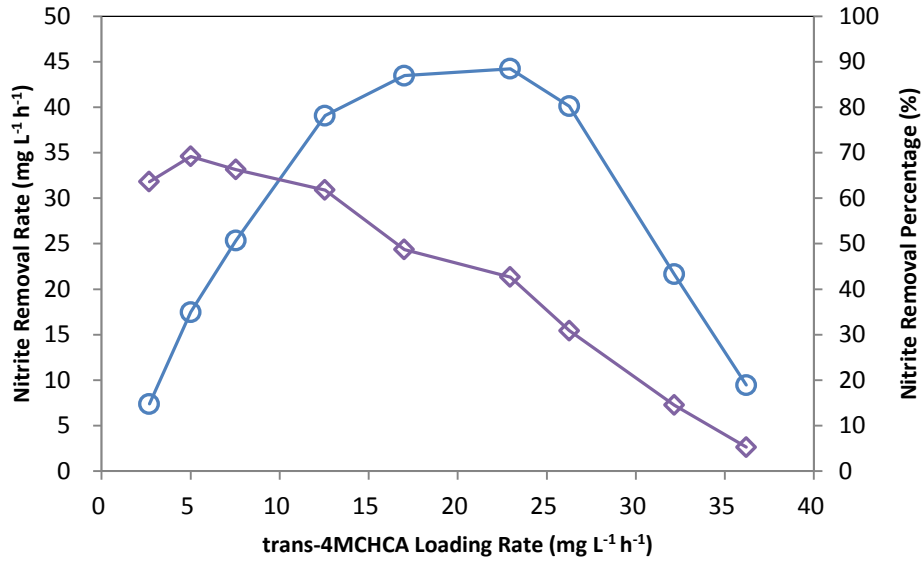


Figure 4.7 Removal rate and removal percentage of nitrite as a function of trans-4MCHCA loading rate in continuous stirred tank reactor (CSTR). ○ removal rate of nitrite; ◇ removal percentage of nitrite.

4.2.2 Determination of Associated Biokinetic Coefficients Using CSTR Data

Using the experimental data obtained in the CSTR various biokinetic coefficients including Y (yield of biomass over trans-4MCHCA consumed), K_e (endogenous rate constant), μ_m (maximum specific growth rate) and K_s (saturation constant) were determined. This was done by fitting the experimental data into Equations 3.15 and 3.21 and the procedure described in section 3.4.2, with the graphical representation for fitting the experimental data into these equations are shown in Figures 4.8 and 4.9. Using the slope and intercept of the line in Figure 4.8, Y and K_e were determined as $0.3 \text{ mg cell mg substrate}^{-1}$ and $\sim 0 \text{ h}^{-1}$ respectively. From Figure 4.9, the value of μ_m and K_s were determined as 0.4 h^{-1} and $20.9 \text{ mg substrate L}^{-1}$, respectively.

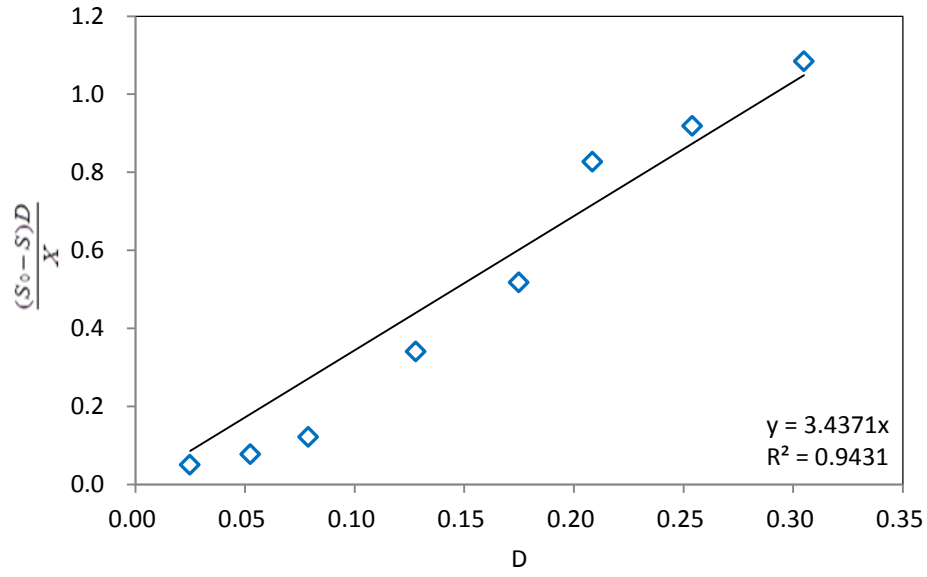


Figure 4.8 Linear plot of $\frac{(S_0 - S)D}{X}$ against D.

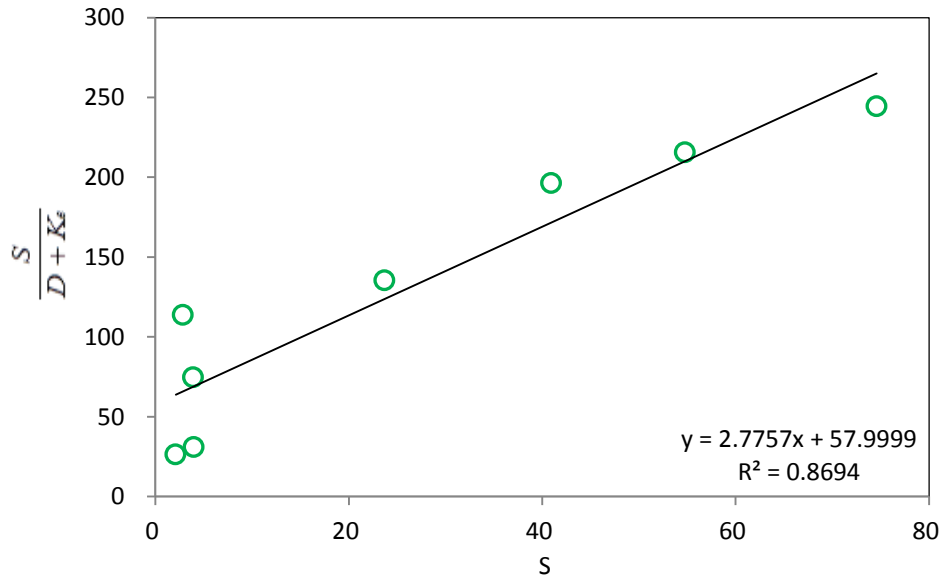


Figure 4.9 Linear plot of $\frac{S}{D + K_e}$ against S.

Table 4.5 compares the biokinetic coefficients obtained in the current work with biokinetic coefficients obtained in a previous work for aerobic biodegradation of trans-4MCHCA in CSTR

with a feed trans-4MCHCA concentration of 500 mg L⁻¹ (Paslawski *et al.*, 2009c). As seen in Table 4.5, the biomass yields (Y) for aerobic and anoxic systems were quite close. The maximum specific growth rate (μ_m) for the anoxic system was about 4.9 times higher than the aerobic system while the saturation constant (K_s) for the aerobic system was about 17.4 times higher than the anoxic system which could be potentially due to higher feed concentration used in the aerobic system.

Table 4.5 Comparison of biokinetic coefficients for aerobic biodegradation (Paslawski *et al.*, 2009c) with anoxic biodegradation (present work) of trans-4MCHCA in CSTR

Biokinetic Coefficients	Aerobic Biodegradation of trans-4MCHCA in CSTR	Anoxic Biodegradation of trans-4MCHCA in CSTR
Y (mg cell mg substrate ⁻¹)	0.3	0.2
K_e (h ⁻¹)	~ 0	~ 0
μ_m (h ⁻¹)	0.1	0.4
K_s (mg substrate L ⁻¹)	363	20.9

4.3 Continuous Biodegradation of trans-4MCHCA with Nitrite in Biofilm Reactor

The effect of volumetric loading rate of trans-4MCHCA on its biodegradation and reduction of nitrite was also examined in the biofilm system at room temperature (24 ± 2 °C). Initial feed concentrations of trans-4MCHCA and nitrite were set at 53.9 ± 5.9 mg L⁻¹ and 498.9 ± 16.6 mg L⁻¹, respectively. Residual trans-4MCHCA and nitrite concentrations were monitored on a regular basis to assess the performance of the biofilm system under different trans-4MCHCA volumetric loading rates. Figure 4.10 shows the steady state concentrations of trans-4MCHCA and nitrite in the effluent observed at various trans-4MCHCA loading rate ranging from 4.1 mg L⁻¹ h⁻¹ to 283.6 mg L⁻¹ h⁻¹ (corresponding residence time: 10.8 h to 0.2 h). As seen in Figure 4.10, for trans-4MCHCA loading rate up to 39.6 mg L⁻¹ h⁻¹ (corresponding residence time: 1.2 h), residual trans-4MCHCA was low (<4 mg L⁻¹), while due to deliberate excess level of nitrite to ensure nitrite was not limiting a residual nitrite concentration around 303 mg L⁻¹ was observed. Increase of the residual trans-4MCHCA and nitrite concentrations were observed with further

increase of loading rate. As shown in Figure 4.10, at the highest trans-4MCHCA loading rate of $283.6 \text{ mg L}^{-1} \text{ h}^{-1}$ (corresponding residence time: 0.2 h), the highest residual trans-4MCHCA and nitrite concentrations were observed at values around 44.1 mg L^{-1} and 465.8 mg L^{-1} , respectively. These were quite close to the feed trans-4MCHCA and nitrite concentrations at $53.9 \pm 5.9 \text{ mg L}^{-1}$ and $498.9 \pm 16.6 \text{ mg L}^{-1}$, respectively.

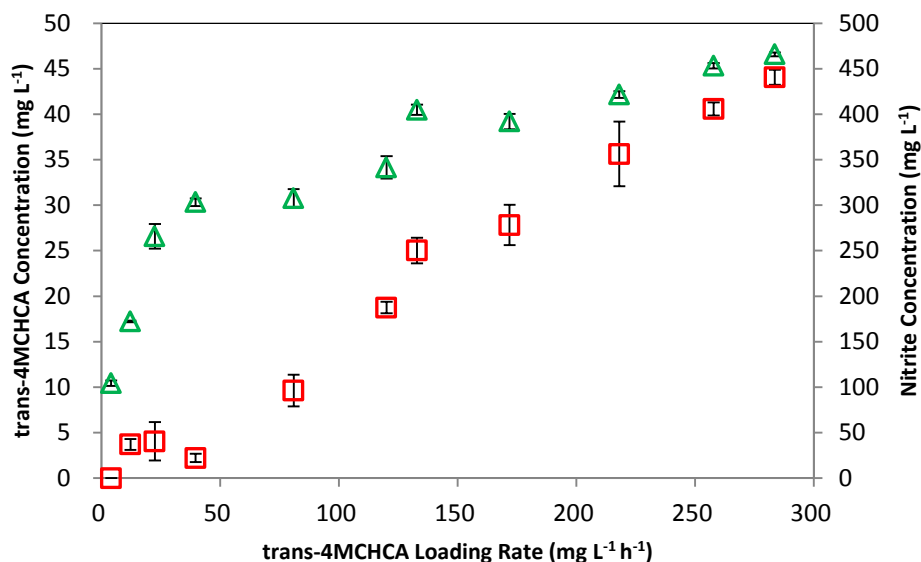


Figure 4.10 Steady-state profiles of trans-4MCHCA and nitrite concentrations observed in the biofilm system at various loading rate of trans-4MCHCA. Values reported are the average data for multiple samplings of the reactor over an extended period equal to three to five residence times after the establishment of steady state. Error bars represent the standard deviations and might not be visible in some cases. \square trans-4MCHCA residual concentration; \triangle nitrite concentration.

Figure 4.11 shows the dependency of trans-4MCHCA removal rate and its removal percentage on trans-4MCHCA loading rate in the biofilm system. The dependency of nitrite removal rate and its removal percentage on trans-4MCHCA loading rate in the biofilm system is shown in Figure 4.12. Generally the removal percentages for both trans-4MCHCA and nitrite decreased with the increase of trans-4MCHCA loading rate. Up to the trans-4MCHCA loading rate of $39.6 \text{ mg L}^{-1} \text{ h}^{-1}$ (corresponding residence time: 1.2 h), the removal percentages for trans-4MCHCA was high ($>95\%$) but due to intentional excess level of nitrite the highest removal percentage for

nitrite was around 40 %. The removal percentages for both trans-4MCHCA and nitrite started to decrease with the further increase of the trans-4MCHCA loading rate. With the highest applied trans-4MCHCA loading rate ($283.6 \text{ mg L}^{-1} \text{ h}^{-1}$) the removal percentages for trans-4MCHCA and nitrite were at their lowest level of 24.1 % and 8.3 %, respectively. The trans-4MCHCA and nitrite removal rates, however, passed through maximum values of $82.2 \text{ mg L}^{-1} \text{ h}^{-1}$ and $361.6 \text{ mg L}^{-1} \text{ h}^{-1}$, respectively, at the trans-4MCHCA loading rate of $171.8 \text{ mg L}^{-1} \text{ h}^{-1}$ (corresponding residence time: 0.3 h). The corresponding removal percentage for trans-4MCHCA and nitrite at this maximum removal rate were 47.8 % and 22.3 %, respectively. With further increase in loading rate (above $171.8 \text{ mg L}^{-1} \text{ h}^{-1}$), decrease in removal rates of both trans-4MCHCA and nitrite was observed.

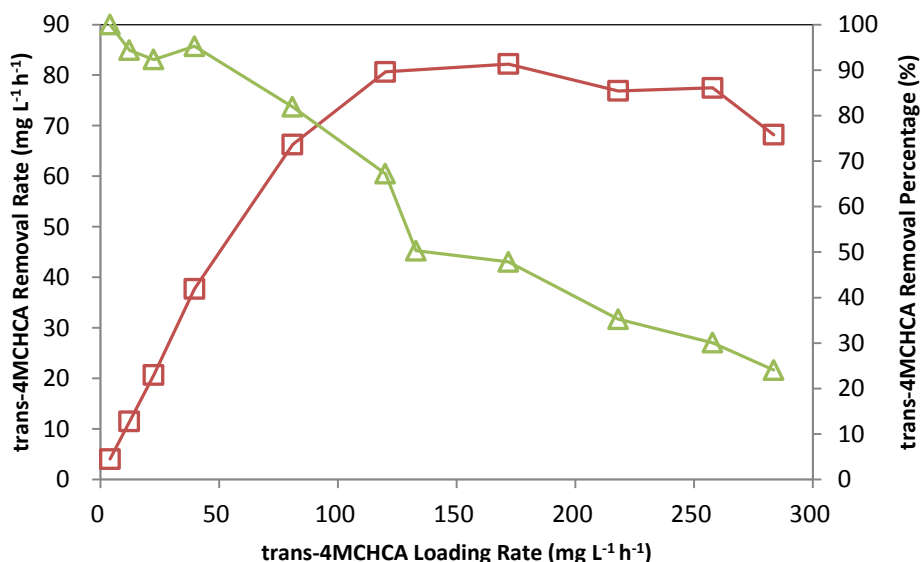


Figure 4.11 Removal rate and removal percentage of trans-4MCHCA as a function of trans-4MCHCA loading rate in the biofilm system. \square removal rate of trans-4MCHCA; \triangle removal percentage of trans-4MCHCA.

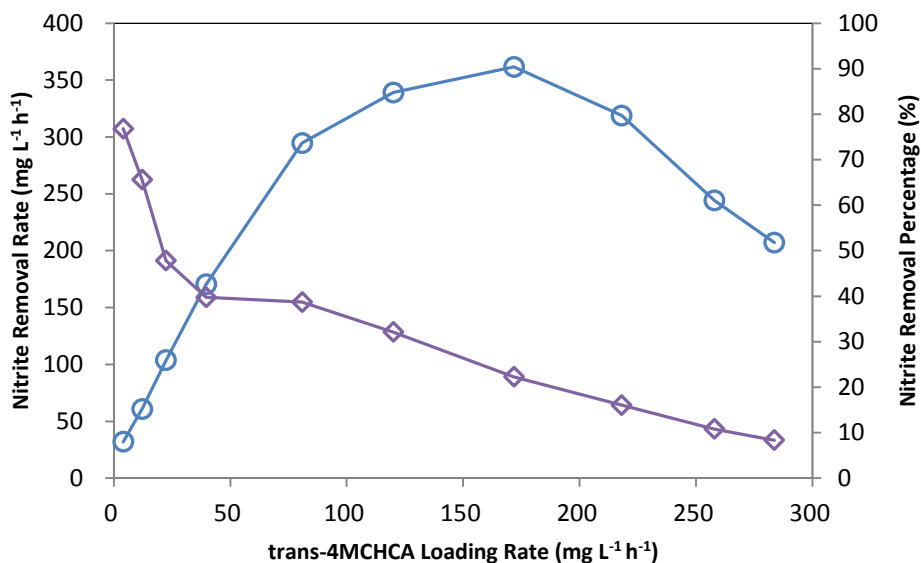


Figure 4.12 Removal rate and removal percentage of nitrite as a function of trans-4MCHCA loading rate in the biofilm system. ○ removal rate of nitrite; ◇ removal percentage of nitrite.

Upon the completion of experiment with a feed containing $53.9 \pm 5.9 \text{ mg L}^{-1}$ trans-4MCHCA and $498.9 \pm 16.6 \text{ mg L}^{-1}$ nitrite, two additional sets of experiment with higher trans-4MCHCA concentrations were carried out to assess the effect of trans-4MCHCA concentration on the biodegradation in the biofilm system. Nitrite concentration was adjusted based on the feed trans-4MCHCA concentration. With $105.3 \pm 1.8 \text{ mg L}^{-1}$ trans-4MCHCA, $471.6 \pm 12.9 \text{ mg L}^{-1}$ nitrite and with $252.7 \pm 6.4 \text{ mg L}^{-1}$ trans-4MCHCA, $815.9 \pm 10.3 \text{ mg L}^{-1}$ nitrite were used. Figures 4.13 and 4.14 show the steady state concentrations of trans-4MCHCA and nitrite, respectively, in the effluent at various trans-4MCHCA loading rate with these higher trans-4MCHCA and nitrite concentrations. As seen in Figure 4.13, with $105.3 \pm 1.8 \text{ mg L}^{-1}$ trans-4MCHCA and $471.6 \pm 12.9 \text{ mg L}^{-1}$ nitrite, the residual trans-4MCHCA concentration remained low ($<5 \text{ mg L}^{-1}$) until the loading rate was increased to $191.1 \text{ mg L}^{-1} \text{ h}^{-1}$ (corresponding residence time: 0.6 h). The residual trans-4MCHCA concentration increased gradually with the further increase of trans-4MCHCA loading rate. With $252.7 \pm 6.4 \text{ mg L}^{-1}$ trans-4MCHCA and $815.9 \pm 10.3 \text{ mg L}^{-1}$ nitrite, the residual trans-4MCHCA concentration remained low ($<3 \text{ mg L}^{-1}$) for loading rate up to $102.2 \text{ mg L}^{-1} \text{ h}^{-1}$ (corresponding residence time: 2.5 h). The residual

trans-4MCHCA concentration increased gradually with the further increase of trans-4MCHCA loading rate.

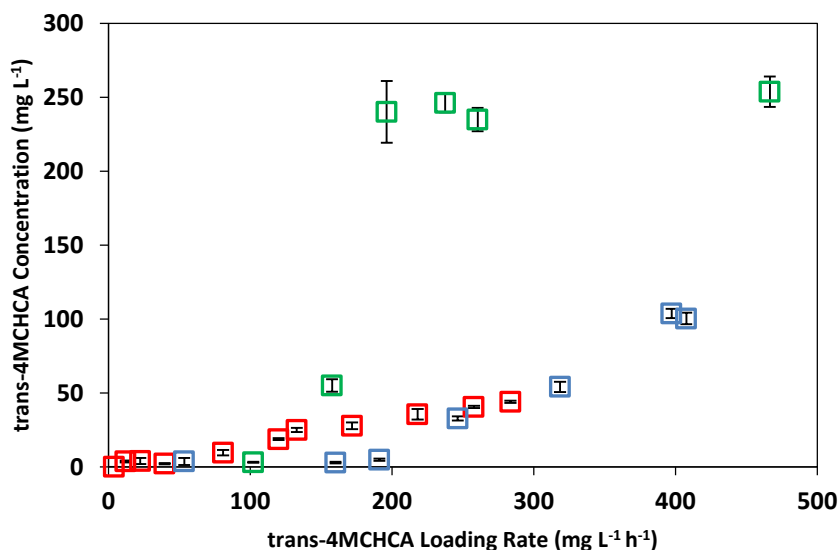


Figure 4.13 Steady-state profile of trans-4MCHCA observed in the biofilm system with various feed trans-4MCHCA and nitrite concentrations. Values reported are the average data for multiple samplings of the reactor over an extended period equal to three to five residence times after the establishment of steady state. Error bars represent the standard deviations and might not be visible in some cases. \square $53.9 \pm 5.9 \text{ mg L}^{-1}$ trans-4MCHCA and $498.9 \pm 16.6 \text{ mg L}^{-1}$ nitrite; \square $105.3 \pm 1.8 \text{ mg L}^{-1}$ trans-4MCHCA and $471.6 \pm 12.9 \text{ mg L}^{-1}$ nitrite; \square $252.7 \pm 6.4 \text{ mg L}^{-1}$ trans-4MCHCA and $815.9 \pm 10.3 \text{ mg L}^{-1}$ nitrite.

As shown in Figure 4.14, for the $105.3 \pm 1.8 \text{ mg L}^{-1}$ trans-4MCHCA and $471.6 \pm 12.9 \text{ mg L}^{-1}$ nitrite, the residual nitrite concentration remained low ($<138.3 \text{ mg L}^{-1}$) until the loading rate was increased to $191.1 \text{ mg L}^{-1} \text{ h}^{-1}$ (corresponding residence time: 0.6 h). The residual nitrite concentration increased gradually with the further increase of trans-4MCHCA loading rate. With $252.7 \pm 6.4 \text{ mg L}^{-1}$ trans-4MCHCA and $815.9 \pm 10.3 \text{ mg L}^{-1}$ nitrite, the residual nitrite concentration remained low ($\sim 0 \text{ mg L}^{-1}$) until the loading rate was increased to $102.2 \text{ mg L}^{-1} \text{ h}^{-1}$ (corresponding residence time: 2.5 h). The residual nitrite concentration increased gradually with the further increase of trans-4MCHCA loading rate.

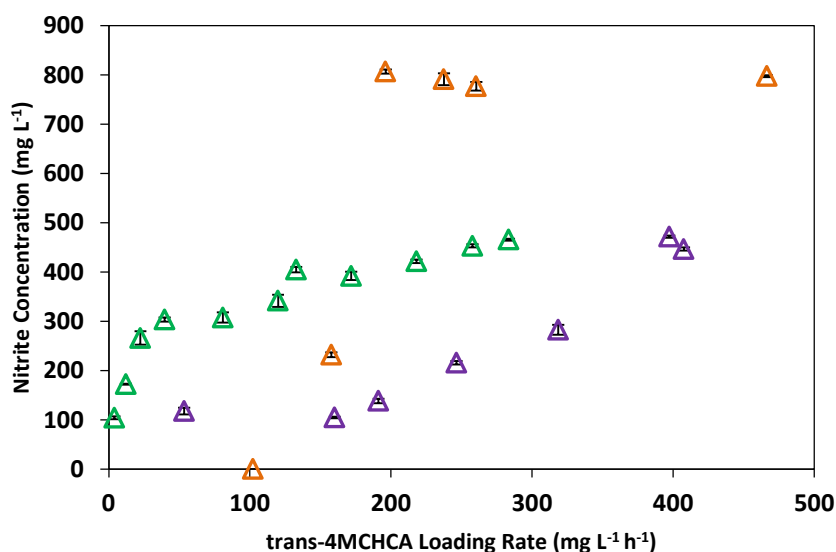


Figure 4.14 Steady-state profile of nitrite observed in the biofilm system with various feed trans-4MCHCA and nitrite concentrations. Values reported are the average data for multiple samplings of the reactor over an extended period equal to three to five residence times after the establishment of steady state. Error bars represent the standard deviations and might not be visible in some cases. ▲ $53.9 \pm 5.9 \text{ mg L}^{-1}$ trans-4MCHCA and $498.9 \pm 16.6 \text{ mg L}^{-1}$ nitrite; △ $105.3 \pm 1.8 \text{ mg L}^{-1}$ trans-4MCHCA and $471.6 \pm 12.9 \text{ mg L}^{-1}$ nitrite; ▲ $252.7 \pm 6.4 \text{ mg L}^{-1}$ trans-4MCHCA and $815.9 \pm 10.3 \text{ mg L}^{-1}$ nitrite.

The removal rates and removal percentages of trans-4MCHCA with various feed trans-4MCHCA and nitrite concentrations were calculated and shown in Figures 4.15 and 4.16 respectively. In all cases trans-4MCHCA removal rate and removal percentage profiles exhibited similar patterns. Data in Figure 4.15 reveals that the trans-4MCHCA removal rates kept increasing with the increases of their loading rates until they reached their maximum values and then started to decrease with further increases of the trans-4MCHCA loading rates. In the experiment with $105.3 \pm 1.8 \text{ mg L}^{-1}$ trans-4MCHCA with $471.6 \pm 12.9 \text{ mg L}^{-1}$ nitrite, removal rate of trans-4MCHCA increased with the increase of trans-4MCHCA and passed through a maximum point ($182.4 \text{ mg L}^{-1} \text{ h}^{-1}$) at a trans-4MCHCA loading rate of $191.1 \text{ mg L}^{-1} \text{ h}^{-1}$ (corresponding residence time: 0.6 h), and then started to decrease with further increase of the trans-4MCHCA loading rate. Similarly with $252.7 \pm 6.4 \text{ mg L}^{-1}$ trans-4MCHCA with $815.9 \pm 10.3 \text{ mg L}^{-1}$ nitrite removal rate of trans-4MCHCA increased with the increase of trans-4MCHCA loading rate and

passed through a maximum value of $121.9 \text{ mg L}^{-1} \text{ h}^{-1}$ at a loading rate of $157.8 \text{ mg L}^{-1} \text{ h}^{-1}$ (corresponding residence time: 1.5 h), and then decreased sharply with further increase of the trans-4MCHCA loading rate.

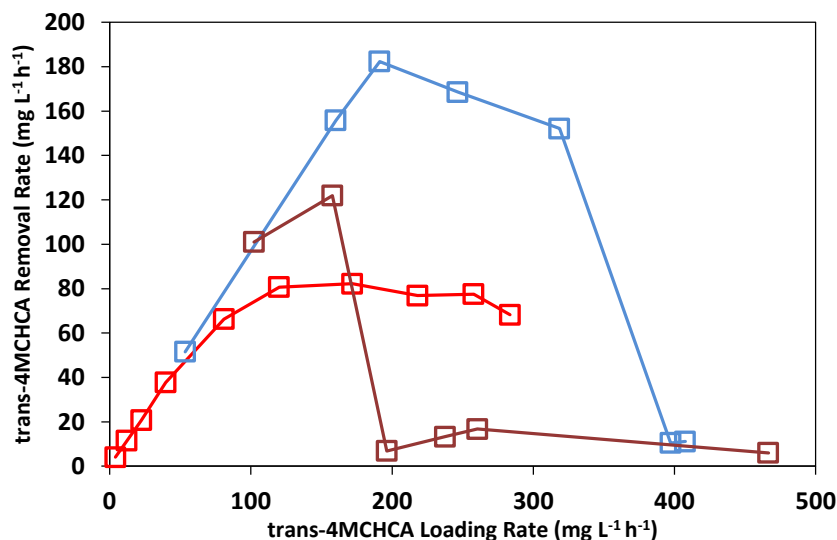


Figure 4.15 Removal rate of trans-4MCHCA as a function of its loading rate in the biofilm system fed with various concentrations of trans-4MCHCA and nitrite. \square $53.9 \pm 5.9 \text{ mg L}^{-1}$ trans-4MCHCA and $498.9 \pm 16.6 \text{ mg L}^{-1}$ nitrite; \square $105.3 \pm 1.8 \text{ mg L}^{-1}$ trans-4MCHCA and $471.6 \pm 12.9 \text{ mg L}^{-1}$ nitrite; \square $252.7 \pm 6.4 \text{ mg L}^{-1}$ trans-4MCHCA and $815.9 \pm 10.3 \text{ mg L}^{-1}$ nitrite.

Data in Figure 4.16 reveals that the trans-4MCHCA removal percentages maintained high at low trans-4MCHCA loading rates and started to decrease with further increases of the trans-4MCHCA loading rates. With $105.3 \pm 1.8 \text{ mg L}^{-1}$ trans-4MCHCA and $471.6 \pm 12.9 \text{ mg L}^{-1}$ nitrite the trans-4MCHCA removal percentage was high ($>95 \%$) up to the trans-4MCHCA loading rate of $191.1 \text{ mg L}^{-1} \text{ h}^{-1}$ (corresponding residence time: 0.6 h), and then started to decreases with further increase of the trans-4MCHCA loading rate. With $252.7 \pm 6.4 \text{ mg L}^{-1}$ trans-4MCHCA and $815.9 \pm 10.3 \text{ mg L}^{-1}$ nitrite the trans-4MCHCA removal percentage was high ($>98 \%$) up to the trans-4MCHCA loading rate of $102.2 \text{ mg L}^{-1} \text{ h}^{-1}$ (corresponding residence time: 2.5 h), and then started to decreases with further increase of the trans-4MCHCA loading rate.

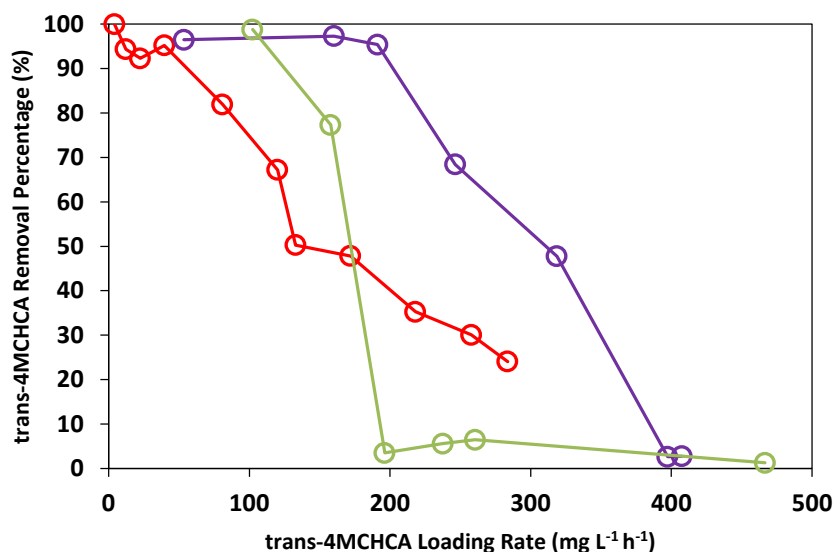


Figure 4.16 Removal percentage of trans-4MCHCA as a function of its loading rate in the biofilm system fed with various concentrations of trans-4MCHCA and nitrite. \circ $53.9 \pm 5.9 \text{ mg L}^{-1}$ trans-4MCHCA and $498.9 \pm 16.6 \text{ mg L}^{-1}$ nitrite; \circ $105.3 \pm 1.8 \text{ mg L}^{-1}$ trans-4MCHCA and $471.6 \pm 12.9 \text{ mg L}^{-1}$ nitrite; \circ $252.7 \pm 6.4 \text{ mg L}^{-1}$ trans-4MCHCA and $815.9 \pm 10.3 \text{ mg L}^{-1}$ nitrite.

The removal rates and removal percentages of nitrite with various feed trans-4MCHCA and nitrite concentrations were calculated and shown in Figures 4.17 and 4.18, respectively. As shown in Figure 4.17 in all cases, similar to the pattern observed with trans-4MCHCA the nitrite removal rates increased with the increases of trans-4MCHCA loading rates until they reached their maximum values and then started to decrease with further increases of the trans-4MCHCA loading rates. With $105.3 \pm 1.8 \text{ mg L}^{-1}$ trans-4MCHCA and $471.6 \pm 12.9 \text{ mg L}^{-1}$ nitrite the maximum nitrite removal rate of $650.1 \text{ mg L}^{-1} \text{ h}^{-1}$ occurred at a loading rate of $191.1 \text{ mg L}^{-1} \text{ h}^{-1}$ (corresponding residence time: 0.6 h). With $252.7 \pm 6.4 \text{ mg L}^{-1}$ trans-4MCHCA and $815.9 \pm 10.3 \text{ mg L}^{-1}$ nitrite, maximum nitrite removal rate and the corresponding trans-4MCHCA loading rate were $379.6 \text{ mg L}^{-1} \text{ h}^{-1}$ and $157.8 \text{ mg L}^{-1} \text{ h}^{-1}$ (corresponding residence time: 1.5 h), respectively.

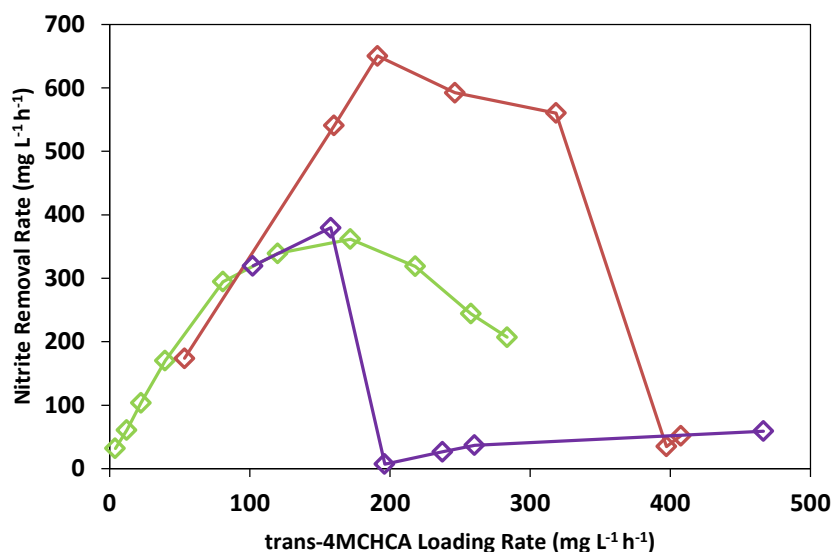


Figure 4.17 Removal rate of nitrite as a function of trans-4MCHCA loading rate in the biofilm system fed with various concentrations of trans-4MCHCA and nitrite. \diamond $53.9 \pm 5.9 \text{ mg L}^{-1}$ trans-4MCHCA and $498.9 \pm 16.6 \text{ mg L}^{-1}$ nitrite; \diamond $105.3 \pm 1.8 \text{ mg L}^{-1}$ trans-4MCHCA and $471.6 \pm 12.9 \text{ mg L}^{-1}$ nitrite; \diamond $252.7 \pm 6.4 \text{ mg L}^{-1}$ trans-4MCHCA and $815.9 \pm 10.3 \text{ mg L}^{-1}$ nitrite.

Data in Figure 4.18 shows that the nitrite removal percentages maintained high at low trans-4MCHCA loading rates and started to decrease with further increases of the trans-4MCHCA loading rates. With $105.3 \pm 1.8 \text{ mg L}^{-1}$ trans-4MCHCA and $471.6 \pm 12.9 \text{ mg L}^{-1}$ nitrite the nitrite removal percentage was high ($>72 \%$) up to the trans-4MCHCA loading rate of $191.1 \text{ mg L}^{-1} \text{ h}^{-1}$ (corresponding residence time: 0.6 h), and then started to decrease with further increase of the trans-4MCHCA loading rate. For the $252.7 \pm 6.4 \text{ mg L}^{-1}$ trans-4MCHCA with $815.9 \pm 10.3 \text{ mg L}^{-1}$ nitrite experiment, the trans-4MCHCA removal percentage was high ($\sim 100 \%$) up to the trans-4MCHCA loading rate of $102.2 \text{ mg L}^{-1} \text{ h}^{-1}$ (corresponding residence time: 2.5 h), and then started to decrease with further increase of the trans-4MCHCA loading rate.

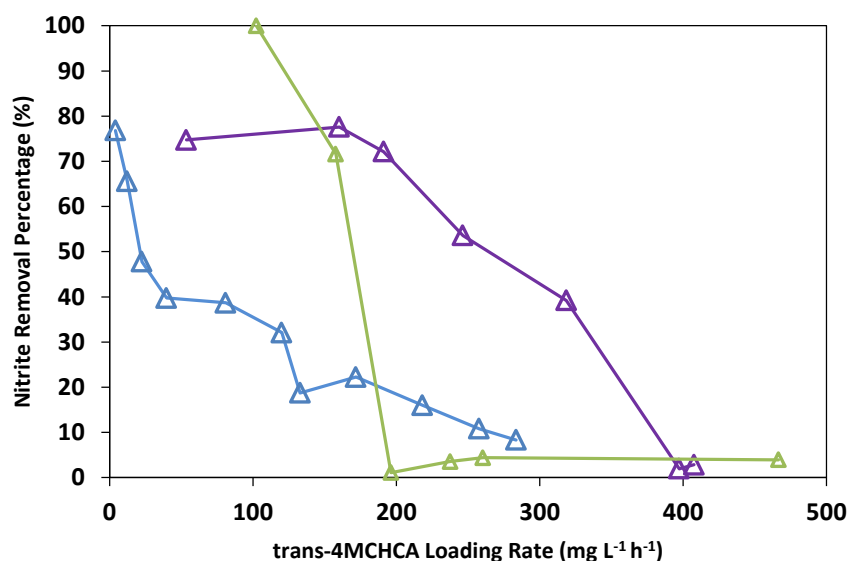


Figure 4.18 Removal percentage of nitrite as a function of trans-4MCHCA loading rate in the biofilm system fed with various concentrations of trans-4MCHCA and nitrite. \triangle $53.9 \pm 5.9 \text{ mg L}^{-1}$ trans-4MCHCA and $498.9 \pm 16.6 \text{ mg L}^{-1}$ nitrite; \triangle $105.3 \pm 1.8 \text{ mg L}^{-1}$ trans-4MCHCA and $471.6 \pm 12.9 \text{ mg L}^{-1}$ nitrite; \triangle $252.7 \pm 6.4 \text{ mg L}^{-1}$ trans-4MCHCA and $815.9 \pm 10.3 \text{ mg L}^{-1}$ nitrite.

4.4 Comparison of trans-4MCHCA Biodegradation with Nitrite in CSTR and Biofilm System

In this section, the performances of the CSTR and the biofilm system are compared. The removal rate profiles of trans-4MCHCA in the CSTR and the biofilm system are compared in Figure 4.19 (A) and the removal rate profiles of nitrite in the CSTR and biofilm system are compared in Figure 4.19 (B), respectively. As seen in Figure 4.19 (A), the maximum trans-4MCHCA removal rate obtained for the CSTR was $14.4 \text{ mg L}^{-1} \text{ h}^{-1}$ at a loading rate of $22.9 \text{ mg L}^{-1} \text{ h}^{-1}$, while it was $82.2 \text{ mg L}^{-1} \text{ h}^{-1}$ and at a loading rate of $171.8 \text{ mg L}^{-1} \text{ h}^{-1}$ for the biofilm system. The maximum trans-4MCHCA removal rate for the biofilm system was around 5.7 times higher than that observed in the CSTR. The highest removal rate in the biofilm reactor and the fact that it was achieved at a much higher loading rate (much shorter residence time) is an expected outcome due to the decoupling of the biomass and hydraulic residence times which allows a much higher biomass hold-up and consequently faster biodegradation rates at shorter residence times. The maximum nitrite removal rates in the CSTR and the biofilm system occurred at the same

trans-4MCHCA loading rate at which the maximum trans-4MCHCA removal rates were observed, with the values for CSTR and biofilm system being $44.2 \text{ mg L}^{-1} \text{ h}^{-1}$ and $361.6 \text{ mg L}^{-1} \text{ h}^{-1}$, respectively (Figure 4.19 (B)). Similar to the pattern observed for tran-4MCHCA, the maximum nitrite removal rate for the biofilm system was around 8.2 times higher than the CSTR.

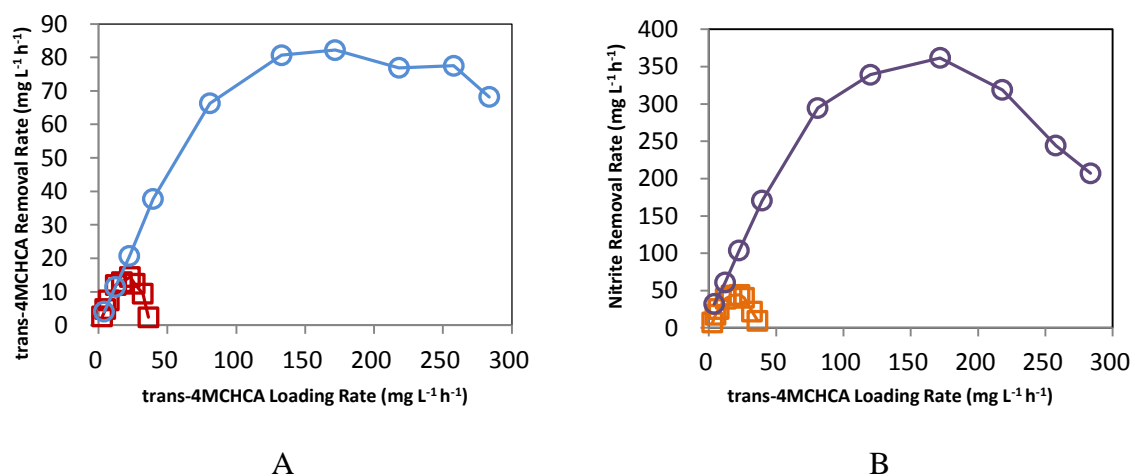


Figure 4.19 Comparison of trans-4MCHCA and nitrite removal rates in the CSTR and biofilm system. Panel (A) \square trans-4MCHCA removal rate profiles of CSTR operating with $101.6 \pm 5.4 \text{ mg L}^{-1}$ trans-4MCHCA and $492.5 \pm 14.8 \text{ mg L}^{-1}$ nitrite; \circ trans-4MCHCA removal rate profiles in biofilm system operating with $53.9 \pm 5.9 \text{ mg L}^{-1}$ trans-4MCHCA and $498.9 \pm 16.6 \text{ mg L}^{-1}$ nitrite; Panel (B) \square nitrite removal rate profiles of CSTR operating with $101.6 \pm 5.4 \text{ mg L}^{-1}$ trans-4MCHCA and $492.5 \pm 14.8 \text{ mg L}^{-1}$ nitrite; \circ nitrite removal rate profiles of biofilm system operating with $53.9 \pm 5.9 \text{ mg L}^{-1}$ trans-4MCHCA and $498.9 \pm 16.6 \text{ mg L}^{-1}$ nitrite.

4.5 Comparison of Anoxic Biodegradation of trans-4MCHCA with Nitrite and Nitrate as Electron Acceptor

4.5.1 Comparison of Biodegradation with Nitrite and Nitrate in a Batch System

Table 4.6 compares the biodegradation rates of trans-4MCHCA at different initial concentrations obtained in the presence of nitrate and nitrite ions as electron acceptors. The nitrate data is taken from an earlier work carried out in our lab (Gunawan *et al.*, 2014). As shown in Table 4.4 the biodegradation of trans-4MCHCA in the presence of nitrate was faster than that with nitrite. This

was specially clear with higher initial trans-4MCHCA concentration of 250 mg L^{-1} , where the biodegradation rate of trans-4MCHCA with nitrate ($4.7 \text{ mg L}^{-1} \text{ h}^{-1}$) was about 6.3 times faster than that with nitrite ($0.8 \text{ mg L}^{-1} \text{ h}^{-1}$), potentially due to inhibitory effect of nitrite as a result of higher nitrite concentration required for degradation of 250 mg L^{-1} trans-4MCHCA.

Table 4.6 Comparison of biodegradation rates of trans-4MCHCA obtained at various initial concentrations at room temperature ($24 \pm 2 \text{ }^{\circ}\text{C}$) with nitrate (Gunawan *et al.*, 2014) and nitrite (present work)

Trans-4MCHCA Concentration (mg L^{-1})	Biodegradation Rate of trans-4MCHCA with Nitrate ($\text{mg L}^{-1} \text{ h}^{-1}$)	Biodegradation Rate of trans-4MCHCA with Nitrite ($\text{mg L}^{-1} \text{ h}^{-1}$)
100	1.4 (0.96) *	0.8 (0.96) *
250	4.7 (0.97) *	0.8 (0.98) *

*The number in the parentheses represents R^2 values.

4.5.2 Comparison of Biodegradation with Nitrite and Nitrate in a CSTR

Figure 4.20 compares the removal rates of trans-4MCHCA as a function of its loading rate in the presence of nitrate and nitrite ions as electron acceptors in the CSTR. The data for biodegradation of trans-4MCHCA with nitrate is taken from an earlier work (Gunawan *et al.*, 2014) where a feed containing trans-4MCHCA and nitrate with respective concentrations of $232.5 \pm 22.9 \text{ mg L}^{-1}$ and $613.7 \pm 10.5 \text{ mg L}^{-1}$ were used. In the present work feed concentrations of trans-4MCHCA and nitrite were $101.6 \pm 5.4 \text{ mg L}^{-1}$ and $492.5 \pm 14.8 \text{ mg L}^{-1}$, respectively. The use of loading rate in presenting the data however allows the comparison of the data despite the differences in feed concentrations. Biodegradation profiles in either case followed similar patterns whereby removal rates of trans-4MCHCA passed through their maximum values with increase in trans-4MCHCA loading rates. The highest trans-4MCHCA removal rate with nitrate as an electron acceptor was $105.4 \text{ mg L}^{-1} \text{ h}^{-1}$ and observed at a trans-4MCHCA loading rate of $157.8 \text{ mg L}^{-1} \text{ h}^{-1}$ (corresponding residence time: 1.7 h), while with nitrite the highest trans-4MCHCA removal rate was $14.4 \text{ mg L}^{-1} \text{ h}^{-1}$ and observed at a trans-4MCHCA loading rate

of $22.9 \text{ mg L}^{-1} \text{ h}^{-1}$ (corresponding residence time: 4.8 h). The maximum trans-4MCHCA removal rate with nitrate was around 7.3 times higher than that with nitrite. The maximum specific removal rates were also calculated by dividing the highest trans-4MCHCA removal rate with corresponding biomass concentration. With nitrate a maximum specific trans-4MCHCA removal rate of $2.9 \text{ mg substrate mg biomass}^{-1} \text{ h}^{-1}$ was achieved which was around 3.1 times higher than the maximum specific trans-4MCHCA removal rate with nitrite ($0.9 \text{ mg substrate mg biomass}^{-1} \text{ h}^{-1}$).

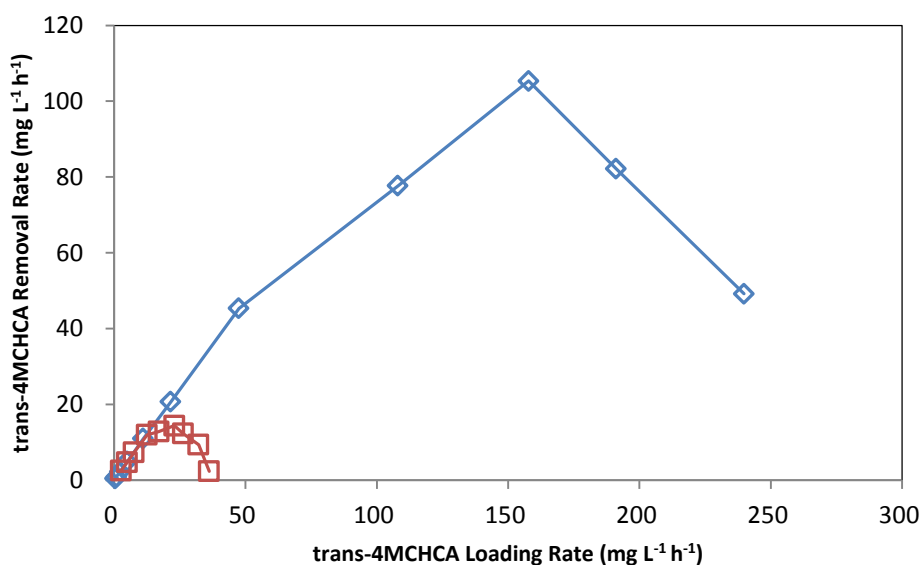


Figure 4.20 Removal rate of trans-4MCHCA as a function of its loading rate in the presence of nitrate and nitrite ions as electron acceptors in the CSTR. \diamond Biodegradation of $232.5 \pm 22.9 \text{ mg L}^{-1}$ trans-4MCHCA with $613.7 \pm 10.5 \text{ mg L}^{-1}$ nitrate (data was taken from Gunawan *et al.*, 2014); \square Biodegradation of $101.6 \pm 5.4 \text{ mg L}^{-1}$ trans-4MCHCA with $492.5 \pm 14.8 \text{ mg L}^{-1}$ nitrite.

4.5.3 Comparison of Biodegradation with Nitrite and Nitrate in a Biofilm System

Figure 4.21 compares the removal rates of trans-4MCHCA as a function of its loading rate in the presence of nitrate and nitrite ions as electron acceptors in the biofilm system. The data for biodegradation of trans-4MCHCA with nitrate is taken from Gunawan *et al.* (2014). The feed concentrations for trans-4MCHCA and nitrate were $50.3 \pm 3.0 \text{ mg L}^{-1}$ and $316.1 \pm 22.8 \text{ mg L}^{-1}$, respectively. In this current work, similar trans-4MCHCA concentration ($53.9 \pm 5.9 \text{ mg L}^{-1}$) and

a nitrite concentration of $498.9 \pm 16.6 \text{ mg L}^{-1}$ were used. As seen in Figure 4.21, two profiles exhibit quite similar patterns whereby removal rates of trans-4MCHCA passed through their maximum values with increases in trans-4MCHCA loading rates. The maximum trans-4MCHCA removal rate in the presence of nitrate was $398.1 \text{ mg L}^{-1} \text{ h}^{-1}$ at a trans-4MCHCA loading rate of $435.8 \text{ mg L}^{-1} \text{ h}^{-1}$ (corresponding residence time: 0.1 h), while the maximum trans-4MCHCA removal rate found in the system with nitrite was $82.2 \text{ mg L}^{-1} \text{ h}^{-1}$ at a trans-4MCHCA loading rate of $171.8 \text{ mg L}^{-1} \text{ h}^{-1}$ (corresponding residence time: 0.3 h). The performance of the biofilm system (in terms of trans-4MCHCA removal rate) with nitrate ions as electron acceptors was about 5.3 times better than that with nitrite ions as electron acceptors. The specific trans-4MCHCA removal rate was not calculated due to technical difficulties in measuring attached biomass concentration in the biofilm reactor.

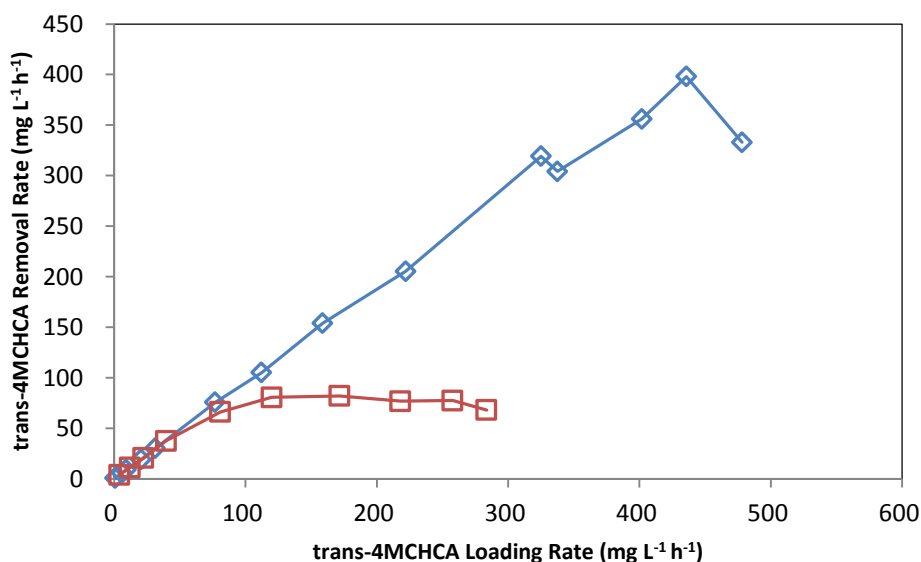


Figure 4.21 Removal rate of trans-4MCHCA as a function of its loading rate in the presence of nitrate and nitrite ions as electron acceptors in the biofilm system. \diamond Biodegradation of $50.3 \pm 3.0 \text{ mg L}^{-1}$ trans-4MCHCA with $316.1 \pm 22.8 \text{ mg L}^{-1}$ nitrate (data was taken from Gunawan *et al.*, 2014); \square Biodegradation of $53.9 \pm 5.9 \text{ mg L}^{-1}$ trans-4MCHCA with $498.9 \pm 16.6 \text{ mg L}^{-1}$ nitrite.

CHAPTER 5 CONCLUSIONS AND RECOMMENDATIONS FOR FUTURE WORK

5.1 Conclusions

Research on aerobic and anoxic biodegradation of model NAs have been conducted as part of earlier works in our research group (Paslawski *et al.*, 2009a, b, c, Huang *et al.*, 2012; D'Souza *et al.*, 2013; Gunawan *et al.*, 2014). The present work investigated the anoxic biodegradation of a surrogate NA (trans-4-methyl-1-cyclohexane carboxylic acid, trans-4MCHCA) using nitrite as an electron acceptor in batch, CSTR and biofilm systems. The anoxic biodegradation of trans-4MCHCA coupled with denitrification (nitrite reduction) was studied as part of an alternative approach for biodegradation of NAs with the intrinsic advantage of eliminating the aeration cost associated with aerobic biodegradation.

The effect of temperature and initial trans-4MCHCA concentration, and the inhibitory effect of nitrite were evaluated in batch system. Results of this batch study revealed that: 1)- the optimum temperature was in the range of 24 to 30 °C, and that biodegradation and denitrification processes did not occur at 10 °C; 2)- increase of initial trans-4MCHCA concentration required higher level of nitrite (as electron acceptor), indicating the coupling of biodegradation and denitrification processes; 3)- nitrite at concentration up to 690 mg L⁻¹ did not have a marked effect on biodegradation but higher concentrations, specially above 920 mg L⁻¹ imposed a strong inhibitory effect.

The effect of dilution rate and trans-4MCHCA loading rate on the anoxic biodegradation of trans-4MCHCA and reduction of nitrite was studied in the CSTR, with a feed containing trans-4MCHCA and nitrite at the average concentrations of 101.6 ± 5.4 and 492.5 ± 14.8 mg L⁻¹, respectively. With dilution rate up to 0.1 h⁻¹, residual trans-4MCHCA concentration was low (<4 mg L⁻¹); Increase of the residual trans-4MCHCA and nitrite concentrations and decrease in the biomass concentration were observed with further increase of the dilution rate. Cell wash-out occurred at a dilution rate of 0.4 h⁻¹ where the trans-4MCHCA, nitrite and biomass

concentrations in the reactor were 95 mg L^{-1} , 475 mg L^{-1} and 3.7 mg L^{-1} , respectively.

For trans-4MCHCA loading rates up to $12.6 \text{ mg L}^{-1} \text{ h}^{-1}$ (corresponding residence time: 7.8 h), the removal percentage of trans-4MCHCA was high (>95 %). The removal percentages of both trans-4MCHCA and nitrite started to decrease with the further increase of trans-4MCHCA loading rate. Increase in trans-4MCHCA loading rate led the trans-4MCHCA and nitrite removal rates to pass through maximum values of 14.4 and $44.2 \text{ mg L}^{-1} \text{ h}^{-1}$, respectively. This occurred at a trans-4MCHCA loading rate of $22.9 \text{ mg L}^{-1} \text{ h}^{-1}$ (corresponding residence time: 4.8 h). The corresponding removal percentage for trans-4MCHCA and nitrite were 62.8 % and 42.7 %, respectively. The maximum trans-4MCHCA removal rate ($14.4 \text{ mg L}^{-1} \text{ h}^{-1}$) was about seven folds lower than the maximum trans-4MCHCA removal rate observed when nitrate was used as an electron acceptor ($105.4 \text{ mg L}^{-1} \text{ h}^{-1}$; Gunawan, 2013). Using the experimental data the biokinetic coefficients Y (biomass yield), K_e (endogenous rate constant), μ_m (maximum specific growth rate) and K_s (saturation constant) were determined as $0.3 \text{ mg cell mg substrate}^{-1}$, $\sim 0 \text{ h}^{-1}$, 0.4 h^{-1} and $20.9 \text{ mg substrate L}^{-1}$, respectively.

The effect of trans-4MCHCA loading rate on the anoxic biodegradation of trans-4MCHCA and the reduction of nitrite was also studied in biofilm system using a feed containing trans-4MCHCA and nitrite at average concentrations of 53.9 ± 5.9 and $498.9 \pm 16.6 \text{ mg L}^{-1}$, respectively. For trans-4MCHCA loading rates up to $39.6 \text{ mg L}^{-1} \text{ h}^{-1}$ (corresponding residence time: 1.2 h), residual trans-4MCHCA was low ($<4 \text{ mg L}^{-1}$); increase of the residual trans-4MCHCA and nitrite concentrations were observed with further increase of trans-4MCHCA loading rate. For trans-4MCHCA loading rate up to $39.6 \text{ mg L}^{-1} \text{ h}^{-1}$ (corresponding residence time: 1.2 h), the removal percentage for trans-4MCHCA was high (>95 %). The removal percentages for both trans-4MCHCA and nitrite started to decrease with the further increase of the trans-4MCHCA loading rate. The trans-4MCHCA and nitrite removal rates passed through maximum values of $82.2 \text{ mg L}^{-1} \text{ h}^{-1}$ and $361.6 \text{ mg L}^{-1} \text{ h}^{-1}$, respectively as

trans-4MCHCA loading rate was increased. This occurred at a trans-4MCHCA loading rate of $171.8 \text{ mg L}^{-1} \text{ h}^{-1}$ (corresponding residence time: 0.3 h). The corresponding removal percentage for trans-4MCHCA and nitrite at this maximum removal rate were 47.8 % and 22.3 %, respectively. The maximum trans-4MCHCA biodegradation rate ($82.2 \text{ mg L}^{-1} \text{ h}^{-1}$) was about five folds lower than the maximum trans-4MCHCA biodegradation rate observed when nitrate was used as an electron acceptor ($435.8 \text{ mg L}^{-1} \text{ h}^{-1}$; Gunawan, 2013).

Comparison of the results obtained under anoxic (with nitrate and nitrite as electron acceptors) and aerobic (with oxygen as electron acceptor) revealed that anoxic biodegradation of NA in the presence of nitrite occurred at rates which were lower than those observed in the presence of nitrate, as well as those obtained under aerobic conditions with oxygen as the electron acceptor.

5.2 Recommendations for Future Work

Future works on the anoxic biodegradation of NAs in a mixture and in OSPW should be carried out to assess the feasibility of industrial application of this approach for treatment of OSPWs. Detailed studies of the anoxic biodegradation aiming to establish the oxidation mechanisms, metabolic pathways and toxicity are recommended as these could play a significant role in understanding the principles of anoxic biodegradation and could lay the foundation of the industrial application of this treatment method. Finally, application of other electron acceptors such as sulphate, ferric iron should be investigated as these electron acceptors may be present in the tailing ponds and thus contribute to anaerobic processes which may occur resulting as part of NAs natural degradation. A thorough feasibility study aiming to compare costs associated with aerobic and anoxic treatment processes is also recommended.

REFERENCES

- Afzal, A., Drzewicz, P., Perez-Estrada, L. A., Chen, Y., Martin, J. W., and Gamal El-Din, M. (2012). Effect of Molecular Structure on the Relative Reactivity of Naphthenic Acids in the UV/H₂O₂ Advanced Oxidation Process. *Environmental Science and Technology*, 46, 10727 - 10734.
- Allen, E. W. (2008). Process water treatment in Canada's oil sands industry: I. target pollutants and treatment objectives. *Journal of Environmental Engineering and Science*, 7(2), 123-138.
- Azad, F. S., Abedi, J., and Iranmanesh, S. (2013). Removal of naphthenic acids using adsorption process and the effect of the addition of salt. *Journal of Environmental Science and Health, Part A*, 48(13), 1649-1654.
- Biryukova, O. V., Fedorak, P. M., and Quideau, S. A. (2007). Biodegradation of naphthenic acids by rhizosphere microorganisms. *Chemosphere*, 67(10), 2058-2064.
- Brown, L. D., Pérez-Estrada, L., Wang, N., El-Din, M. G., Martin, J. W., Fedorak, P. M., et al. (2013). Indigenous microbes survive in situ ozonation improving biodegradation of dissolved organic matter in aged oil sands process-affected waters. *Chemosphere*, 93(11), 2748-2755.
- Brient, J. A., Wessner, P. J., and Doyle, M. N. (1995). Naphthenic acids, in Kroschwitz, J. I. (Ed.), *Encyclopedia of Chemical Technology*, vol. 16, fourth ed., pp. 1017 – 1029. New York, NY: John Wiley and Sons.
- Bessa, E., Sant'Anna, G.L., and Dezotti, J. (1999). Photocatalysis: An approach to the treatment of oil field produced waters. *Journal of Advanced Oxidation Technologies* 4: 196–202.
- Clemente, J. S., Prasad, N. G. N., MacKinnon, M. D., and Fedorak, P. M. (2003). A statistical comparison of naphthenic acids characterized by gas chromatography–mass spectrometry. *Chemosphere*, 50(10), 1265-1274.
- Canadian Association of Petroleum Producers (CAPP). (2014). Crude Oil Forecast, Markets and Transportation. Retrieved from <http://www.capp.ca/getdoc.aspx?DocId=247759&DT=NTV>. Accessed on Aug 24, 2014.
- Canadian Association of Petroleum Producers (CAPP). (2011). The Facts on Oil Sands. Retrieved from <http://www.capp.ca/getdoc.aspx?DocId=178979&>. Accessed on Aug 24, 2014.

Damasceno, F. C., Gruber, L. D. A., Geller, A. M., Vaz de Campos, M. C., Gomes, A. O., Guimaraes, R. C. L., et al. (2014). Characterization of naphthenic acids using mass spectroscopy and chromatographic techniques: Study of technical mixtures. *Analytical Methods*, (3), 807-816.

Dominski, M. (2007). Surface mined oil sand: tailings practices, performance, and projections. Alberta Energy and Utilities Board. In Proceedings of the 3rd International Heavy Oil Conference, March 5 – 7, 2007, Calgary, Alta. Alberta Energy and Utilities Board.

Del Rio, L. F., Hadwin, A. K. M., Pinto, L. J., MacKinnon, M. D., and Moore, M. M. (2006). Degradation of naphthenic acids by sediment micro-organisms. *Journal of Applied Microbiology*, 101(5), 1049-1061.

Doll, T. E., and Frimmel, F. H. (2005). Removal of selected persistent organic pollutants by heterogeneous photocatalysis in water. *Catalysis Today*, 101(3–4), 195-202.

D'souza, L. (2012). Co-biodegradation of Linear and Cyclic Naphthenic Acids in a Circulating Packed Bed Bioreactor. M.Sc. Thesis, Univ. of Saskatchewan, Saskatoon, Canada.

D'Souza, L., Sami, Y., Nemati, M., and Headley, J. (2013). Continuous co-biodegradation of linear and cyclic naphthenic acids in circulating packed-bed bioreactors. *Environmental Progress and Sustainable Energy*.

Dokholyan, V.K.; A.K.Magomedov (1983). Effects of sodium naphthenate on survival and some physiological-biochemical parameters of some fishes. *Journal of Ichthyology*. 23, 125–128.

Evans, W. C. (1977). Biochemistry of the bacterial catabolism of aromatic compounds in anaerobic environments. *Nature*, 270(5632), 17-22.

Foght, J. (2008). Anaerobic biodegradation of aromatic hydrocarbons: Pathways and prospects. *Journal of Molecular Microbiology and Biotechnology*, 15(2-3), 93-120.

Goff, K. L., Peru, K., Wilson, K. E., and Headley, J. V. (2014). Evaluation of biologically mediated changes in oil sands naphthenic acid composition by *chlamydomonas reinhardtii* using negative-ion electrospray orbitrap mass spectrometry. *Journal of Phycology*, 50(4), 727-735.

Gunawan, Y. (2013). Anaerobic biodegradation of a naphthenic acid under denitrifying conditions . M.Sc. Thesis, Univ. of Saskatchewan, Saskatoon, Canada.

Gunawan, Y., Nemati, M., and Dalai, A. (2014). Biodegradation of a surrogate naphthenic acid under denitrifying conditions. *Water Research*, 51(0), 11-24.

Government of Alberta. (2014). Oil Sands - Alberta's Clean Energy Future – Water Retrieved from <http://www.oilsands.alberta.ca/water.html> Accessed on August 6, 2014

Han, X., Scott, A. C., Fedorak, P. M., Bataineh, M., and Martin, J. W. (2008). Influence of molecular structure on the biodegradability of naphthenic acids. *Environmental Science and Technology*, 42(4), 1290-1295.

Headley, J. V., Tanapat, S., Putz, G., and Peru, K. M. (2002a). Biodegradation kinetics of geometric isomers of model naphthenic acids in Athabasca river water. *Canadian Water Resources Journal*, 27(1), 25-42.

Headley, J. V., Peru, K. M., McMartin, D. W., and Winkler, M. (2002b). Determination of dissolved naphthenic acids in natural waters by using negative- ion electrospray mass spectrometry. *Journal of AOAC International*, 85(1), 182.

Herman, D. C., Fedorak, P. M., MacKinnon, M. D., and Costerton, J. W. (1994). Biodegradation of naphthenic acids by microbial populations indigenous to oil sands tailings. *Canadian Journal of Microbiology*, 40, 467-477.

Holowenko, F. M., MacKinnon, M. D., and Fedorak, P. M. (2002). Characterization of naphthenic acids in oil sands wastewaters by gas chromatography-mass spectrometry. *Water Research*, 36(11), 2843-2855.

Hsu, C. S., Dechert, G. J., Robbins, W. K., and Fukuda, E. K. (2000). Naphthenic acids in crude oils characterized by mass spectrometry. *Energy and Fuels*, 14(1), 217-223.

Hrudey, S.E. (1975). Characterization of Wastewaters from the Great Canadian Oil Sands Bitumen Extraction and Upgrading Plant. Environment Canada Surveillance Report no. EPS 5NM-WP-75-6.

Hwang, G., Dong, T., Islam, M. S., Sheng, Z., Pérez-Estrada, L. A., Liu, Y., et al. (2013). The impacts of ozonation on oil sands process-affected water biodegradability and biofilm formation characteristics in bioreactors. *Bioresource Technology*, 130(0), 269-277.

Huang, L. Y. (2011). Bioremediation of Naphthenic Acids in a Circulating Packed Bed Bioreactor. M.Sc. Thesis, Univ. of Saskatchewan, Saskatoon, Canada.

Huang, J., Nemati, M., Hill, G., and Headley, J. (2012). Batch and Continuous Biodegradation of Three Model Naphthenic Acids in a Circulating Packed-bed Bioreactor. *Journal of Hazardous Materials*, 201 - 202, 132 - 140.

- Islam, M. S., Moreira, J., Chelme-Ayala, P., and Gamal El-Din, M. (2014). Prediction of naphthenic acid species degradation by kinetic and surrogate models during the ozonation of oil sands process-affected water. *Science of the Total Environment*, 493(0), 282-290.
- Johnson, R. J., Smith, B. E., Sutton, P. A., McGenity, T. J., Rowland, S. J., and Whitby, C. (2011). Microbial biodegradation of aromatic alkanolic naphthenic acids is affected by the degree of alkyl side chain branching. *International Society for Microbial Ecology*, 5(3), 486-496.
- Johnson, R. J., Smith, B. E., Rowland, S. J., and Whitby, C. (2013). Biodegradation of alkyl branched aromatic alkanolic naphthenic acids by *Pseudomonas putida* KT2440. *International Biodeterioration and Biodegradation*, 81(0), 3-8.
- Jones, D. M., Watson, J. S., Meredith, W., Chen, M., and Bennett, B. (2001). Determination of naphthenic acids in crude oils using nonaqueous ion exchange solid-phase extraction. *Analytical Chemistry*, 73(3), 703-707.
- Knight, R.L., Kadlec, R.H., Ohlendorf, H.M. (1999) The use of treatment wetlands for petroleum industry effluents. *Environmental Science and Technology* 33(7), 973–980.
- Linsebigler, A. L., Lu, G., Yates, J. T. (1995). Photocatalysis on TiO₂ Surfaces: Principles, Mechanisms, and Selected Results. *Chemical Reviews*, 95 (3), 735 – 758.
- MacKinnon, M. D. and Boerger, H. (1986). Description of Two Treatment Methods for Detoxifying Oil Sands Tailings Pond Water. *Water Pollution Research Journal of Canada*, 21 (4), 496 - 512.
- McMartin, D.W. (2003) Persistence and fate of acidic hydrocarbons in aquatic environments: naphthenic acids and resin acids. Ph.D. thesis; University of Saskatchewan, Canada.
- McMartin, D. W., Headley, J. V., Friesen, D. A., Peru, K. M., and Gillies, J. A. (2004) Photolysis of Naphthenic Acids in Natural Surface Water. *Journal of Environmental Science and Health, Part A - Toxic/Hazardous Substances and Environmental Engineering*, A39 (6), 1361 - 1383.
- Martin, J. W., Han, X., Peru, K. M., and Headley, J. V. (2008). Comparison of high- and low-resolution electrospray ionization mass spectrometry for the analysis of naphthenic acid mixtures in oil sands process water. *Rapid Communications in Mass Spectrometry: RCM*, 22(12), 1919.
- Martin, J. W., Barri, T., Han, X., Fedorak, P. M., El-Din, M., Perez, L., et al. (2010). Ozonation of oil sands process-affected water accelerates microbial bioremediation. *Environmental Science and Technology*, 44(21), 8350-8356.

- Masliyah, J., Zhou, Z. J., Xu, Z., Czarnecki, J., and Hamza, H. (2004). Understanding water-based bitumen extraction from Athabasca oil sands. *The Canadian Journal of Chemical Engineering*, 82(4), 628-654.
- McKenzie, N., Yue, S., Liu, X., Ramsay, B. A., and Ramsay, J. A. (2014). Biodegradation of naphthenic acids in oils sands process waters in an immobilized soil/sediment bioreactor. *Chemosphere*, 109(0), 164-172.
- Mishra, S., Meda, V., Dalai, A. K., Headley, J. V., Peru, K. M., and McMartin, D. W. (2010a). Microwave treatment of naphthenic acids in water. *Journal of Environmental Science and Health, Part A*, 45(10), 1240-1247.
- Mishra, S., Meda, V., Dalai, A. K., McMartin, D. W., Headley, J. V., and Peru, K. M. (2010b). Photocatalysis of naphthenic acids in water. *Journal of Water Resource and Protection*, 02(07), 644.
- Misiti, T. M., Tezel, U., Tandukar, M., and Pavlostathis, S. G. (2013a). Aerobic biotransformation potential of a commercial mixture of naphthenic acids. *Water Research*, 47(15), 5520-5534.
- Misiti, T., Tandukar, M., Tezel, U., and Pavlostathis, S. G. (2013b). Inhibition and biotransformation potential of naphthenic acids under different electron accepting conditions. *Water Research*, 47(1), 406-418.
- Misiti, T., Tezel, U., and Pavlostathis, S. G. (2013c). Fate and effect of naphthenic acids on oil refinery activated sludge wastewater treatment systems. *Water Research*, 47(1), 449-460.
- Paslawski, J. (2008). The Kinetics of Biodegradation of trans-4-methyl-1-cyclohexane carboxylic acid. Ph.D. Thesis, Univ. of Saskatchewan, Saskatoon, Canada.
- Paslawski, J. C., Nemati, M., Hill, G. A., and Headley, J. V. (2009a). Model for biodegradation of a naphthenic acid in an immobilized cell reactor. *The Canadian Journal of Chemical Engineering*, 87(3), 507-513.
- Paslawski, J., Headley, J., Hill, G., and Nemati, M. (2009b). Biodegradation kinetics of trans-4-methyl-1-cyclohexane carboxylic acid. *Biodegradation*, 20(1), 125-133.
- Paslawski, J., Nemati, M., Hill, G., and Headley, J. (2009c). Biodegradation kinetics of trans-4-methyl-1-cyclohexane carboxylic acid in continuously stirred tank and immobilized cell bioreactors. *Journal of Chemical Technology and Biotechnology*, 84(7), 992-1000.

Pereira, A. S., Islam, M. S., Gamal El-Din, M., and Martin, J. W. (2013). Ozonation degrades all detectable organic compound classes in oil sands process-affected water; an application of high-performance liquid chromatography/obitrap mass spectrometry. *Rapid Communications in Mass Spectrometry*, 27(21), 2317-2326.

Quesnel, D. M., Bhaskar, I. M., Gieg, L. M., and Chua, G. (2011). Naphthenic acid biodegradation by the unicellular alga *dunaliella tertiolecta*. *Chemosphere*, 84(4), 504-511.

Quagraine, E. K., Peterson, H. G., and Headley, J. V. (2005). In Situ Bioremediation of Naphthenic Acids Contaminated Tailing Pond Waters in the Athabasca Oil Sands Region- Demonstrated Field Studies and Plausible Options: A Review. *Journal of Environmental Science and Health, Part A: Toxic/Hazardous Substances and Environmental Engineering*, 40, 685-722.

Rogers, V. V., Wickstrom, M., Liber, K., and MacKinnon, M. D. (2002). Acute and subchronic mammalian toxicity of naphthenic acids from oil sands tailings. *Toxicological Sciences*, 66(2), 347-355.

Scarlett, A. G., Reinardy, H. C., Henry, T. B., West, C. E., Frank, R. A., Hewitt, L. M., et al. (2013). Acute toxicity of aromatic and non-aromatic fractions of naphthenic acids extracted from oil sands process-affected water to larval zebrafish. *Chemosphere*, 93(2), 415-420.

Scott, A. C., MacKinnon, M. D., and Fedorak, P. M. (2005). Naphthenic acids in Athabasca oil sands tailings waters are less biodegradable than commercial naphthenic acids. *Environmental Science and Technology*, 39(21), 8388.

Scott, A. C., Zubot, W., MacKinnon, M. D., Smith, D. W., and Fedorak, P. M. (2008). Ozonation of oil sands process water removes naphthenic acids and toxicity. *Chemosphere*, 71(1), 156-160.

Shuler, M. and Kargi, F. (2002). *Bioprocess Engineering Basic Concepts* (2nd Edition). Saddle River, NJ: Prentice Hall.

Smith, B. E., Lewis, C. A., Belt, S. T., Whitby, C., and Rowland, S. J. (2008). Effects of alkyl chain branching on the biotransformation of naphthenic acids. *Environmental Science and Technology*, 42(24), 9323-9328.

Toor, N. S., Franz, E. D., Fedorak, P. M., MacKinnon, M. D., and Liber, K. (2013a). Degradation and aquatic toxicity of naphthenic acids in oil sands process-affected waters using simulated wetlands. *Chemosphere*, 90(2), 449-458.

Toor, N. S., Han, X., Franz, E., MacKinnon, M. D., Martin, J. W., and Liber, K. (2013b). Selective biodegradation of naphthenic acids and a probable link between mixture profiles and aquatic toxicity. *Environmental Toxicology and Chemistry*, 32(10), 2207-2216.

Videla, P. P., Farwell, A. J., Butler, B. J., and Dixon, D. G. (2009). Examining the microbial degradation of naphthenic acids using stable isotope analysis of carbon and nitrogen. *Water, Air, and Soil Pollution*, 197(1-4), 107-119.

Yen, T., Marsh, W., MacKinnon, M., and Fedorak, P. (2004) Measuring Naphthenic Acids Concentrations in Aqueous Environmental Samples by Liquid Chromatography. *Journal of Chromatography A*, 1033 (1), 83 – 90.

Zubot, W., MacKinnon, M. D., Chelme-Ayala, P., Smith, D. W., and Gamal El-Din, M. (2012). Petroleum coke adsorption as a water management option for oil sands process-affected water. *Science of the Total Environment*, 427–428(0), 364-372.

APPENDIX A

A1 Gas Chromatography (GC) Calibration Curve

Calibration Curve for Gas Chromatography was generated using six trans-4MCHCA standard solutions (10, 20, 40, 60, 80 and 100 mg L⁻¹) in sterilized modified McKinney's medium. The average retention time for trans-4MCHCA was 14.0 ± 0.5 minutes. The calibration curve for trans-4MCHCA is shown in Figure A.3.

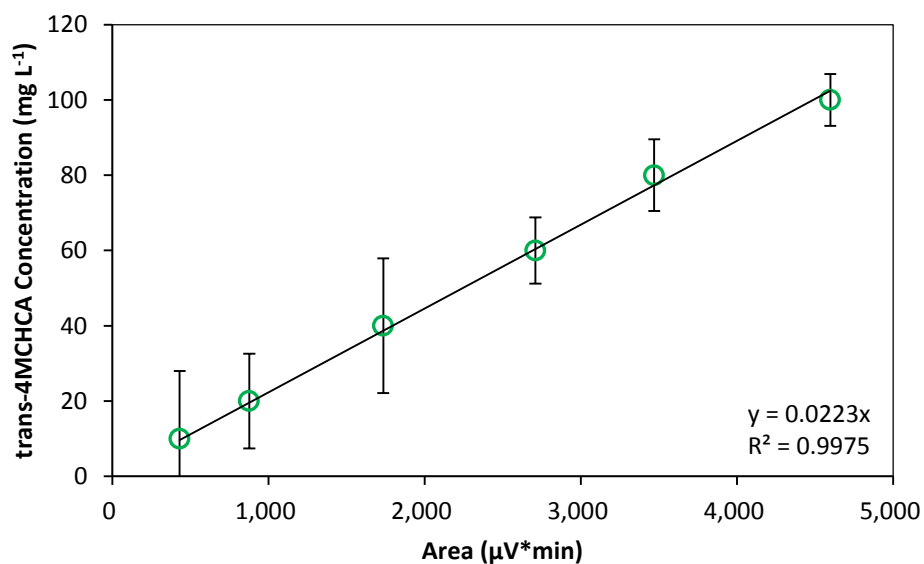


Figure A.1 Calibration curve developed for various trans-4MCHCA concentrations. Error bars represent standard deviations in three trans-4MCHCA concentration readings.

A2 Ion Chromatography (IC) Calibration Curve

Calibration Curve for Ion Chromatography was generated using six nitrite standard solutions (0, 5, 10, 15, 20 and 25 mg L⁻¹) in sterilized modified McKinney's medium. The average retention time for nitrite was 4.52 ± 0.1 minutes. The calibration curve for nitrite is shown in Figure A.2.

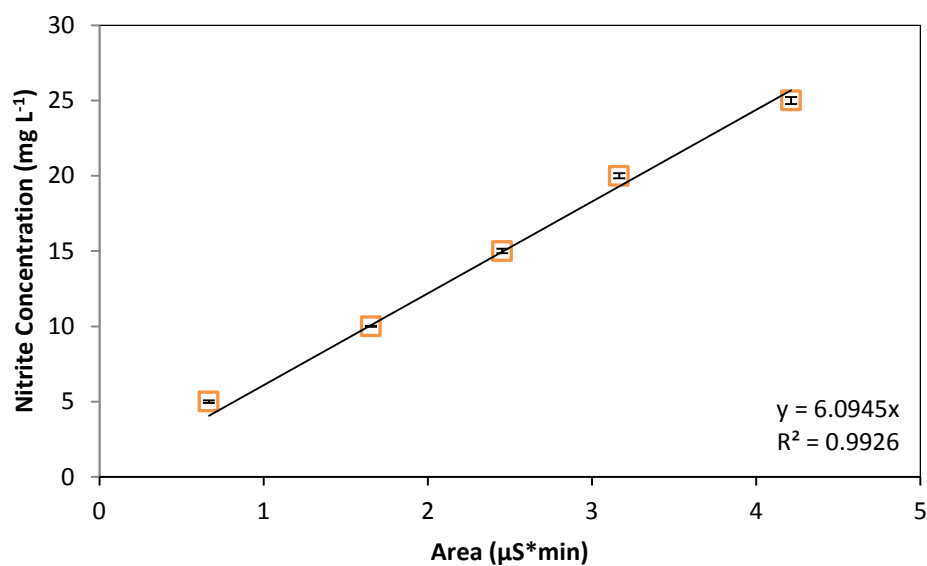


Figure A.2 Calibration curve developed for various nitrite concentrations. Error bars represent standard deviations in four nitrite concentration readings.

A3 Biomass Calibration Curve

Optical Density (OD) of the samples was measured throughout the research work (for both batch experiment and CSTR experiment) using spectrophotometer at a wavelength of 620 nm to record the growth of the bacteria. Dry weight of the biomass for the culture that was used in this research work was measured using one batch experiment with 100 mg L^{-1} of trans-4MCHCA and 460 mg L^{-1} of nitrite at the end of its exponential phase. A portion of a large sample taken at the end of the experiment was used to determine the biomass concentration in terms of the dry weight per volume and the remaining part was diluted 2, 4 and 10 times to determine their OD and their corresponding biomass concentration. The linear relationship between OD and biomass dry weight concentration is shown in Figure A.1.

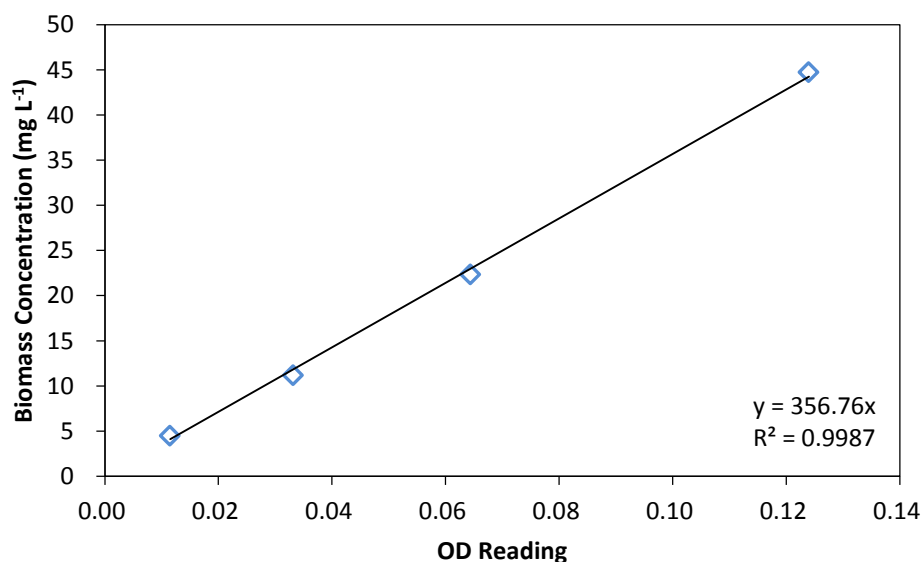


Figure A.3 Biomass calibration curve.

APPENDIX B

B1 Samples of Gas Chromatogram

Figure B.2 shows the elution time of trans-4MCHCA using gas chromatography. The elution time of trans-4MCHCA was 14.1 minutes in this chromatogram.

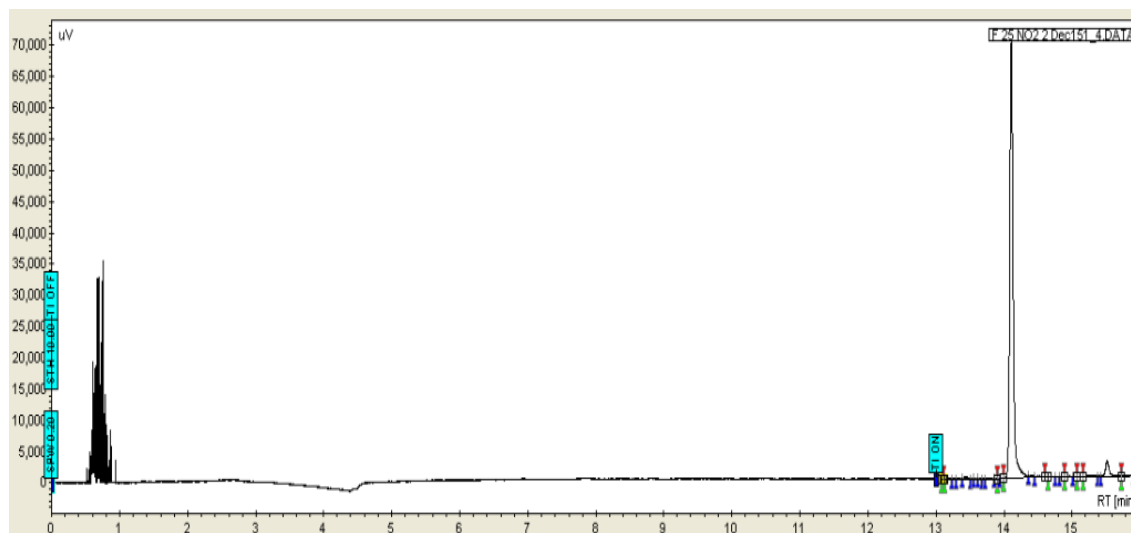


Figure B.1 The representative Varian-430 GC chromatogram of trans-4MCHCA.

B2 Sample of Ion Chromatogram

Figure B.1 shows the elution time of nitrite ion using ion chromatography. The elution time of nitrite was 4.6 minutes in this chromatogram.

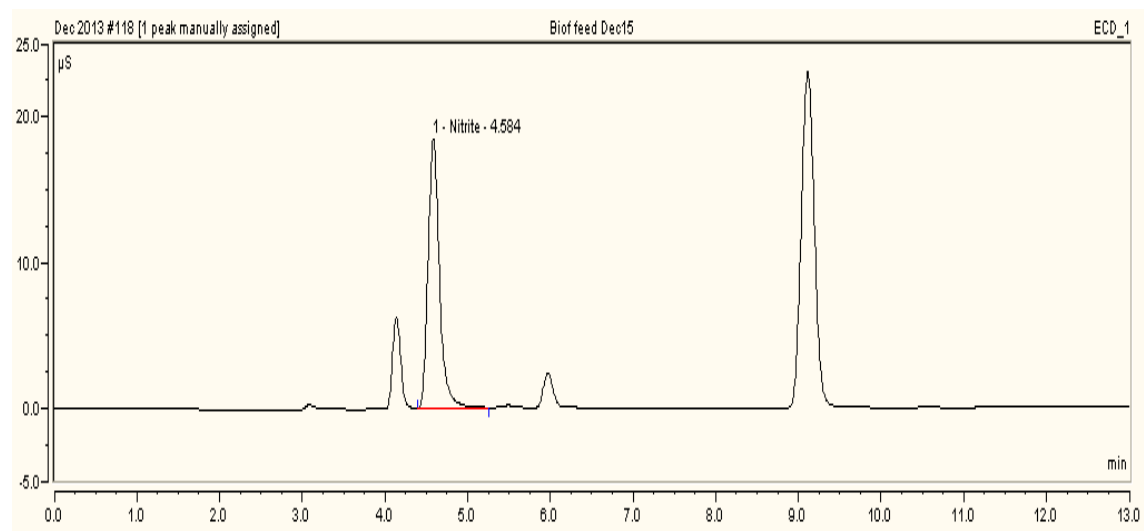


Figure B.2 The representative Dionex ICS-2500 IC chromatogram of nitrite.

APPENDIX C

Sample Calculations

Dilution rate for the continuous stirred tank reactor (CSTR) and hydraulic residence time (HRT), trans-4MCHCA loading rate, trans-4MCHCA removal rate, trans-4MCHCA removal percentage, nitrite removal rate and nitrite removal percentage for both CSTR and biofilm system were calculated using the following procedures.

$$D = Q/V \quad (C.1)$$

For example, at a flow rate of 71.3 mL h^{-1} , with a working volume of 200 mL, CSTR had a dilution rate of 0.4 h^{-1} .

$$\text{HRT} = V/Q \quad (C.2)$$

For example, at a flow rate of 71.3 mL h^{-1} for the CSTR, with a working volume of 200 mL, CSTR had a hydraulic residence time of 2.8 h; at a flow rate of 132 mL h^{-1} for the biofilm system, with a working volume of 27 mL, biofilm system had a hydraulic residence time of 0.2 h.

$$\text{Loading rate} = (S_0/\text{HRT}) \quad (C.3)$$

For example, at a feed trans-4MCHCA concentration of 101.6 mg L^{-1} for the CSTR, with a HRT of 2.8 h, CSTR had a trans-4MCHCA loading rate of $36.1 \text{ mg L}^{-1} \text{ h}^{-1}$; at a feed trans-4MCHCA concentration of 58.0 mg L^{-1} for the biofilm system, with a HRT of 0.2 h, biofilm system had a trans-4MCHCA loading rate of $290.1 \text{ mg L}^{-1} \text{ h}^{-1}$.

$$\text{Removal rate} = (S_0 - S)/\text{HRT} \quad (C.4)$$

For example, at a feed trans-4MCHCA concentration of 101.6 mg L^{-1} and a residual trans-4MCHCA concentration of 94.8 mg L^{-1} for the CSTR, with a HRT of 2.8 h, CSTR had a trans-4MCHCA removal rate of $2.4 \text{ mg L}^{-1} \text{ h}^{-1}$; at a feed trans-4MCHCA concentration of 58.0 mg L^{-1} and a residual trans-4MCHCA concentration of 44.1 mg L^{-1} for the biofilm system, with a HRT of 0.2 h, biofilm system had a trans-4MCHCA removal rate of $69.8 \text{ mg L}^{-1} \text{ h}^{-1}$.

$$\text{Removal Percentage} = ((S_0 - S) / S_0) * 100 \% \quad (\text{C.5})$$

For example, at a feed trans-4MCHCA concentration of 101.6 mg L^{-1} and a residual trans-4MCHCA concentration of 94.8 mg L^{-1} for the CSTR, CSTR had a trans-4MCHCA removal percentage of 6.7 %; at a feed trans-4MCHCA concentration of 58.0 mg L^{-1} and a residual trans-4MCHCA concentration of 44.1 mg L^{-1} for the biofilm system, biofilm system had a trans-4MCHCA removal percentage of 24.1 %.

APPENDIX D

Determination of Biokinetic Coefficients from CSTR Data

Overall eight different dilution rates were selected for determination of biokinetic coefficients from CSTR data. Their corresponding residual trans-4MCHCA concentration and biomass concentration are shown in Table D.1. The average feed trans-4MCHCA was 101.6 mg L⁻¹. Based on Equations 3.15 and 3.21, the terms used for plotting and determination of coefficients (Figures 4.8 and 4.9 in the main text) were calculated and shown in Table D.1.

Table D.1 Data for CSTR modelling

Dilution Rate (h ⁻¹)	Residual trans-4MCHCA Concentration (mg L ⁻¹)	Biomass Concentration (mg L ⁻¹)	$(S_0-S)D/X$	$S/(D+K_e)$
0.0	2.8	49.0	0.1	113.8
0.1	3.9	66.1	0.1	74.8
0.1	2.1	64.8	0.1	26.5
0.1	4.0	36.7	0.3	31.1
0.2	23.7	26.3	0.5	135.5
0.2	40.9	15.3	0.8	196.4
0.3	54.8	12.9	0.9	215.7
0.3	74.6	7.6	1.1	244.6

APPENDIX E

Data for Control Experiments

For the batch experiment, negative control experiment using McKinney's medium containing 100 mg L^{-1} trans-4MCHCA and 460 mg L^{-1} nitrite in the absence of inoculum was conducted to demonstrate that abiotic degradation did not occur. Concentrations profiles in the negative control experiment are shown in Figure E.1.

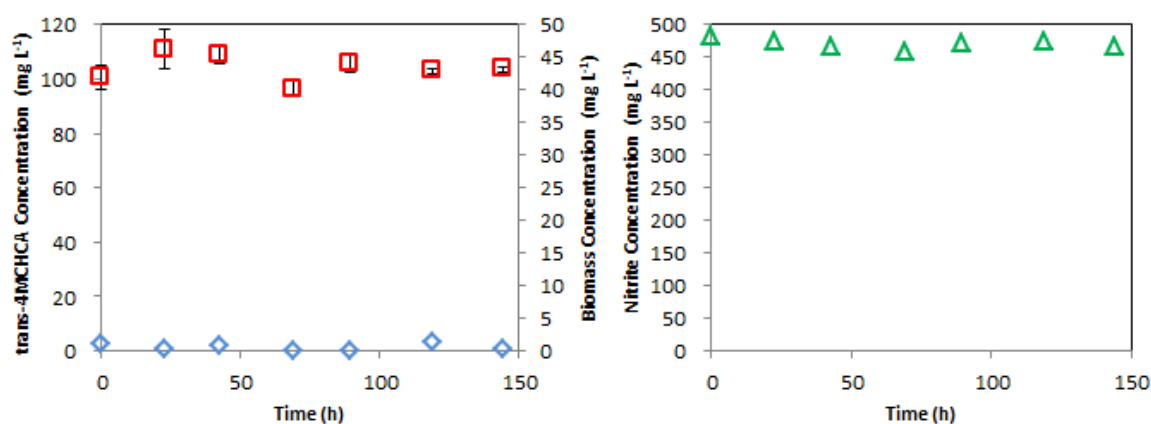


Figure E.1 Control experiments with 100 mg L^{-1} trans-4MCHCA and 460 mg L^{-1} nitrite in the absence of inoculum. The error bars represent the standard deviations of multiple tests on each sample taken from the system and they may not be visible in some cases. \diamond Biomass concentration; \square trans-4MCHCA concentration; \triangle Nitrite ion concentration.

For the CSTR experiment, Two sets of negative control experiments were carried out:

- 1)- McKinney's modified medium containing 100 mg L^{-1} trans-4MCHCA and 460 mg L^{-1} nitrite with no inoculum was fed to the CSTR. Two different flow rates of 9.4 and 18.3 mL h^{-1} were tested in this negative control experiment and each flow rate was maintained for three days. The result of this set of negative control experiment is shown in Table E.1.
- 2)- McKinney's modified medium containing 100 mg L^{-1} trans-4MCHCA with no nitrite was fed to a CSTR which contained McKinney modified medium with 100 mg L^{-1} trans-4MCHCA and 460 mg L^{-1} nitrite inoculated with a seven-day old stock culture and already undergone batch biodegradation (i.e. CSTR contained bacterial population but trans-4MCHCA and nitrite were

already consumed) to confirm that nitrite was required as the terminal electron acceptor and also to assess the extent of potential aerobic biodegradation, if any. One flow rate of 10.7 mL h⁻¹ was tested in this negative control experiment and it was maintained for six days. The result of this set of negative control experiment is shown in Table E.2.

Table E.1 Control experiment with 100 mg L⁻¹ trans-4MCHCA and 460 mg L⁻¹ nitrite in the absence of inoculum

Date	Time	Flow Rate (mL h ⁻¹)	Biomass Concentration (mg L ⁻¹)	Trans-4MCHCA Concentration (mg L ⁻¹)	Nitrite Concentration (mg L ⁻¹)
Feed trans-4MCHCA Concentration				101.1	483.6
20140324	16:55	9.4	1.0	100.7	490.9
20140325	15:21		1.4	99.9	502.8
20140326	11:32		0.2	102.2	488.2
Feed trans-4MCHCA Concentration				108.5	482.7
20140327	14:08	18.3	0.4	95.8	457.6
20140328	10:27		1.4	108.1	460.3
20140329	15:58		1.4	104.7	464.0

Table E.2 Control experiment with 100 mg L⁻¹ trans-4MCHCA in the absence of nitrite

Date	Time	Flow Rate (mL h ⁻¹)	Biomass Concentration (mg L ⁻¹)	Trans-4MCHCA Concentration (mg L ⁻¹)
Feed trans-4MCHCA Concentration				98.1
20140315	17:23	10.7	6.9	90.0
20140316	18:37		4.9	87.4
20140317	10:12		4.6	90.7
Feed trans-4MCHCA Concentration				105.2
20140318	9:36	10.7	7.4	90.2
20140319	10:26		5.5	91.4
20140320	12:41		5.9	91.7